HOKKAIDO UNIVERSITY

Title	Immobilization of Heavy Metals by Metakaolin-Based K-Geopolymer
Author(s)	Pramesti, Prihutami
Degree Grantor	北海道大学
Degree Name	博士(工学)
Dissertation Number	甲第16134号
Issue Date	2024-09-25
DOI	https://doi.org/10.14943/doctoral.k16134
Doc URL	https://hdl.handle.net/2115/93382
Type	doctoral thesis
File Information	Pramesti_Prihutami.pdf

Hokkaido University Collection of Scholarly and Academic Papers : HUSCAP

Immobilization of Heavy Metals by Metakaolin-Based K-Geopolymer

(メタカオリンを用いたカリウム型ジオポリマーによる重金属の不溶化)

by

PRAMESTI PRIHUTAMI
S.T. (2017), M.Eng. (2020)

DISSERTATION
Presented in Partial Fulfilment of the Requirements for the Degree of

DOCTOR OF PHILOSOPHY

in
Graduate School of Engineering
of the

HOKKAIDO
UNIVERSITY

Japan

Approved by the committee in charge,
Tsutomu Sato, *Chair*
Tsubasa Otake
Yogarajah Elakneswaran

August 2024

For my mother (Priyati), my father (Is Hadri Utomo), my aunt (Sri Wiryanti), my sister (Pradhaninggar Prihutami), and my brother (Nugraha Prihutama)

ABSTRACT

Liquid and solid waste from anthropogenic activities commonly contain heavy metals, such as mercury, cadmium, lead, and zinc. These metals exist in wastes in various concentrations and combinations. Exposure to these metals can cause damage to the nervous and reproductive systems, skeleton, liver, kidneys, cardiovascular and respiratory systems. Due to their high toxicity, environmental contamination caused by heavy metals from waste has become a concern. The contamination may occur from the direct disposal of industrial wastes, such as sludge and fly ash, in landfills. Heavy metals may undergo desorption from the sludge. These metals can also leach out from fly ash due to their presence as soluble chloride or sulfate salt. Aside from common industrial activities, fly ash is also produced from municipal solid waste incineration at the Fukushima Dai-Ichi Nuclear Power Plant. This waste contains not only heavy metals but also radioactive cesium. Consequently, an appropriate treatment to stabilize a wide variety of wastes containing heavy metals is needed. One of the potential binders for solidification/stabilization treatment is geopolymer. Studies have shown the excellency of sodium-activated geopolymer to immobilize metal cations. However, each study concluded different kinds of immobilization mechanisms within a particular metal due to the variety of uses of aluminosilicate precursors, metal concentrations, and mixing procedures. Therefore, clarification of the mechanisms is needed to predict their long-term stability. The long-term stability can also be expected with the use of potassium-activated geopolymer instead of sodium. Despite its prominent advantages, potassium-activated geopolymer is less studied. This dissertation explores the use of potassium-activated geopolymer to immobilize heavy metals. This research aims to understand heavy metals immobilization mechanisms to propose geopolymer use in stabilizing contaminated wastes.

Chapter 1 of the dissertation provides a comprehensive background for this study. It introduces the potential of geopolymers, particularly potassium-activated ones, in immobilizing heavy metals. The chapter concludes with the study objectives.

Chapter 2 presents a literature review on geopolymer, including its component and formation process. This chapter also summarizes previous studies on heavy metals immobilization using this material.

Chapter 3 investigates the effect of mixing procedure and heavy metal concentration on cadmium and mercury speciation in potassium-activated geopolymer. This chapter suggests that the mixing procedure can control their final speciation and geopolymer characteristics. This chapter also shows the difference of mercury immobilization in various concentrations and highlights the applicability of geopolymer to manage waste of various cadmium concentrations.

Chapter 4 elucidates the immobilization mechanisms of zinc, cadmium, mercury, and lead in potassium-activated geopolymer through the use of various analytical

instruments. Factors affecting the mechanisms, including their similarities and differences, are also explained.

Chapter 5 focuses on immobilizing mercury in potassium-activated geopolymer. This chapter shows the success of using hydrosulfide as an additive. This chapter also highlights the effect of different methods and mercury-to-sulfur ratios on immobilization.

Chapter 6 shows the effect of hydrosulfide addition on the immobilization of other metals, namely zinc, cadmium, and lead, by observing their leaching behavior in deionized water. The chapter reveals that hydrosulfide addition brings a positive effect on immobilization.

Finally, **Chapter 7** provides a summary and general conclusion of the study, highlighting the findings and implications as well as suggesting directions for future research.

ACKNOWLEDGMENTS

Throughout my educational journey, I received support from various parties, for which my gratitude knows no bounds. My heartfelt love and gratitude go to my family for their never-ending prayers and unwavering support. Their trust and encouragement allowed me to reach where I am today.

I am deeply grateful to Prof. Tsutomu Sato for giving me the invaluable opportunity to conduct research and pursue a doctoral degree. His exceptional guidance, understanding, support, and kindness have greatly influenced my growth on the academic and personal fronts. It is a great honor to become one of his students.

I would like to extend my gratitude to Prof. Tsubasa Otake and Dr. Yogarajah Elakneswaran. Their guidance and support have been critical in the progression of my study.

I am immensely grateful to Dr. Ryosuke Kikuchi, Dr. Yoko Ohtomo, Dr. Kiyofumi Kurumisawa, and Dr. Masaji Kato. They provided me with thoughtful feedback and support through this academic journey.

My acknowledgment extends to Ms. Ayumi Uesugi, Ms. Junko Hasegawa, Ms. Kumiko Kinoshita, Ms. Yoshie Hoshi, Ms. Yuka Ishioka, and Ms. Mika Sueda. Their care and kind support have helped my academic and personal life in Japan.

I am indebted to Mr. Uchida, Mr. Wang, and Mr. Sawa from the Open Facility Division, Mr. Keita Suzuki from the Laboratory of XPS Analysis, Mr. Naoya Nakagawa from the FCC Instrumental Analysis and Management Support Office, and Ms. Reina Ishikawa from the Technical Center Technology Department of the Faculty of Engineering for training me to operate various analytical instruments and assisting me during the analysis.

I am particularly grateful to my research team, Chaerun Raudhatul Islam and Yusuke Ohya. They have been great teammates who readily helped and taught me many things. Their warm friendship, even before we met in person, has been invaluable.

I am grateful to my laboratory members, to Haruki Matsukawa, Masaki Saito, Arata Katsumata, Tobimaru Ishiwata, Naito Yamashita, Takahiro Daimon, Joseph Godirilwe, Dwi Vidya Sari, Zhang Zixuan, Yutaro Kobayashi, Hkaung Htut San, Frances Chikanda, Monthicha Rawangphai, Ebiyo Misganu Geleti, Sereyroith Tum, Yuto Nishiki, Tetsuya Fujimura, Asuka Sugawara, Haruna Asai, Nono Kimotsuki, Reo Suma, Yasuhiro Nagashima, Keisuke Nasuno, Akua Hoshi, Wang Shuai, Amidu Makwinja, Mutungwa David Mwai, Fugo Nakamura, Kanya Kimura, Mitsutaka Kojima, Koichi Furukawa, Koki Toyata, Ryoya Sato, Tsujimoto Kenichiro, Hajime Iwaki, and Masaki Takeda. Their warm friendship and support have been meaningful throughout my journey.

I extend my heartfelt gratitude to Yoan Felanny Lembono, Sukamto, Willy Angraini, Kayyis Muayadah Lubba, Tovika Berlinasari, and Aditya Irfan Witono, who have accompanied me from the very beginning, as well as other Indonesian friends in Hokkaido. Their friendship in this place far away from home has been heartwarming.

I am also grateful to my teachers, especially Prof. Himawan Tri Bayu Murti Petrus, Dr. Agus Prasetya, Prof. Wahyudi Budi Sediawan, and Prof. Hary Sulistyo, for their guidance and encouragement through my academic pursuit.

Lastly, I would like to acknowledge the Ministry of Education, Culture, Sports, Science and Technology (MEXT) of Japan for granting me a scholarship and making my doctoral study possible.

TABLE OF CONTENTS

LIST OF FIGURES

LIST OF TABLES

CHAPTER 1: GENERAL INTRODUCTION

1.1 Background of the study

1.1.1 Heavy Metals and Their Harmful Effects

Heavy metals are a group of elements with a relatively high density compared to water. This group includes metals such as cadmium (Cd), mercury (Hg), chromium (Cr), lead (Pb), copper (Cu), zinc (Zn), nickel (Ni), and metalloids like arsenic (As). Heavy metals are nonbiodegradable, have rich coordination chemistry, and can bind with many functional groups in the biomolecules [1]. While trace amounts of some metals, such as Cr, Cu, Ni, and Zn, are essential for various biochemical and physiological functions, high amounts can induce metabolic abnormalities [2]. Some other metals, such as As, Cd, Hg, and Pb, are non-essential in any amount and are considered harmful [3].

Heavy metals are naturally occurring elements on the earth's crust. However, anthropogenic activities have contributed to the high occurrence of these metals in the ecosystems [4]. Activities from several industries, fossil fuel combustion, waste incineration, and mining provide the metals with increased bioavailability and mobility [5]. These metals are contained in liquid and solid wastes and some fractions are prone to release to the environment. Environmental contamination by heavy metals has become a concern due to their negative implications for ecosystems. Once released, these metals can persist in the ecosystems for long periods and damage aquatic life [6]. Heavy metals can also accumulate in every stage of the food chain through soil contamination [7]. Migration of these metals into the groundwater is possible, increasing the risk of drinking water contamination and posing a threat to human health [8]. Several clinical effects of heavy metals are provided in Table 1-1.

Table 1-1. Clinical effects of several heavy metals [9], [10], [11], [12], [13]

Heavy Metal	Clinical Effects
Cadmium	Diarrhea, bone disease (osteomalacia and osteoporosis), kidney disease, lung damage, and prostate cancer
Mercury	Nausea, diarrhea, lung damage, birth defects, permanent damage to the brain and nervous system
Chromium	Skin irritation, ulcers, breathing problems, DNA damage, and lung cancer
Lead	Anemia, hypertension, hallucination, birth defects, renal dysfunction, and brain damage
Copper	Acute nausea, diarrhea, red blood cell destruction, kidney and liver damage
Zinc	Nausea, abdominal pain, anemia, and dizziness
Nickel	Allergy, kidney disease, lung fibrosis, and nasal cancer
Arsenic	Nausea, diarrhea, cardiac abnormalities, skin and respiratory cancer

1.1.2 Waste Containing Heavy Metals

Heavy metals are contained in various wastes, including wastewater and fly ash [14], [15], [16]. Several industries leading to the production of heavy metals-containing wastes are mentioned in Table 1-2. In wastewater, heavy metals are present as ions. This

form poses a higher risk for environmental contamination. Further treatment is then required to remove metal ions from the wastewater and reduce their mobility. One of the common treatments with low capital cost and simple operation is by coprecipitation with iron oxyhydr(oxides) [17]. This process includes the addition of iron salt coagulants to the wastewater [18]. Iron(III) hydrolyses to produce hydrated Fe(III) species and fastly grows into iron oxyhydr(oxides). The first hydrolysis product is commonly ferrihydrite with a high specific surface area and adsorption capacity [19]. After the adsorption of heavy metals, the final waste is ferric sludge.

Table 1-2. Source of several heavy metals in wastes [20], [21]

Heavy Metal	Source
Cadmium	Mining, smelting, and photovoltaic cells
Mercury	Coal power plant, mining, paper and paint industries
Chromium	Leather industry, canning industry, and steel manufacture
Lead	Mining, electroplating, and batteries manufacture
Copper	Paint manufacture, mining, electronics and cables industries
Zinc	Brass coating, mining, and refineries
Nickel	Electroplating, stainless steel and zinc storage battery industries
Arsenic	Coal power plant, mining, electronics and glass production

Not only wastewater, but heavy metals are also present in the by-product of coal or solid waste combustion. This combustion produces two types of waste, fly ash and bottom ash. Fly ash is a lighter and smaller combustion product collected in a scrubber or baghouse accounting for 90% of the by-product. Meanwhile, bottom ash is heavier and resides at the bottom of the chamber. Compared to bottom ash, heavy metals accumulate more in fly ash. Their concentration in fly ash is relatively higher with the decrease in particle size [22]. A fraction of these metals exist in water-soluble species, either as chloride or sulfate salt [23]. The content of heavy metals varies widely, as seen in Table 1-3. Aside from each metal having a different concentration within a waste, heavy metals are also present in various combinations. In addition, the metals may present alongside a radioactive, such as fly ash from municipal solid waste incineration of the Fukushima Daiichi Nuclear Power Plant accident. Radioactive cesium (Cs) is found in fly ash with approximately 60% available as a chloride salt [24]. Various metals, concentrations, and radioactive coexistence indicate the wide variety of wastes containing heavy metals.

Table 1-3. Heavy metals content in solid wastes [25], [26], [27]

Waste	Content (mg/kg)							
	Cd	Hg	Cr	Pb	Cu	Zn	Ni	As
Sludge	0.21 – 2.77	0.67 – 19.50	10 – 136	0 – 79	28 – 1150	154 – 2970	9 – 262	12.1 – 41.6
Fly ash	0.25 – 464	0.001 – 46	18 – 1460	35 – 19,130	28.1 – 6647	59.6 – 66,450	10.5 – 335	9 – 163

1.1.3 Waste Disposal

The disposal of solid wastes containing heavy metals needs to consider their content and species to prevent the risk of contamination. Fly ash containing heavy metals and radioactive requires stabilization before its final disposal. As of now, sludge and regular fly ash are commonly dumped in landfills. However, this kind of disposal can instigate secondary environmental contamination through contact with rainfall and soil moisture [28]. This water may desorb heavy metals from the sludge. It also dissolves soluble heavy metal species in fly ash. Therefore, there is a need to stabilize those wastes instead of directly disposing them in landfills. Among others, solidification/stabilization technology is deemed to be the most reasonable. This technology includes the addition of a binder to the waste to make a more stable solid waste. One of the most established binders is Portland cement. This binder is cheap and has been used widely to solidify and stabilize sludge and fly ash [29], [30].

Portland cement is a hydraulic binder from the calcination of limestone and siliceous matter at around 1450˚C with a main hydration product of C-S-H (calcium silicate hydrate) [31]. Due to the use of limestone and very high calcination temperature, the production of this binder emits a lot of CO_2. For every ton of cement, 0.73-0.85 tons of CO_2 is released [32]. This has become a major drawback as the world is leading to carbon neutrality by 2050. Vulnerability to acidic attack is another drawback of Portland cement. Decomposition and mechanical properties degradation of this binder are available as acid attacks calcium hydroxide and other hydration products of the matrix [33]. Portland cement is also unsuitable to immobilize some metals. Zinc and copper tend to hinder its hydration process [34]. The cement matrix also cannot hold cesium for the long term. A study about cesium incorporation into cement results in a high leaching rate with around 80% of the element leached out after 360 days [35].

Recently, geopolymer emerged as an alternative to Portland cement. Unlike cement, geopolymer is a binder with a great ability to immobilize cesium [35]. Sodium-activated geopolymer is also known to have an excellent immobilization effect for heavy metals [36]. This binder shares the same characteristics as Portland cement as it has a simple manufacturing process and hardens at low temperatures [37], [38]. However, the use of geopolymer for the solidification/stabilization of waste containing aluminosilicate content like fly ash is more beneficial as it relatively does not increase the final waste volume. Geopolymer production also emits a lower amount of CO_2 compared to cement [39]. Additionally, this material is acid-resistant, stable at high temperatures, and has low permeability [40], [41].

1.1.4 Present Challenge in Using Geopolymer as Solid Wastes Binder

Despite the many advantages of geopolymer, research interest in this material has only grown recently [42]. Studies on heavy metal immobilization have only been conducted in sodium-activated geopolymers [43], [44], [45]. Several metals that have been intensively investigated are zinc, cadmium, mercury, and lead. However, there is still no conclusive result on the immobilization mechanisms of those metals. Instead, mechanisms for each particular metal are concluded differently. This causes difficulty in

predicting the long-term stability of heavy metals in geopolymer. These results are probably caused by different kinds of aluminosilicate precursors, heavy metal concentrations, and mixing procedures in the previous studies. Aluminosilicate precursors for geopolymer varied from fly ash, bottom ash, slag, and drinking water treatment residue, to metakaolin, [44], [46], [47], [48]. Among those, metakaolin produces a purer geopolymer since its main components are SiO_2 and Al_2O_3.

Concern about the long-term ability of Na-geopolymer to immobilize heavy metals arises due to its transformation into zeolite even at low temperatures [49], [50]. The transformation from amorphous to more ordered structure may cause a shrinking of the ring structures and cause the initially retained heavy metals to leach out. This phenomenon may work differently with the use of K-geopolymer. This type of geopolymer remains amorphous at low temperatures and enhances the possibility of keeping heavy metals incorporated in geopolymer for a long time [51].

Aside from the long-term prospect of immobilizing heavy metals, practicality during manufacturing is an important factor. Sodium activator possesses lower flowability compared to potassium one [52], [53]. Mixing a sodium activator of this flowability with solid waste may bring difficulty, resulting in parts of the waste remaining in its initial forms. This way, the heavy metals in waste are not stabilized and are prone to contaminating the environment. Meanwhile, a potassium activator allows better mixing of waste during geopolymerization to produce a homogeneous final waste. Despite its superiority, potassium-activated geopolymer is less studied. Further research in this area is required to encourage the application of geopolymer in waste handling.

1.2 Study Focus and Objectives

The exploration of potassium-activated geopolymer for immobilizing heavy metals opens the opportunity to manufacture final waste of longer stability. This approach not only provides an alternative to Portland cement but also offers a binder with high potential to treat a wide variety of waste containing heavy metals, including various combinations of heavy metals, various heavy metal concentrations, and the coexistence of radioactive. Understanding the immobilization mechanisms of heavy metals in a simple geopolymer system is intriguing and essential. The theoretical understanding lays a foundation for further use of geopolymer in waste disposal. The primary objectives of this study are:

- Understanding the immobilization mechanisms of zinc, cadmium, mercury, and lead in metakaolin-based K-geopolymer.
- Proposing methods to make solidified/stabilized wastes containing heavy metals.

Addressing the current research gap, particularly about K-geopolymer and heavy metals immobilization, the potential impact of this study on long-term waste stabilization with a wide variety of waste emphasizes its significance.

1.3 References

[1] J. Briffa, E. Sinagra, and R. Blundell, “Heavy metal pollution in the environment and their toxicological effects on humans,” *Heliyon*, vol. 6, no. 9, pp. 1–26, Sep. 2020, doi: 10.1016/j.heliyon.2020.e04691.

[2] M. Bibi, Samiullah, F. Behlil, S. Afzal, and Sahifa, “Essential and non-essential heavy metals sources and impacts on human health and plants,” *Pure and Applied Biology*, vol. 12, no. 2, pp. 835–847, Jun. 2023, doi: 10.19045/bspab.2023.120083.

[3] H. Ali and E. Khan, “Bioaccumulation of non-essential hazardous heavy metals and metalloids in freshwater fish. Risk to human health,” *Environ Chem Lett*, vol. 16, no. 3, pp. 903–917, Sep. 2018, doi: 10.1007/s10311-018-0734-7.

[4] J. P. Vareda, A. J. M. Valente, and L. Durães, “Assessment of heavy metal pollution from anthropogenic activities and remediation strategies: A review,” *J Environ Manage*, vol. 246, pp. 101–118, Sep. 2019, doi: 10.1016/j.jenvman.2019.05.126.

[5] H. Ali, E. Khan, and I. Ilahi, “Environmental chemistry and ecotoxicology of hazardous heavy metals: Environmental persistence, toxicity, and bioaccumulation,” *J Chem*, vol. 2019, 2019, doi: 10.1155/2019/6730305.

[6] Khushbu, R. Gulati, Sushma, A. Kour, and P. Sharma, “Ecological impact of heavy metals on aquatic environment with reference to fish and human health,” *Journal of Applied and Natural Science*, vol. 14, no. 4, pp. 1471–1484, 2022, doi: 10.31018/jans.v14i4.3900.

[7] P. Nyiramigisha, Komariah, and Sajidan, “Harmful Impacts of Heavy Metal Contamination in the Soil and Crops Grown Around Dumpsites,” *Reviews in Agricultural Science*, vol. 9, pp. 271–282, 2021.

[8] Z. Ullah *et al.*, “Groundwater contamination through potentially harmful metals and its implications in groundwater management,” *Front Environ Sci*, vol. 10, pp. 1–13, Nov. 2022, doi: 10.3389/fenvs.2022.1021596.

[9] M. Mahurpawar, “Effects of heavy metals on human health,” *Social Issues and Environmental Problems*, pp. 1–7, 2015.

[10] P. B. Tchounwou, C. G. Yedjou, A. K. Patlolla, and D. J. Sutton, “Heavy metal toxicity and the environment,” *EXS*, vol. 101, pp. 133–164, 2012, doi: 10.1007/978-3-7643-8340-4_6.

[11] M. Araya, M. Olivares, and F. Pizarro, “Copper in human health,” *International Journal of Environment and Health*, vol. 1, no. 4, pp. 608–620, 2007, doi: 10.1504/IJENVH.2007.018578.

[12] L. M. Plum, L. Rink, and H. Hajo, “The essential toxin: Impact of zinc on human health,” *Int J Environ Res Public Health*, vol. 7, no. 4, pp. 1342–1365, 2010, doi: 10.3390/ijerph7041342.

[13] G. Genchi, A. Carocci, G. Lauria, M. S. Sinicropi, and A. Catalano, “Nickel: Human health and environmental toxicology,” *Int J Environ Res Public Health*, vol. 17, no. 3, pp. 1–21, Feb. 2020, doi: 10.3390/ijerph17030679.

[14] N. A. A. Qasem, R. H. Mohammed, and D. U. Lawal, “Removal of heavy metal ions from wastewater: a comprehensive and critical review,” *NPJ Clean Water*, vol. 4, no. 1, pp. 1–36, Dec. 2021, doi: 10.1038/s41545-021-00127-0.

[15] V. K. Sangal, S. Rajoria, and M. Vashishtha, “Heavy Metal Ions in Wastewater: A Review on Detection and Toxicity,” *Chem Eng Process Tech*, vol. 8, no. 3, pp. 1082–1087, 2023.

[16] A. Altlkulaç *et al.*, “Assessment of the Enrichment of Heavy Metals in Coal and Its Combustion Residues,” *ACS Omega*, vol. 7, no. 24, pp. 21239–21245, Jun. 2022, doi: 10.1021/acsomega.2c02308.

[17] M. A. Barakat, “New trends in removing heavy metals from industrial wastewater,” *Arabian Journal of Chemistry*, vol. 4, no. 4, pp. 361–377, Oct. 2011, doi: 10.1016/j.arabjc.2010.07.019.

[18] F. Younas *et al.*, “Current and emerging adsorbent technologies for wastewater treatment: Trends, limitations, and environmental implications,” *Water (Basel)*, vol. 13, no. 2, pp. 1–25, Jan. 2021, doi: 10.3390/w13020215.

[19] Y. Wang *et al.*, “Stability and Transformation of Ferrihydrite Coprecipitated with Metals: Dependence of Choice of Iron Salt Precursor,” *ACS Earth Space Chem*, vol. 7, no. 12, pp. 2475–2488, Dec. 2023, doi: 10.1021/acsearthspacechem.3c00225.

[20] M. Rafique, S. Hajra, M. B. Tahir, S. S. A. Gillani, and M. Irshad, “A review on sources of heavy metals, their toxicity and removal technique using physico-chemical processes from wastewater,” *Environmental Science and Pollution Research*, vol. 29, no. 11, pp. 16772–16781, Mar. 2022, doi: 10.1007/s11356-022-18638-9.

[21] P. B. Angon *et al.*, “Sources, effects and present perspectives of heavy metals contamination: Soil, plants and human food chain,” *Heliyon*, vol. 10, no. 7, pp. 1–15, Apr. 2024, doi: 10.1016/j.heliyon.2024.e28357.

[22] Y. Tang, J. Pan, B. Li, S. Zhao, and L. Zhang, “Residual and ecological risk assessment of heavy metals in fly ash from co-combustion of excess sludge and coal,” *Sci Rep*, vol. 11, no. 1, pp. 1–11, Dec. 2021, doi: 10.1038/s41598-021-81812-5.

[23] W. Chen, Y. Wang, Y. Sun, G. Fang, and Y. Li, “Release of soluble ions and heavy metal during fly ash washing by deionized water and sodium carbonate solution,” *Chemosphere*, vol. 307, pp. 1–8, Nov. 2022, doi: 10.1016/j.chemosphere.2022.135860.

[24] Y. Koike, K. Fujii, R. Saito, N. Ogawa, and A. Ohbuchi, “Chemical State Analysis of Heavy Metals and Radioactive Cesium in Municipal Solid Waste Incineration Fly Ash Contaminated with Radioactive Cesium Released by the FDNPP Accident,” *Analytical Sciences*, vol. 37, no. 11, pp. 1565–1570, 2021, doi: 10.2116/analsci.21P022.

[25] D. Xiao, H. Li, Y. Wang, G. Wen, and C. Wang, “Distribution Characteristics of Typical Heavy Metals in Sludge from Wastewater Plants in Jiangsu Province (China) and Their Potential Risks,” *Water (Basel)*, vol. 15, no. 2, pp. 1–13, Jan. 2023, doi: 10.3390/w15020313.

[26] G. C. Kisku, S. Yadav, R. K. Sharma, and M. P. S. Negi, “Potential environmental pollution hazards by coal based power plant at Jhansi (UP) India,” *Environ Earth Sci*, vol. 67, no. 7, pp. 2109–2120, Dec. 2012, doi: 10.1007/s12665-012-1651-x.

[27] W. Zucha, G. Weibel, M. Wolffers, and U. Eggenberger, “Inventory of MSWI fly ash in Switzerland: Heavy metal recovery potential and their properties for acid leaching,” *Processes*, vol. 8, no. 12, pp. 1–13, Dec. 2020, doi: 10.3390/pr8121668.

[28] A. Iravanian and S. O. Ravari, “Types of Contamination in Landfills and Effects on the Environment: A Review Study,” in *IOP Conference Series: Earth and Environmental Science*, IOP Publishing Ltd, Dec. 2020, pp. 1–8. doi: 10.1088/1755-1315/614/1/012083.

[29] Army Environmental Policy Institute, “Solidification Technologies for Restoration of Sites Contaminated with Hazardous Wastes,” 1998.

[30] U.S. Environmental Protection Agency, “Treatment Technologies For Mercury in Soil, Waste, and Water,” 2007.

[31] I. G. Richardson, “The nature of C-S-H in hardened cements,” *Cem Concr Res*, vol. 29, pp. 1131–1147, 1999.

[32] Z. He, X. Zhu, J. Wang, M. Mu, and Y. Wang, “Comparison of CO2 emissions from OPC and recycled cement production,” *Constr Build Mater*, vol. 211, pp. 965–973, Jun. 2019, doi: 10.1016/j.conbuildmat.2019.03.289.

[33] S. Goyal, M. Kumar, D. S. Sidhu, and B. Bhattacharjee, “Resistance of Mineral Admixture Concrete to Acid Attack,” *Journal of Advanced Concrete Technology*, vol. 7, no. 2, pp. 273–283, 2009.

[34] M. Liu, Y. Zhao, Z. Yu, and Z. Cao, “Binding of Cu(II) and Zn(II) in Portland cement immobilization systems: Effect of C-A-S-H composition,” *Cem Concr Compos*, vol. 131, pp. 1–11, Aug. 2022, doi: 10.1016/j.cemconcomp.2022.104602.

[35] R. I. Chaerun *et al.*, “Retention mechanism of cesium in chabazite embedded into metakaolin-based alkali activated materials,” *J Hazard Mater*, vol. 440, pp. 1–10, Oct. 2022, doi: 10.1016/j.jhazmat.2022.129732.

[36] Z. Ji and Y. Pei, "Immobilization efficiency and mechanism of metal cations (Cd2+, Pb2+ and Zn2+) and anions (AsO43- and Cr2O72-) in wastes-based geopolymer," *J Hazard Mater*, vol. 384, pp. 1–11, Feb. 2020, doi: 10.1016/j.jhazmat.2019.121290.

[37] P. Sajan, T. Jiang, C. K. Lau, G. Tan, and K. Ng, "Combined effect of curing temperature, curing period and alkaline concentration on the mechanical properties of fly ash-based geopolymer," *Cleaner Materials*, vol. 1, pp. 1–13, Dec. 2021, doi: 10.1016/j.clema.2021.100002.

[38] A. M. Mustafa Al Bakria, H. Kamarudin, M. Bin Hussain, I. Khairul Nizar, Y. Zarina, and A. R. Rafiza, "The effect of curing temperature on physical and chemical properties of geopolymers," in *Physics Procedia*, Elsevier B.V., 2011, pp. 286–291. doi: 10.1016/j.phpro.2011.11.045.

[39] J. Davidovits, "Geopolymer cement to minimize carbon-dioxde greenhouse-warming," *Ceramic Transactions*, vol. 37, no. 1, pp. 165–182, 1993, [Online]. Available: https://www.researchgate.net/publication/284682578

[40] J. L. Provis and S. A. Bernal, "Geopolymers and related alkali-activated materials," *Annu Rev Mater Res*, vol. 44, pp. 299–327, 2014, doi: 10.1146/annurev-matsci-070813-113515.

[41] K. Srinivasan and A. Sivakumar, "Geopolymer Binders: A Need for Future Concrete Construction," *ISRN Polymer Science*, vol. 2013, pp. 1–8, Jul. 2013, doi: 10.1155/2013/509185.

[42] J. Matsimbe, M. Dinka, D. Olukanni, and I. Musonda, "A Bibliometric Analysis of Research Trends in Geopolymer," *Materials*, vol. 15, no. 19, pp. 1–20, Oct. 2022, doi: 10.3390/ma15196979.

[43] X. Wei *et al.*, "Structural Evolution of Geopolymers Incorporated with Heavy Metals: Solidification Mechanism of Pb2+ and Cd2+," *Journal of Physical Chemistry C*, vol. 127, no. 39, pp. 19563–19573, Oct. 2023, doi: 10.1021/acs.jpcc.3c03924.

[44] J. Zhang, J. L. Provis, D. Feng, and J. S. J. van Deventer, "Geopolymers for immobilization of Cr6+, Cd2+, and Pb2+," *J Hazard Mater*, vol. 157, no. 2–3, pp. 587–598, Sep. 2008, doi: 10.1016/j.jhazmat.2008.01.053.

[45] Z. Ji, L. Su, and Y. Pei, "Synthesis and toxic metals (Cd, Pb, and Zn) immobilization properties of drinking water treatment residuals and metakaolin-based geopolymers," *Mater Chem Phys*, vol. 242, pp. 1–9, Feb. 2020, doi: 10.1016/j.matchemphys.2019.122535.

[46] G. Qian, D. D. Sun, and J. H. Tay, "Immobilization of mercury and zinc in an alkali-activated slag matrix," *J Hazard Mater*, vol. 101, no. 1, pp. 65–77, Jul. 2003, doi: 10.1016/S0304-3894(03)00143-2.

[47] Z. Ji and Y. Pei, “Geopolymers produced from drinking water treatment residue and bottom ash for the immobilization of heavy metals,” *Chemosphere*, vol. 225, pp. 579–587, Jun. 2019, doi: 10.1016/j.chemosphere.2019.03.056.

[48] Q. Wan, F. Rao, S. Song, and Y. Zhang, “Immobilization forms of ZnO in the solidification/stabilization (S/S) of a zinc mine tailing through geopolymerization,” *Journal of Materials Research and Technology*, vol. 8, no. 6, pp. 5728–5735, Nov. 2019, doi: 10.1016/j.jmrt.2019.09.040.

[49] P. Rożek, M. Król, and W. Mozgawa, “Geopolymer-zeolite composites: A review,” *J Clean Prod*, vol. 230, pp. 557–579, Sep. 2019, doi: 10.1016/j.jclepro.2019.05.152.

[50] P. De Silva and K. Sagoe-Crenstil, “Medium-term phase stability of Na2O-Al2O3-SiO2-H2O geopolymer systems,” *Cem Concr Res*, vol. 38, no. 6, pp. 870–876, Jun. 2008, doi: 10.1016/j.cemconres.2007.10.003.

[51] B. Liu *et al.*, “Insights into the microstructure of hydrothermal synthesized nanoscale k2o-al2o3-sio2-h2o particles,” *Nanomaterials*, vol. 10, no. 1, pp. 1–18, Jan. 2020, doi: 10.3390/nano10010063.

[52] A. C. Constâncio Trindade, I. Curosu, M. Liebscher, V. Mechtcherine, and F. de Andrade Silva, “On the mechanical performance of K- and Na-based strain-hardening geopolymer composites (SHGC) reinforced with PVA fibers,” *Constr Build Mater*, vol. 248, pp. 1–16, Jul. 2020, doi: 10.1016/j.conbuildmat.2020.118558.

[53] M. Uehara, “New Concrete with Low Environmental Load Using the Geopolymer Method,” *QR of RTRI*, vol. 51, no. 1, pp. 1–7, 2010.

CHAPTER 2: LITERATURE REVIEW ON GEOPOLYMER AND HEAVY METALS IMMOBILIZATION

2.1 Geopolymer

2.1.1 Definition

Geopolymer derives from the word "geo" which means "earth" in Greek and "polymer" [1]. The word "geo" corresponds to Si and Al which make up a huge percent of the earth's crust. The word "polymer" correlates to the material structure made up of Si and Al monomers. Geopolymer terminology refers to an alkali-activated material consisting of amorphous to semi-crystalline 3-dimensional aluminosilicate networks [2]. This material consists of alumina and silica tetrahedra joined alternately by sharing oxygen atoms [3]. The four-coordinated aluminium with respect to oxygen creates a negative charge imbalance. Thus, the presence of cations, namely Na^+ or K^+ from the activator is essential to maintain electric neutrality within the geopolymer [4]. Geopolymer has a similar chemical composition to zeolite and differs in crystallinity and alternating framework [5]. Another important terminology of geopolymer that differs from other alkali-activated materials is the absence or the little presence of calcium [6]. Alkali-activated materials with high calcium content have a gel structure of C-(A)-S-H (calcium (alumina) silicate hydrate) in a disordered tobermorite-like structure [6]. Meanwhile, the structure of geopolymer is dominantly N-A-S-H (sodium aluminosilicate hydrate) or K-A-S-H (potassium aluminosilicate hydrate) as shown in Figure 2-1 [2]. This highly cross-linked aluminosilicate gel is assumed to be limited by Loewenstein's rule, which states that the formation of Al-O-Al linkages is energetically unstable, making every aluminium to be in the $Al(OSi)_4$ environment [7], [8]. Nonetheless, previous studies indicated the possibility of Al-O-Al linkages on low Si/Al ratios [9].

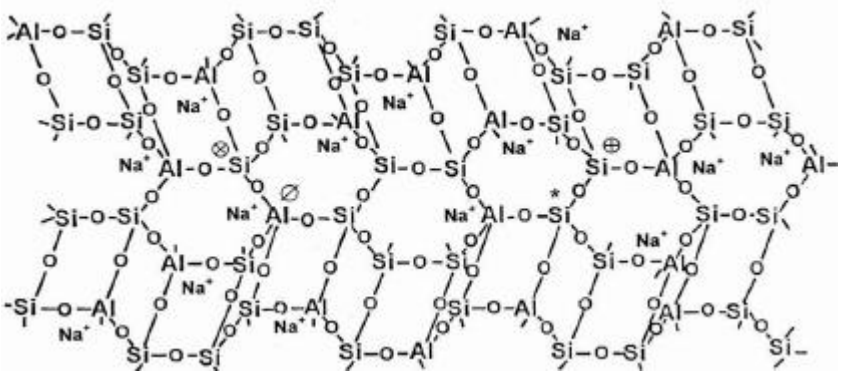

Figure 2-1. A proposed structure of geopolymer [2]

2.1.2 Geopolymerization Process

Geopolymer formed from the polymerization reaction of alkali activator and aluminosilicate precursor. Alkali activators are commonly alkali hydroxides, alkali silicates, or a combination of both [10]. Alkali hydroxides are used to maintain a high solution pH and play an important role in the dissolution of aluminosilicate precursor [4]. Alkali silicates act as an additional source of SiO_2 and as the initiator for the polymerization reaction [11]. Depending on the alkaline used, geopolymer is divided into

sodium and potassium-activated. In this study, focus is given to potassium-activated geopolymer.

Aluminosilicate sources having been used for the geopolymerization process include blast furnace slag, fly ash, municipal solid waste incineration bottom ash, mine tailing, rice husk ash, bagasse ash, sewage sludge ash, waste glass, and metakaolin [12], [13], [14], [15], [16], [17]. Aside from SiO_2 and Al_2O_3, CaO content is important to define geopolymer. As mentioned before, a high amount of calcium in the system leads to C-(A)-S-H formation, a completely different structure from geopolymer [6]. Accounting for the small number of calcium content, metakaolin is the best precursor to produce a simple geopolymer system [18]. It is a manufactured product from the calcination of kaolinite between 600-800˚C [19]. The basic structure of kaolinite initially consists of a silica tetrahedra layer and an alumina octahedra layer parallelly arranged and connected via oxygen atoms [20]. Calcination changes alumina octahedra into tetrahedra, reforming the structure to amorphous. This amorphousness accounts for the highly reactive nature of metakaolin [21].

The geopolymerization process begins with the dissolution of metakaolin by a potassium activator. Hydroxide ions (OH^-) play a pivotal role in depolymerizing and dissolving the precursor into hydroxyl silanol and aluminol. Reaction with OH^- dissolves silica in the form of $SiO(OH)_3^-$ and $SiO_2(OH)_2^{2-}$ [22]. At a pH of around 13 to 14, the dominant species is initially $SiO_2(OH)_2^{2-}$. Silica species then transform mainly into $SiO(OH)_3^-$ with a decreasing pH of until around 12. This species bonds with K^+ to achieve charge stability [23]. The formation of ≡Si-O-K is crucial for allowing the condensation reaction. Simultaneously, OH^- reacts with alumina to form $Al(OH)_4^-$. In the next step, silanol condenses into ≡Si-O-Si≡, promoted by high pH conditions. The reactive aluminol also tends to bond with a non-bonding oxygen atom from silanol. Aluminol and silanol form another oligomer of ≡Si-O-Al≡, while the OH^- group from the aluminol bonds with K^+ from the silanol. These oligomers continue forming a polymeric structure through covalent bonding and condensation reactions. During this process, KOH is liberated and re-participates in polycondensation. Geopolymer hardens with the expulsion of H_2O and KOH. It is worth noting that the role of K^+ and OH^- is not only for the dissolution of aluminosilicate but also as a catalyst for the condensation reaction [24]. Thus, KOH leach out from the hardened material in approximately the same amount as was added during the manufacturing. The whole process is simultaneously done with K^+ balancing negative charges from alumina tetrahedra. The overall process is summarized by the following reactions [2].

$$n(Si_2O_5, Al_2O_2) + 2nSiO_2 + 4nH_2O \xrightarrow{KOH} n(OH)_3\text{-Si-O-Al}^{(-)}\text{-O-Si-}(OH)_3 \quad (2.1)$$

$$\text{with } (OH)_2 \text{ on Al}$$

$$n(OH)_3\text{-Si-O-Al}^{(-)}\text{-O-Si-}(OH)_3 \xrightarrow{KOH} K^+\text{-(-Si-O-Al}^{(-)}\text{-O-Si-O)} + nH_2O \quad (2.2)$$

$$\text{with } (OH)_2 \text{ on Al; with O on Si-O-Al}^{(-)}\text{-O-Si-O}$$

K-geopolymer exhibits superior flowability than Na-geopolymer, enhancing its practical use during manufacturing[25], [26]. The produced geopolymer is also better at maintaining its amorphous structure [27]. Therefore, any application that benefits from this structure will be stable in the long term. K-geopolymer is also denser and more stable at elevated temperatures than the sodium counterpart with higher residual compressive strength and lower volumetric shrinkage, mass loss, and cracking damage [28], [29].

2.2 Heavy Metals Immobilization in Geopolymer

Immobilization studies of heavy metals have been conducted before in Na-geopolymer. Previous studies employ various aluminosilicate precursors, from metallurgical slag, fly ash, bottom ash, and drinking water treatment residue, to metakaolin [30], [31], [32], [33]. The content of these precursors is provided in Table 2-1. The CaO content in previous studies ranges between 0.4 – 40.31 wt.%. Since a relatively high amount of calcium is present in some precursors, the possibility of complex geopolymer-C-(A)-S-H formation cannot be ruled out [34]. Consequently, the reported heavy metals immobilization effect may also be contributed by the C-(A)-S-H framework. Qian *et al.* (2003) reported the contribution of this framework in the immobilization of Hg when metallurgical slag with high calcium content was used as a precursor [30]. Meanwhile, the use of fly ash with a relatively lower calcium content immobilized Hg through adsorption onto an N-A-S-H structure [35].

Table 2-1. Composition of several aluminosilicate precursors [30], [31], [32], [33]

Precursor	Content (wt.%)		
	SiO_2	Al_2O_3	CaO
Metallurgical slag	34.47	9.47	40.31
Fly ash	46.4	28.3	5.1
Bottom ash	43.51	23.24	10.52
Drinking water treatment residue	21.25	23.1	9.36
Metakaolin	50.62	46.21	0.4

In general, previous studies suggest that geopolymer has a positive immobilization effect on heavy metals [36]. Several metals like Pb, Cd, Zn, Cr, and Cu achieve a high immobilization efficiency of more than 90% [37], [38]. The immobilization of heavy metals is postulated to happen through four types of mechanism [39]:

1. Ion exchange with Na^+ or K^+ to balance the negative charge of alumina tetrahedra
2. Covalent bonding to the aluminosilicate network
3. Precipitations of hydroxides, carbonates, or silicates
4. Physical encapsulation by low permeability geopolymer

Among all the above, covalent bonding between heavy metals with the geopolymer framework seems to ensure the long-term immobilization effect as long as the

geopolymer structure is preserved. However, the condition in which a particular mechanism is preferred over the others has not been reported. Therefore, a specific mechanism cannot be aimed.

Nonetheless, this area of study is not free from contradictive results. A study by Ji and Pei (2020) indicates that the immobilization effect of chromium in the form of $Cr_2O_7^{2-}$ is in the lower degree, having a completely different result from the study by Wang, *et al*. (2018) with an immobilization rate reaching 99.963% [36], [40]. This opposite result is due to the different forms of Cr added into the system, namely Cr^{3+} and $Cr_2O_7^{2-}$. In addition, arsenic added as AsO_4^{3-} has the same result as $Cr_2O_7^{2-}$, indicating the low capability of geopolymer in immobilizing heavy metal anions. The differences in both studies suggest that considering the available ion species during geopolymerization is important as it highly affects metal immobilization.

Accordingly, at least three kinds of studies have been conducted to enlighten the immobilization mechanisms of cadmium in geopolymer. A thermodynamics study by El-Eswed (2020) mentioned that Cd is expected to turn into $Cd(OH)_2$ at highly alkaline conditions. However, this hydroxide has high solubility and exists as oxyanions at high pH [39]. The oxyanions cannot attach to the negatively charged alumina tetrahedra, thus physical encapsulation is claimed to be an irrefutable mechanism. However, experimental studies suggest different kinds of mechanisms. A study by Zhang, *et al*. (2008) found that Cd is immobilized as a hydroxide precipitate ($Cd(OH)_2$) when added as cadmium nitrate salt [38]. Meanwhile, another study by Ji, *et al*. (2020) shows that the addition of cadmium nitrate solution changes Si, Al, and O environment, indicating Cd immobilization through Si-O-Cd and Al-O-Cd bonding [37]. Both experimental studies did not take thermodynamics calculations into account. Therefore, the exact thermodynamically-predicted species is unknown.

Referring to the solubility diagram in Figure 2-2, Cd species does not only depend on pH but also on activity which equals its concentration. Zhang, *et al.* (2008) and Ji, *et al.* (2020) used 0.5 wt.% and 2 and 4 wt.% of Cd in their experiments. These concentrations are considered high and induce the formation of $Cd(OH)_2$, explaining the formation of hydroxide species in Zhang, *et al*. (2008) study. Only with the use of low Cd concentration does oxyanion become the dominant species. However, the correlation between heavy metal concentration and immobilization mechanisms is not reported.

Different from Zhang, *et al.* (2008) result, research by Ji, *et al*. (2020) employing also high cadmium concentration suggests a completely different immobilization mechanism of Si-O-Cd and Al-O-Cd bonding. Both experimental studies differ in the form of Cd added into the system, namely salt and dissolved ions. However, neither study explains whether this factor contributes to the immobilization mechanisms of the metal.

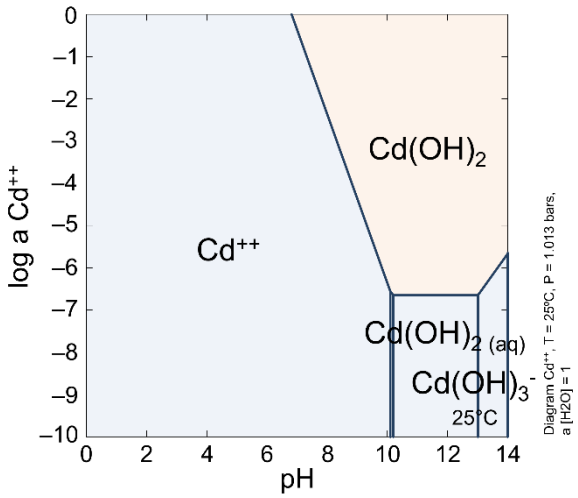

Figure 2-2. Solubility diagram of Cd-H_2O system calculated with Visual MINTEQ database

Wan, *et al*. (2019) studied the immobilization forms of ZnO in the solidification/stabilization of Zn mine tailing by geopolymer [41]. The results show that ZnO is nonreactive in the geopolymerization process and is immobilized through physical encapsulation. A small amount of ZnO dissolves into Zn^{2+} in an acid-leaching test. According to the solubility diagram of Zn in Figure 2-3, ZnO species is stable at the geopolymerization condition, which is highly alkaline. During acid leaching, Zn^{2+} can leach out from the geopolymer due to the high solubility of ZnO species. This study has a good correlation with thermodynamics data. When the final speciation of heavy metal is known or can be expected, its immobilization effect in geopolymer can be predicted with the help of thermodynamics calculation.

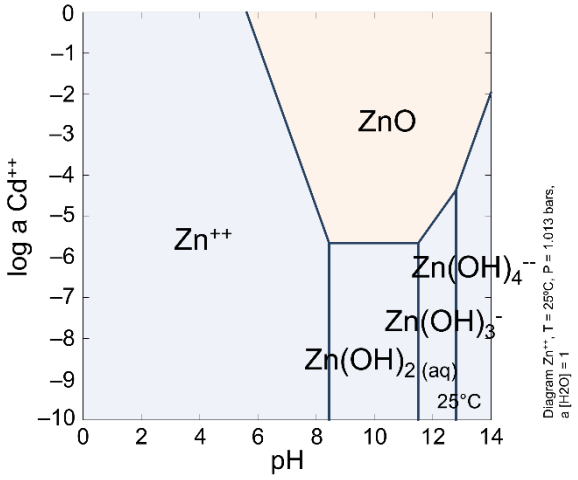

Figure 2-3. Solubility diagram of Zn-H_2O system from calculated with Visual MINTEQ database

El-Eswed (2020) employs thermodynamics calculation to predict the stability of several heavy metal precipitates [39]. Predictions are made for metal hydroxides and

silicates since geopolymerization enables the metals to come in contact with OH^- and SiO_3^{2-}. The calculation is also done for metal sulfides as those forms usually exist in solid waste. The results of the calculation are provided in Table 2-2.

Table 2-2. Solubility of Several Heavy Metal Precipitates in Water

Precipitate	Solubility (mg/L)
$Pb(OH)_2$	0.031
$Cd(OH)_2$	1.4
$Zn(OH)_2$	0.13
$CdSiO_3$	6.83×10^{-3}
$ZnSiO_3$	9.25×10^{-4}
PbS	6.6×10^{-9}
CdS	10×10^{-9}
ZnS	2.1×10^{-7}

Thermodynamics calculation shows that the stability of heavy metal precipitates is in the order of metal sulfides > metal silicates > metal hydroxides. The study indicates that the presence of sulfide and an increase in silicate have positive effects on heavy metal immobilization. However, an experimental study will be needed to prove the proposed postulate.

2.3 References

[1] H. Castillo, H. Collado, T. Droguett, M. Vesely, P. Garrido, and S. Palma, "State of the art of geopolymers: A review," *E-Polymers*, vol. 22, no. 1, pp. 108–124, Jan. 2022, doi: 10.1515/epoly-2022-0015.

[2] J. Davidovits, "PROPERTIES OF GEOPOLYMER CEMENTS," in *Alkaline Cements and Concretes*, 1994, pp. 131–149. [Online]. Available: www.geopolymer.org

[3] J. Davidovits, "Geopolymers: Ceramic-like inorganic polymers," *Journal of Ceramic Science and Technology*, vol. 8, no. 3, pp. 335–350, 2017, doi: 10.4416/JCST2017-00038.

[4] K. Komnitsas and D. Zaharaki, "Geopolymerisation: A review and prospects for the minerals industry," *Miner Eng*, vol. 20, no. 14, pp. 1261–1277, Nov. 2007, doi: 10.1016/j.mineng.2007.07.011.

[5] J. G. S. Van Jaarsveld, J. S. J. Van Deventer, and L. Lorenzeni, "THE POTENTIAL USE OF GEOPOLYMERIC MATERIALS TO IMMOBILISE TOXIC METALS: PART I. THEORY AND APPLICATIONS," *Miner Eng*, vol. 10, no. 7, pp. 659–669, 1997.

[6] J. L. Provis and S. A. Bernal, “Geopolymers and related alkali-activated materials,” *Annu Rev Mater Res*, vol. 44, pp. 299–327, 2014, doi: 10.1146/annurev-matsci-070813-113515.

[7] B. Walkley, X. Ke, O. H. Hussein, S. A. Bernal, and J. L. Provis, “Incorporation of strontium and calcium in geopolymer gels,” *J Hazard Mater*, vol. 382, pp. 1–10, Jan. 2020, doi: 10.1016/j.jhazmat.2019.121015.

[8] J. Davidovits, “Solid-Phase Synthesis of a Mineral Blockpolymer by Low Temperature Polycondensation of Alumino-Silicate Polymers: Na-poly(sialate) or Na-PS and Characteristics,” in *IUPAC Symposium on Long-Term Properties of Polymers and Polymeric Materials*, 1976, pp. 1–14. [Online]. Available: https://www.researchgate.net/publication/329864876

[9] P. Duxson, J. L. Provis, G. C. Lukey, F. Separovic, and J. S. J. Van Deventer, “29Si NMR study of structural ordering in aluminosilicate geopolymer gels,” *Langmuir*, vol. 21, no. 7, pp. 3028–3036, Mar. 2005, doi: 10.1021/la047336x.

[10] M. Nodehi and V. M. Taghvaee, “Alkali-Activated Materials and Geopolymer: a Review of Common Precursors and Activators Addressing Circular Economy,” *Circular Economy and Sustainability*, vol. 2, no. 1, pp. 165–196, Mar. 2022, doi: 10.1007/s43615-021-00029-w.

[11] Z. Yahya, M. M. A. B. Abdullah, K. Hussin, K. N. Ismail, R. A. Razak, and A. V. Sandu, “Effect of solids-to-liquids, Na2SiO3-to-NaOH and curing temperature on the palm oil boiler ash (Si + Ca) geopolymerisation system,” *Materials*, vol. 8, no. 5, pp. 2227–2242, 2015, doi: 10.3390/ma8052227.

[12] V. Chanakya Varma, T. V Nagaraju, J. Raju, S. Subhan Alisha, and M. Chaitanya, “Understanding the potential role of precursor content in the geopolymer concrete strength development,” *Mater Today Proc*, May 2023, doi: 10.1016/j.matpr.2023.05.227.

[13] G. Furtos, D. Prodan, C. Sarosi, D. Popa, M. Moldovan, and K. Korniejenko, “The Precursors Used for Developing Geopolymer Composites for Circular Economy—A Review,” *Materials*, vol. 17, no. 7, pp. 1–17, Apr. 2024, doi: 10.3390/ma17071696.

[14] M. Sitarz, T. Zdeb, J. Castro Gomes, E. Grünhäuser Soares, and I. Hager, “The immobilisation of heavy metals from sewage sludge ash in geopolymer mortars,” *MATEC Web of Conferences*, vol. 322, pp. 1–8, 2020, doi: 10.1051/matecconf/202032201026.

[15] G. Huang, Y. Ji, L. Zhang, J. Li, and Z. Hou, “Advances in understanding and analyzing the anti-diffusion behavior in complete carbonation zone of MSWI bottom ash-based alkali-activated concrete,” *Constr Build Mater*, vol. 186, pp. 1072–1081, Oct. 2018, doi: 10.1016/j.conbuildmat.2018.08.038.

[16] M. E. Küçük, T. Kinnarinen, J. Timonen, O. Mulari, and A. Häkkinen, “Characterisation of industrial side streams and their application for the production of geopolymer composites,” *Minerals*, vol. 11, no. 6, pp. 1–17, Jun. 2021, doi: 10.3390/min11060593.

[17] M. R. El-Naggar and M. I. El-Dessouky, “Re-use of waste glass in improving properties of metakaolin-based geopolymers: Mechanical and microstructure examinations,” *Constr Build Mater*, vol. 132, pp. 543–555, Feb. 2017, doi: 10.1016/j.conbuildmat.2016.12.023.

[18] T. da S. Rocha, D. P. Dias, F. C. C. França, R. R. de S. Guerra, and L. R. da C. de O. Marques, “Metakaolin-based geopolymer mortars with different alkaline activators (Na+ and K+),” *Constr Build Mater*, vol. 178, pp. 453–461, Jul. 2018, doi: 10.1016/j.conbuildmat.2018.05.172.

[19] W. N’cho, A. Gharzouni, J. Jouin, A. Aimable, I. Sobrados, and S. Rossignol, “Effect of mixing metakaolins: methodological approach to estimate metakaolin reactivity,” *Ceram Int*, vol. 49, no. 12, pp. 1–21, 2023, doi: 10.1016/j.ceramint.2023.03.157ï.

[20] G. M. H. W. M. Burnett, “Structure of Kaolinite,” *Nature*, vol. 156, pp. 661–662, 1945.

[21] N. Janosevic, S. Djoric-Veljkovic, G. Toplicic-Curcic, and J. Karamarkovic, “Properties of geopolymers,” *Facta universitatis - series: Architecture and Civil Engineering*, vol. 16, no. 1, pp. 45–56, 2018, doi: 10.2298/fuace161226004j.

[22] N. Ranjbar, C. Kuenzel, J. Spangenberg, and M. Mehrali, “Hardening evolution of geopolymers from setting to equilibrium: A review,” *Cem Concr Compos*, vol. 114, pp. 1–19, Nov. 2020, doi: 10.1016/j.cemconcomp.2020.103729.

[23] Z. Moujoud, S. Sair, H. Ait Ousaleh, I. Ayouch, A. El Bouari, and O. Tanane, “Geopolymer composites reinforced with natural Fibers: A review of recent advances in processing and properties,” *Constr Build Mater*, vol. 388, pp. 1–22, Jul. 2023, doi: 10.1016/j.conbuildmat.2023.131666.

[24] D. Khale and R. Chaudhary, “Mechanism of geopolymerization and factors influencing its development: A review,” *J Mater Sci*, vol. 42, no. 3, pp. 729–746, Feb. 2007, doi: 10.1007/s10853-006-0401-4.

[25] A. C. Constâncio Trindade, I. Curosu, M. Liebscher, V. Mechtcherine, and F. de Andrade Silva, “On the mechanical performance of K- and Na-based strain-hardening geopolymer composites (SHGC) reinforced with PVA fibers,” *Constr Build Mater*, vol. 248, pp. 1–16, Jul. 2020, doi: 10.1016/j.conbuildmat.2020.118558.

[26] M. Uehara, “New Concrete with Low Environmental Load Using the Geopolymer Method,” *QR of RTRI*, vol. 51, no. 1, pp. 1–7, 2010.

[27] B. Liu *et al.*, “Insights into the microstructure of hydrothermal synthesized nanoscale k2o-al2o3-sio2-h2o particles,” *Nanomaterials*, vol. 10, no. 63, pp. 1–18, Jan. 2020, doi: 10.3390/nano10010063.

[28] M. Lizcano, H. S. Kim, S. Basu, and M. Radovic, “Mechanical properties of sodium and potassium activated metakaolin-based geopolymers,” *J Mater Sci*, vol. 47, no. 6, pp. 2607–2616, Mar. 2012, doi: 10.1007/s10853-011-6085-4.

[29] A. Hosan, S. Haque, and F. Shaikh, “Compressive behaviour of sodium and potassium activators synthetized fly ash geopolymer at elevated temperatures: A comparative study,” *Journal of Building Engineering*, vol. 8, pp. 123–130, Dec. 2016, doi: 10.1016/j.jobe.2016.10.005.

[30] G. Qian, D. D. Sun, and J. H. Tay, “Immobilization of mercury and zinc in an alkali-activated slag matrix,” *J Hazard Mater*, vol. 101, no. 1, pp. 65–77, Jul. 2003, doi: 10.1016/S0304-3894(03)00143-2.

[31] Z. Ji and Y. Pei, “Geopolymers produced from drinking water treatment residue and bottom ash for the immobilization of heavy metals,” *Chemosphere*, vol. 225, pp. 579–587, Jun. 2019, doi: 10.1016/j.chemosphere.2019.03.056.

[32] Q. Wan, F. Rao, S. Song, and Y. Zhang, “Immobilization forms of ZnO in the solidification/stabilization (S/S) of a zinc mine tailing through geopolymerization,” *Journal of Materials Research and Technology*, vol. 8, no. 6, pp. 5728–5735, Nov. 2019, doi: 10.1016/j.jmrt.2019.09.040.

[33] B. I. El-Eswed, O. M. Aldagag, and F. I. Khalili, “Efficiency and mechanism of stabilization/solidification of Pb(II), Cd(II), Cu(II), Th(IV) and U(VI) in metakaolin based geopolymers,” *Appl Clay Sci*, vol. 140, pp. 148–156, May 2017, doi: 10.1016/j.clay.2017.02.003.

[34] E. Gomaa, S. Sargon, C. Kashosi, A. Gheni, and M. A. ElGawady, “Mechanical Properties of High Early Strength Class C Fly Ash-Based Alkali Activated Concrete,” *Transp Res Rec*, vol. 2674, no. 5, pp. 430–443, May 2020, doi: 10.1177/0361198120915892.

[35] S. Donatello, A. Fernández-Jiménez, and A. Palomo, “An assessment of Mercury immobilisation in alkali activated fly ash (AAFA) cements,” *J Hazard Mater*, vol. 213–214, pp. 207–215, Apr. 2012, doi: 10.1016/j.jhazmat.2012.01.081.

[36] Z. Ji and Y. Pei, “Immobilization efficiency and mechanism of metal cations (Cd2+, Pb2+ and Zn2+) and anions (AsO43- and Cr2O72-) in wastes-based geopolymer,” *J Hazard Mater*, vol. 384, pp. 1–11, Feb. 2020, doi: 10.1016/j.jhazmat.2019.121290.

[37] Z. Ji, L. Su, and Y. Pei, “Synthesis and toxic metals (Cd, Pb, and Zn) immobilization properties of drinking water treatment residuals and metakaolin-

based geopolymers," *Mater Chem Phys*, vol. 242, pp. 1–9, Feb. 2020, doi: 10.1016/j.matchemphys.2019.122535.

[38] J. Zhang, J. L. Provis, D. Feng, and J. S. J. van Deventer, "Geopolymers for immobilization of Cr6+, Cd2+, and Pb2+," *J Hazard Mater*, vol. 157, no. 2–3, pp. 587–598, Sep. 2008, doi: 10.1016/j.jhazmat.2008.01.053.

[39] B. I. El-Eswed, "Chemical evaluation of immobilization of wastes containing Pb, Cd, Cu and Zn in alkali-activated materials: A critical review," *J Environ Chem Eng*, vol. 8, no. 5, pp. 1–9, Oct. 2020, doi: 10.1016/j.jece.2020.104194.

[40] Y. Wang, F. Han, and J. Mu, "Solidification/stabilization mechanism of Pb(II), Cd(II), Mn(II) and Cr(III) in fly ash based geopolymers," *Constr Build Mater*, vol. 160, pp. 818–827, Jan. 2018, doi: 10.1016/j.conbuildmat.2017.12.006.

[41] Q. Wan, F. Rao, S. Song, and Y. Zhang, "Immobilization forms of ZnO in the solidification/stabilization (S/S) of a zinc mine tailing through geopolymerization," *Journal of Materials Research and Technology*, vol. 8, no. 6, pp. 5728–5735, Nov. 2019, doi: 10.1016/j.jmrt.2019.09.040.

CHAPTER 3. EFFECT OF MIXING PROCEDURES AND CONCENTRATIONS ON THE IMMOBILIZATION OF HEAVY METALS IN K-GEOPOLYMER

3.1 Introduction

Cadmium and mercury are heavy metals with high levels of toxicity [1]. Exposure to cadmium can damage the skeleton, kidneys, liver, and respiratory and cardiovascular systems. Mercury causes adverse health effects on the kidneys, liver, lungs, and reproductive and nervous systems [2]. These elements are contained in various industrial wastes, such as fly ash and wastewater [3], [4], [5]. Iron adsorbent sludge from wastewater treatment and fly ash are usually disposed of in landfills [6]. As such, the leaching of heavy metals from fly ash is possible, because some metals occur as soluble chloride or sulfate salts [7], [8]. The adsorbed heavy metals can also undergo desorption [9]. These solid wastes require safe solidification/stabilization techniques to prevent secondary waste contamination.

Geopolymers are one option for the solidification/stabilization of solid wastes, as they possess excellent properties, including acid and thermal resistance, low permeability, and low CO_2 emissions as compared to Portland cement [10]. Geopolymer is an alkali-activated material with little or no calcium that has a three-dimensional framework developed by the dissolution, polycondensation, and hardening of an aluminosilicate precursor in an alkali activator [10], [11], [12]. This material has a negative charge from the alumina tetrahedra structure balanced by Na^+ or K^+ from the activator [13]. A Na-geopolymer is structurally similar to zeolite and can transform into this secondary stable phase even at low temperatures [14]. Compared to Na-geopolymer, K-geopolymer remains amorphous and is denser and stronger [14], [15], [16].

Previous studies have investigated the ability of Na-geopolymer to immobilize heavy metals, but none has investigated K-geopolymer. Although further study of heavy metal retention during the transformation of Na-geopolymer to zeolite is required, Na-geopolymer has an excellent ability to retain metal cations [17]. The cations are thought to be retained by: (1) ion exchange; (2) covalent bonding to the aluminosilicate network; (3) precipitation as hydroxides, silicates, or carbonates; and (4) physical encapsulation by the low-permeability geopolymer [18]. Covalent bonding is thought to be the most favorable for stabilizing the heavy metals. K-geopolymer may retain such bonding on longer timescales due to its stability.

Previous studies have proposed different immobilization mechanisms for cadmium and mercury, presented in Table 3-1. These differences are possibly due to variations in the aluminosilicate precursors and heavy metal concentrations in each study. The presence of calcium in the precursor leads to the formation of a complex C–(A)–S–H system that participates in metal immobilization [19], [20]. Heavy metal speciation is also controlled by the metals' activity in the system, which is correlated with their concentration. In addition to these factors, the mixing procedure might also influence the results. Zhang et al. [21] mixed precursors with cadmium nitrate and added the Na-activator later. This process made the cadmium form a hydroxide precipitate. Distinctly, El-Eswed et al. [22] mixed cadmium nitrate with water before adding the precursors. The addition of the Na-activator then followed this step. This procedure incorporated cadmium into the alkali-activated material through an exchange with other cations. The mixing variance is also found in the effort to immobilize mercury. Donatello et al. [20] mixed mercury (II) chloride with a precursor before adding the alkali activator. In contrast,

Qian et al. [23] first added mercury (II) nitrate to the alkali activator. While both procedures led to similar immobilization mechanisms for mercury oxide and mercury silicate, other mechanisms also occurred, such as incorporation into C–S–H, absorption onto N–A–S–H, and HgS precipitation. These results highlight the influence of the aluminosilicate precursor composition.

Table 3-1. Previous studies on the immobilization of heavy metals by Na-geopolymer

Researcher	Metal	Aluminosilicate Precursor	Metal Concentration (wt.%)	Mechanisms
Zhang *et al.* [21]	Cd	Fly ash + sand	0.5	$Cd(OH)_2$ precipitate
El-Eswed *et al.* [22]	Cd	Zeolite + kaolinite	0.001 and 0.006	Cation exchange
Ji and Pei [24]	Cd	Bottom ash + drinking water treatment residue	1, 2, and 4	Covalent bonding
Qian *et al.* [23]	Hg	Blast furnace slag	0.5 and 2	Hg-silicate precipitate; C-S-H lattice incorporation; Physical encapsulation of HgO
Donatello *et al.* [20]	Hg	Fly ash	0.5 and 5	HgS; HgO/Hg-silicate; Hg absorbed onto N-A-S-H

Predicting the long-term stability of heavy metals in a geopolymer is challenging because the immobilization forms are not entirely conclusive. As such, the effects of heavy metal concentrations and the mixing processes need to be investigated. This was difficult in previous studies due to the use of various aluminosilicate precursors for geopolymer production. In this study, a metakaolin-based geopolymer was used as the standard geopolymer. Metakaolin, consisting mainly of silica and alumina, produces a model geopolymer system that is easy to characterize [16]. K-geopolymer is used rather than a Na-geopolymer to fill the research gap.

3.2 Materials and Methods

3.2.1 Materials

Metakaolin from Sobueclay Co., Ltd. (Japan) was used as the aluminosilicate precursor for the geopolymer. The metakaolin has a chemical composition of mainly SiO_2 and Al_2O_3, with minimal CaO as presented in Table 3-2. The alkali activator used in the manufacturing process was a mixture of potassium silicate solution, potassium hydroxide, and ultrapure water. The molar ratio of SiO_2:K_2O:H_2O was kept constant at 1:1:13 to ensure the highest workability of the geopolymer [11]. Potassium silicate solution was obtained from Fujifilm Wako Pure Chemical Corporation, Japan, with K_2O and SiO_2

contents of 21.90 and 29.00 wt.%, respectively. The potassium hydroxide was obtained from Kanto Chemical Co., Inc., Japan, and had a purity of 86.0 wt.%. Cadmium chloride 2.5-hydrate with a purity of 98.0% (Kanto Chemical Co., Inc., Japan) and mercury (II) chloride with a purity of 99.5 wt.% (Fujifilm Wako Pure Chemical Corporation, Japan) were used as artificial pollutants.

Table 3-2. Chemical composition of the Sobueclay metakaolin.

Component	Percentage (wt.%)
SiO_2	51.25
Al_2O_3	45.82
TiO_2	1.19
Fe_2O_3	0.58
Na_2O	0.06
K_2O	0.15
CaO	0.23
MgO	0.02
P_2O_5	0.13

3.2.2 Methods

3.2.2.1 Sample Preparation

A geopolymer control was made by mixing 1.3 g of metakaolin with an alkali activator containing 1.2 g of potassium silicate and 0.4 g of potassium hydroxide. The amount of this alkali activator was adjusted to the Al_2O_3 content in the metakaolin to obtain an Al_2O_3:K_2O molar ratio of 1. The mixture was stirred for 15 min, poured into PVC molds (1.3 cm diameter × 1.5 cm height), and covered with parafilm on both sides. The samples were cured for 24 h at 40°C and another 24 h at 25°C before demolding. The upper and bottom parts of the hardened samples were then separated for solid analysis.

Cadmium and mercury geopolymers were produced using three different mixing procedures, namely Salt, Ion, and Salt-AA.

i. Salt: The heavy metal was solid mixed with metakaolin in its original salt form. The mixture was then blended with the alkali activator before molding.

ii. Ion: The heavy metal–geopolymer was prepared in a similar way to Salt mixing procedure, but the heavy metal salt was first dissolved in ultrapure water. The solution was then poured onto metakaolin and later added to a mixture of potassium hydroxide and potassium silicate.

iii. Salt-AA: The heavy metal–geopolymer was produced in reverse order to the Salt mixing procedure, as the salt was first mixed with the alkali activator before being combined with metakaolin.

The above procedures were followed by the same method to make geopolymer control. The experiments were carried out at a heavy metal concentration of 0.5 wt.%. Further experiments using the Ion mixing procedure were then conducted at other concentrations ranging from 0.02 to 1.00 wt.%. Figure 3-1 shows the initial concentrations and pH values in the experiments, as well as the predicted forms of cadmium and mercury.

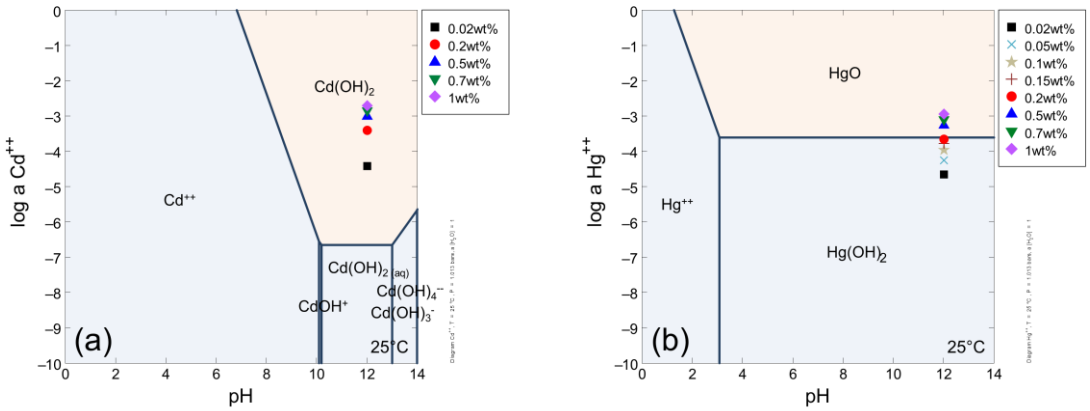

Figure 3-1. Solubility diagrams of (a) cadmium and (b) mercury calculated with the Visual MINTEQ database, along with the initial concentrations and pH values of the experiments

3.2.2.2 Leaching Test

A leaching test was performed using the ANSI/ANS-16.1-2003 standard. Geopolymer samples weighing 3.4 g each were submerged in 88 mL of deionized water and then moved into a new batch of deionized water after 30 s, 2 h, 7 h, and 1, 2, 3, 4, 5, 19, 47, and 90 d. The temperature during leaching was kept constant at 25°C.

3.2.2.3 Liquid Sample Analysis

The pH values of the leachates were measured with a W-22XD pH meter (Horiba, Japan). Heavy metal concentrations in the leachates were analyzed using an iCAP RQplus inductively coupled plasma mass spectrometry (ICP-MS; Thermo Scientific, USA). The custom assurance standard XSTC-331 (SPEX CertiPrep; Seishin Trading Company, Japan) and a mercury standard solution (Hg 1000; Fujifilm Wako Pure Chemical Corporation, Japan) were used to make a calibration standard containing 0.01–10 ppb cadmium and mercury. Indium and bismuth were used as internal standards.

3.2.2.4 Solid Sample Analysis

The geopolymer control, cadmium geopolymer, and mercury geopolymer samples were analyzed by X-ray diffraction (RINT2100; Rigaku; Japan) to determine their crystallography. The CuKα radiation source was operated at 30 kV and 20 mA. The scanning was conducted at 0.02°/s at 2θ = 2°–70°. Samples were also examined with an XploRA PLUS Raman microscope (Horiba, Japan). The spectra were collected using a 532 nm excitation wavelength with a 50× objective lens, 100 µm entrance slit, and 1800 groove/mm grating.

3.3 Results and Discussion

3.3.1 Effect of Mixing Procedure

3.3.1.1 Effect of Mixing Procedure on Cadmium Immobilization

All the mixing procedures yielded high immobilization efficiencies with <0.012% of the cadmium leached at the end of the leaching test. Although all procedures resulted in very low levels of leaching, differences in leaching behavior were observed (Figure 3-2a). The Salt and Salt-AA mixing procedures yielded similar results, in which the amount of leached cadmium increased after 90 d of leaching. In comparison, the Ion mixing

procedure resulted in more constant cadmium leaching from day 19 onwards. These differences occurred even when the leachate pH values were similar and decreased over time from 12 to ~8.5 (Figure 3-2b). The results indicate that the Salt and Salt-AA procedures produce strongly pH-dependent cadmium species, whereas the Ion mixing procedure does not.

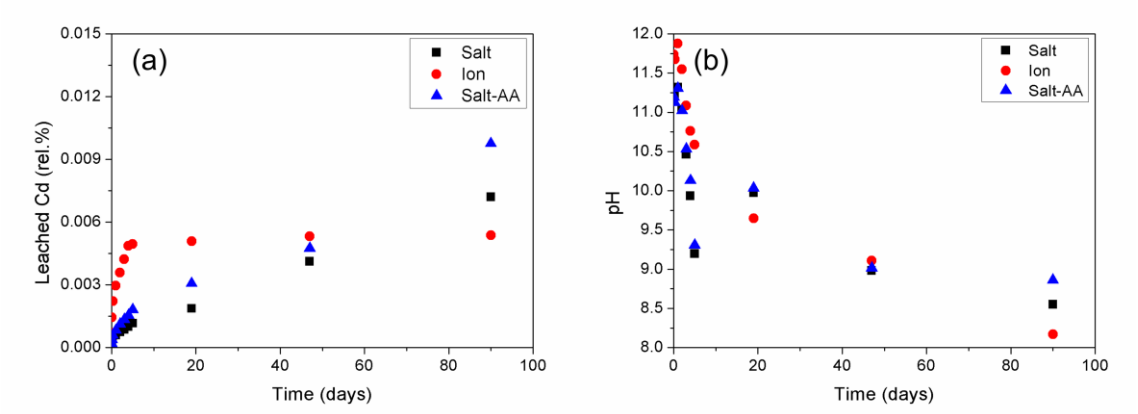

Figure 3-2. (a) Cumulative amount of leaching relative to the initial amount of cadmium and (b) leachate pH values of the cadmium geopolymers after various mixing procedures

The X-ray diffraction patterns (Figure 3-3) are consistent with the leaching data because the Salt and Salt-AA samples are similar to each other and different from the Ion samples. All samples exhibit a broad hump in the patterns centered at ~28°. This hump is due to amorphous silica and is a characteristic of the geopolymer peak [25]. In addition, the samples made by the Salt and Salt-AA mixing procedures exhibit sharp peaks at 18.9°, 29.5°, 35.3°, 49.0°, 52.3°, and 56.1° due to the presence of Cd(OH)2 (Figure 3-3a and 3-3c). Both procedures resulted in the formation of $Cd(OH)_2$, which later settles into the bottom part of the geopolymer due to its high density. Unlike Salt and Salt-AA, the Ion mixing procedure does not lead to $Cd(OH)_2$ formation.

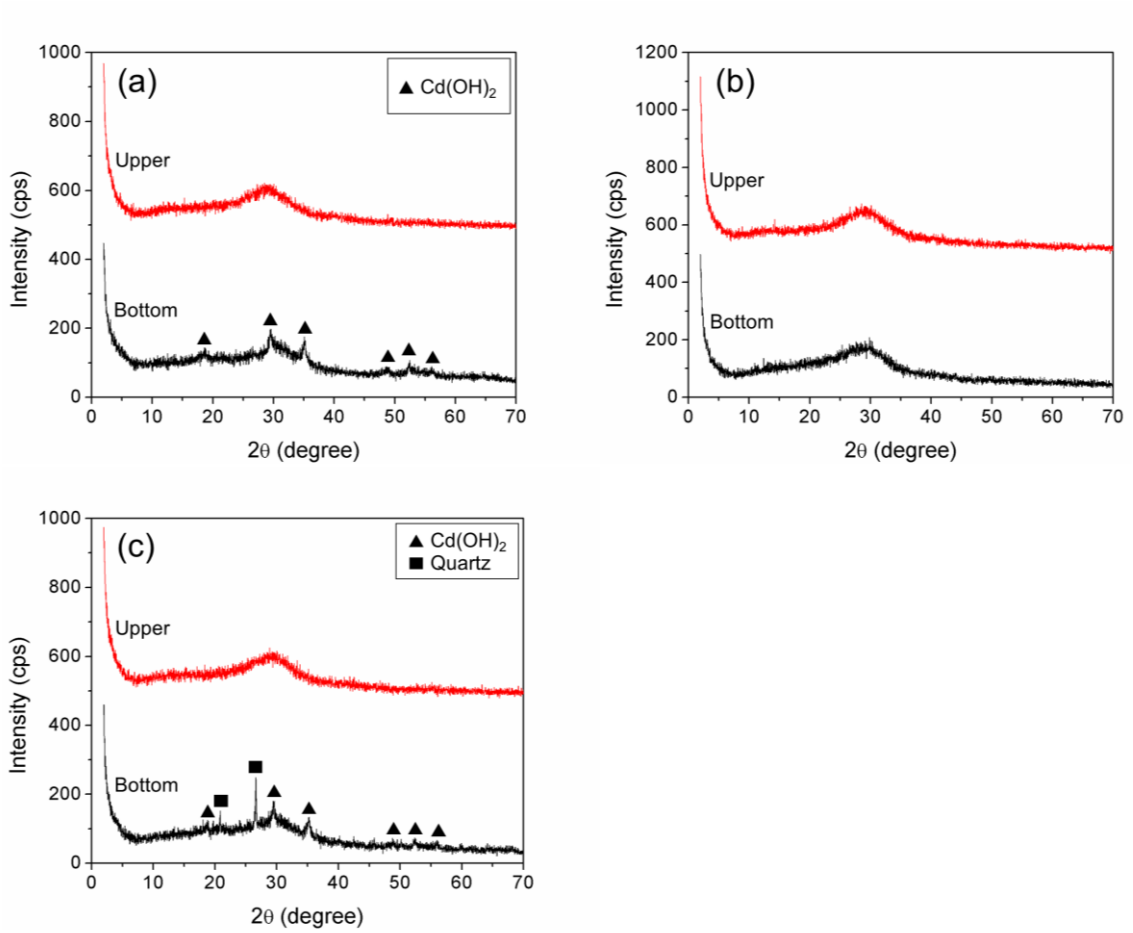

Figure 3-3. X-ray diffraction patterns of the upper and bottom parts of the cadmium geopolymer made by the (a) Salt, (b) Ion, and (c) Salt-AA mixing procedures

Raman spectroscopy was used to detect changes in covalent bonds due to cadmium incorporation. The control sample exhibits prominent peaks at 396, 502, 570, and 637 cm^{-1}, which correspond to the Si–O–Al bending mode, Si–O–Si stretching vibration from long chains (C5,6,7) and short chains, and T–O symmetric stretching mode [26], [27], [28], [29]. The 851 and 1056 cm^{-1} peaks are due to Si–O symmetric stretching [28]. The upper parts of the Salt, Ion, and Salt-AA samples have similar spectra to the geopolymer control sample, suggesting that no differences in covalent bonds can be observed by Raman spectroscopy (Figure 3-4b). The bottom parts of the Ion samples also have identical spectra (Figure 3-4a). However, a new peak at 231 cm^{-1} characterizes the Salt and Salt-AA samples. The original geopolymer peak at 396 cm^{-1}, corresponding to the Si–O–Al bending mode for these samples, is also accompanied by a high-intensity peak at 382 cm^{-1}. Both sharp peaks correspond to the vibrational modes of the $Cd(OH)_2$ lattice [30]. Similar to the XRD results, $Cd(OH)_2$ was only observed at the bottom parts of samples made by the Salt and Salt-AA mixing procedures. Hydroxide formation can explain the increasing leaching of these samples. After 90 d of leaching, the leachate pH is as low as 8.5, which triggers the dissolution of $Cd(OH)_2$ into its ionic constituents (Figure 3-1a).

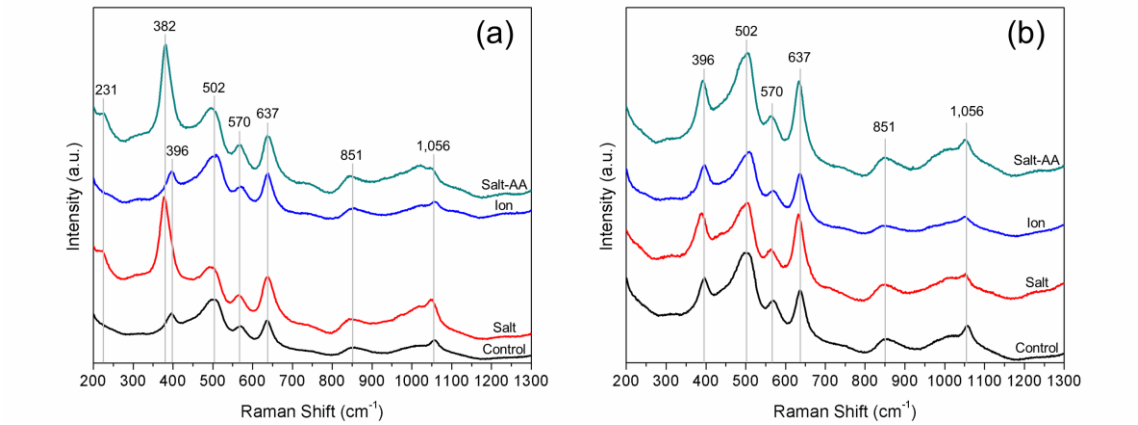

Figure 3-4. Raman spectra of the (a) bottom and (b) upper parts of the cadmium geopolymers after various mixing procedures

3.3.1.2 Effect of Mixing Procedure on Mercury Immobilization

Unlike cadmium, all the mixing procedures led to high mercury leaching of >70% (maximum of 95.6%), suggesting mercury was poorly retained in the geopolymer. The leaching was similar for all mixing procedures. Figure 3-5a shows the increasing amount of mercury leached until the last day of the experiments, and Figure 3-5b shows the pH data. No significant difference is evident between the three samples as the pH decreases from ~12 to 8.5 with time. The similar trends indicate mercury speciation was identical in the three samples.

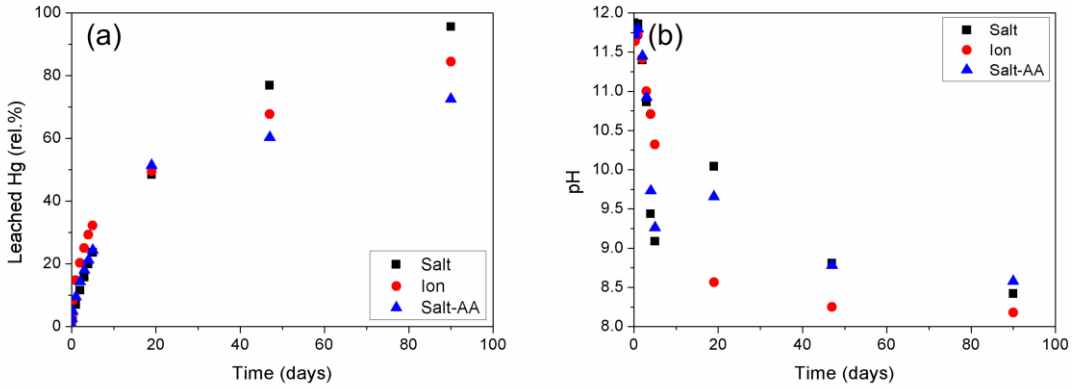

Figure 3-5. (a) Cumulative amount of leaching relative to the initial amount of mercury and (b) leachate pH values of the mercury geopolymers after various mixing procedures

The X-ray diffraction patterns for the bottom parts of the mercury geopolymers made by the Salt and Salt-AA mixing procedures (Figure 3-6) show that, apart from the amorphous silica peak, there are peaks at 30.1°, 31.5°°, 37.3°, 50.3°, 56.4°, and 62.0°, which correspond to mercury oxide. Like cadmium, this metal oxide forms during manufacturing and settles due to its high density. The Ion mixing procedure did not result in different XRD patterns between the bottom and upper parts of the geopolymers.

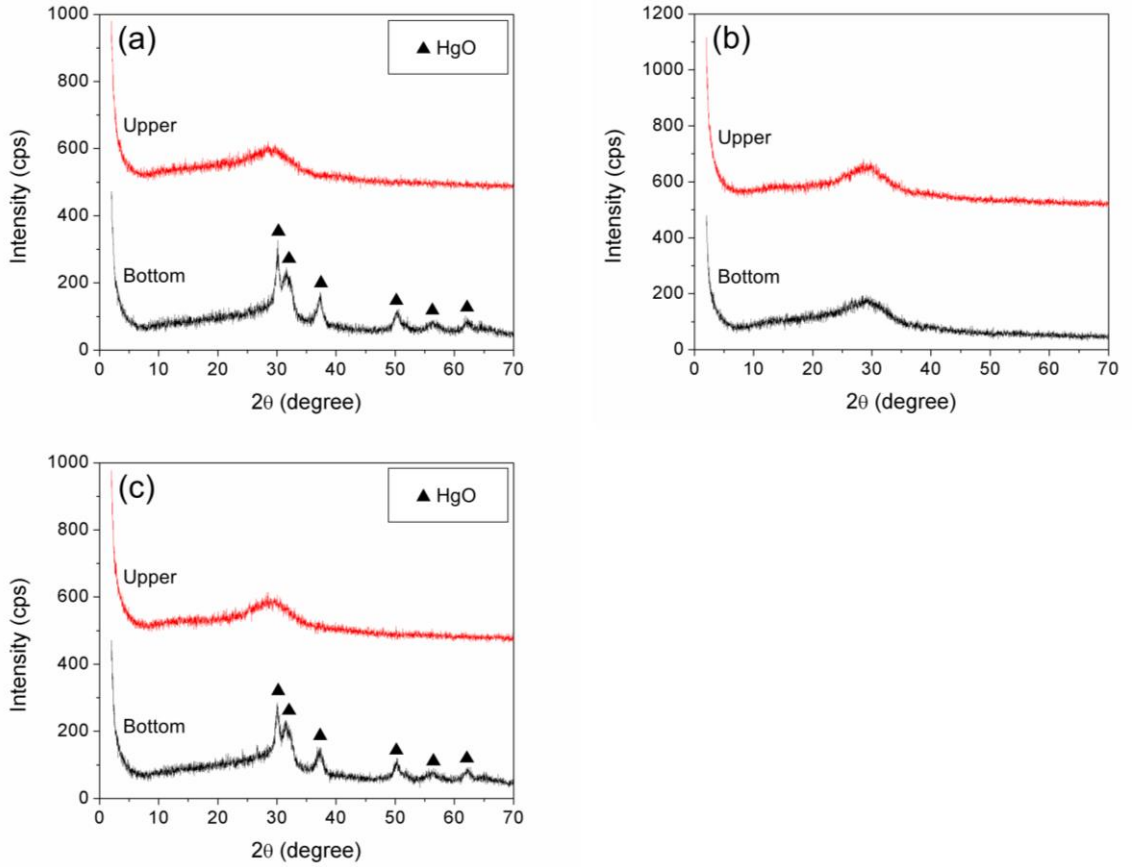

Figure 3-6. X-ray diffraction patterns of mercury geopolymers made by the (a) Salt, (b) Ion, and (c) Salt-AA mixing procedures

Other results that compare the two parts of the mercury geopolymer are shown in Figure 3-7. The analyzed samples exhibit all the peaks shown by the geopolymer control sample, including the Si–O–Al bending mode at 396 cm^{-1}, υs (Si–O–Si) at 502 and 570 cm^{-1}, T–O symmetric stretching mode at 637 cm^{-1}, and υs (Si–O-) at around 851 and 1056 cm^{-1} [26], [27], [28], [29]. In addition, a new peak at 320 cm^{-1} due to Hg–O stretching characterizes the bottom parts of samples (Figure 3-7a) [31]. This peak is evident for the Salt and Salt-AA samples, confirming the formation of mercury oxide, as is evident from the X-ray diffraction patterns. Although not detected by X-ray diffraction, the Hg–O covalent bonding in the samples made by the Ion mixing procedure is apparent from the Raman spectroscopy. This result is consistent with the mercury solubility diagram (Figure 3-1b). Moreover, this mercury species is found in the bottom and upper parts of the mercury geopolymer, which is not the case for the Salt and Salt-AA samples.

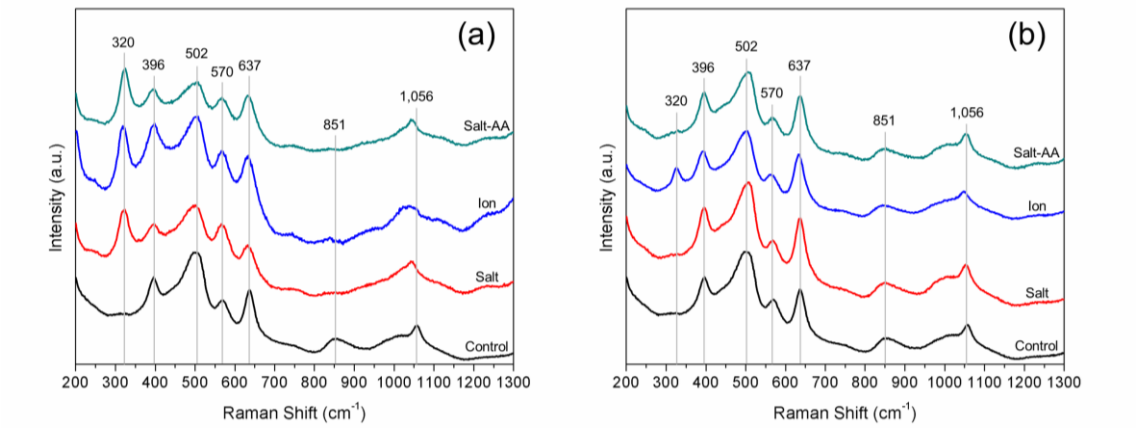

Figure 3-7. Raman spectra of the (a) bottom and (b) upper parts of the mercury geopolymers after various mixing procedures

In general, the Salt and Salt-AA procedures yielded similar results. Mixing the heavy metal salts with the precursor or the alkali activator first produces geopolymers with residing heavy metals. This highlights the insignificant effects of the mixing sequence in determining the heavy metal immobilization. Rather, heavy metals being in salt form at the initial stage for both cases is essential in defining their similarity. Under highly alkaline conditions, OH^- from the activator acts as a precipitant, which removes chloride to make metal hydroxide or oxide. In contrast, the Ion mixing procedure produces a more homogeneous geopolymer. It is beneficial to introduce dissolved heavy metals before geopolymerization to ensure they can move more freely and be more evenly distributed. Although the Ion sample for mercury produced the same species as the Salt and Salt-AA mixing procedures, this was not the case for cadmium.

3.3.2 Effect of the Initial Heavy Metal Concentration

3.3.2.1 Effect of the Initial Heavy Metal Concentration on Cadmium Immobilization

Different concentrations of cadmium geopolymers leach a minimal amount of Cd into water (Figure 3-8a). Up to the last day of the tests, <0.025% of the cadmium was leached, and this value was constant from day 19. This was the case even when the leachate pH decreased to 8.5 (Figure 3-8b). During the leaching tests, the geopolymers absorbed water and released OH^-. Geopolymers with initially high alkalinity lost a large amount of OH^- during the earlier leaching stage and gradually became less alkaline. The identical leaching behavior in all tests indicates the cadmium may have been immobilized in the same form in all concentrations.

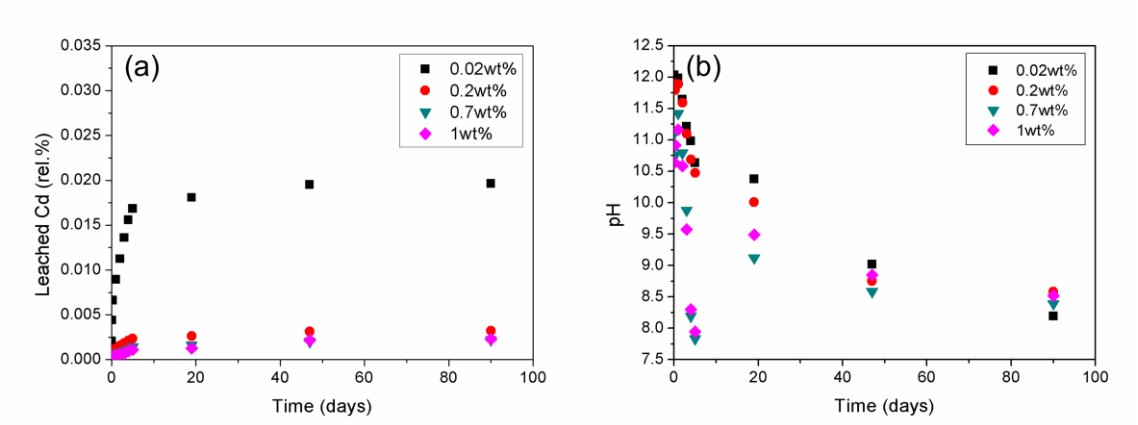

Figure 3-8. (a) Cumulative amount of leaching relative to the initial amount of cadmium and (b) leachate pH values of the cadmium geopolymers produced at various initial concentrations

The cadmium solubility diagram in Figure 3-1a shows that the expected cadmium form in the geopolymer is $Cd(OH)_2$ for all given concentrations. However, the solid sample analyses suggest there was no hydroxide formation, even at cadmium concentrations as high as 1 wt.%. The X-ray diffraction spectra in Figure 3-9a show that the cadmium geopolymers consist mainly of amorphous silica. In addition, the Raman spectra in Figure 3-9b show that the cadmium geopolymers have the same bands as the geopolymer control sample.

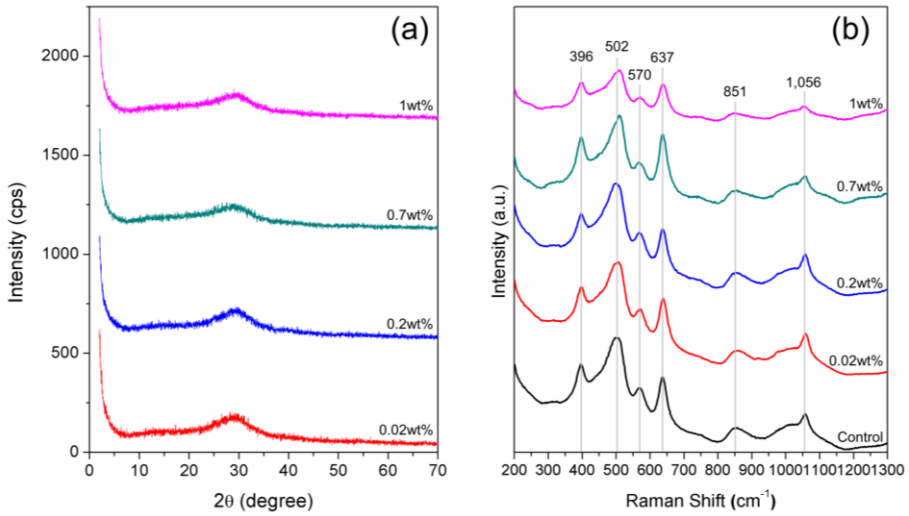

Figure 3-9. (a) X-ray diffraction patterns and (b) Raman spectra of the geopolymers at various cadmium concentrations

3.3.2.2 Effect of the Initial Heavy Metal Concentration on Mercury Immobilization

Figure 3-1b shows that the main mercury species varies according to its concentration in a system. For concentrations of >0.2 wt.%, mercury is expected to occur mainly as HgO, while at lower concentrations, mercury is in the soluble $Hg(OH)_2$ form. Extra samples with 0.05, 0.10, and 0.15 wt.% of Hg were prepared to investigate how these two different phases affect the immobilization. The leaching results are shown in Figure 3-10. Over a similar pH range, Hg tends to have an increasing leaching pattern.

High mercury concentrations result in high leaching values, showing that Hg is weakly immobilized. Meanwhile, mercury concentrations of 0.02 and 0.05 wt.% exhibit lower leaching. The leaching pattern also tends to be constant, especially for 0.02 wt.%. The results show that Hg is more immobilized when in low concentrations and suggest different immobilization mechanisms.

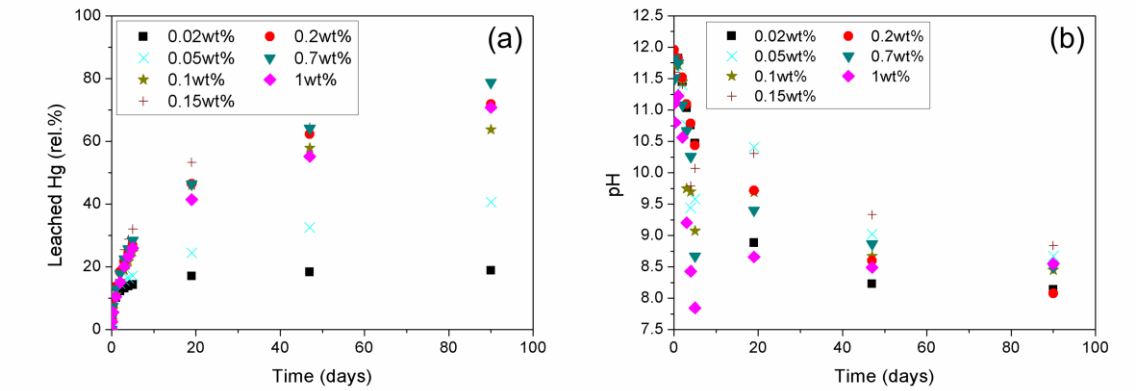

Figure 3-10. (a) Cumulative amount of leaching relative to the initial amount of mercury and (b) leachate pH values of the mercury geopolymer with variable initial concentrations

X-ray diffraction analysis identified the mercury speciation in the 0.7 and 1 wt.% mercury geopolymer as HgO (Figure 3-11a). This is also consistent with the Raman spectroscopic data (Figure 3-11b). In addition to the high-concentration samples, the HgO band at 320 cm^{-1} is evident for the lower-concentration samples. Raman spectroscopy detects HgO in samples with mercury concentrations as low as 0.1 wt.%. The band intensity increases with increasing concentration.

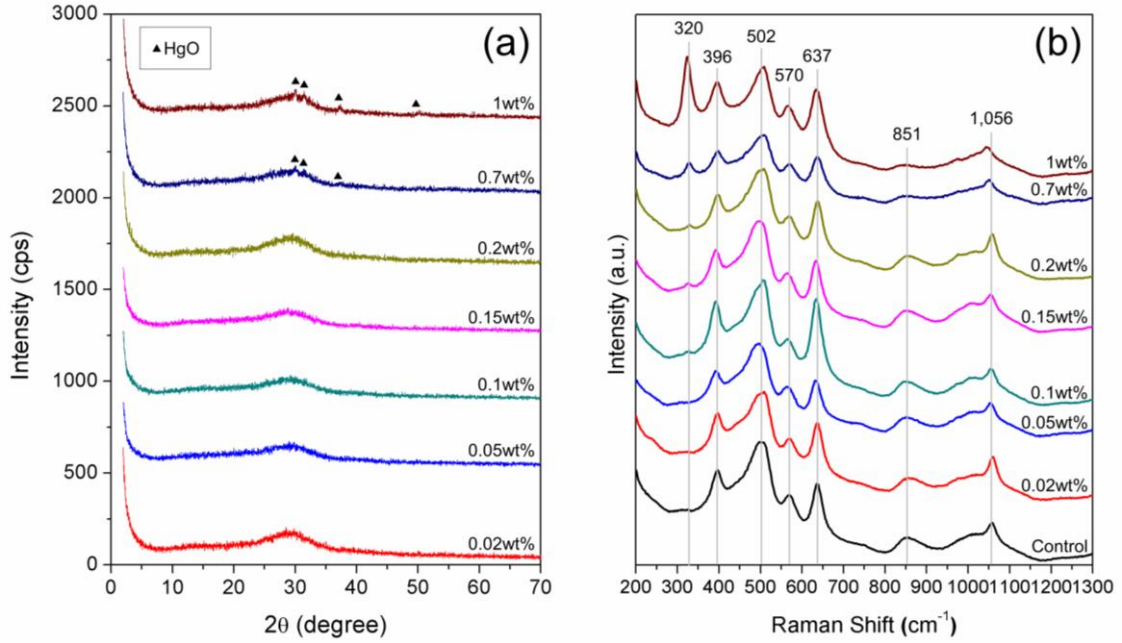

Figure 3-11. (a) X-ray diffraction patterns and (b) Raman spectra of the geopolymers at various mercury concentrations

Although Hg still requires more work, geopolymer is an excellent candidate to retain Cd. Its immobilization form can be controlled by the incorporation method. This study has identified a procedure to process Cd-containing waste that results in the most favorable immobilization form. Providing Cd in its ion form is ideal for geopolymerization. When processing actual waste, mixing fly ash or iron sludge with water first is recommended to dissolve the soluble or desorbed Cd. Subsequently, blending the waste with metakaolin is necessary to adjust the aluminosilicate content. The next step is the addition of an alkali activator. For waste containing calcium, such as fly ash, the formation of C–(A)–S–H may need to be eliminated, as this matrix immobilizes cadmium as $Cd(OH)_2$ [32], [33]. Therefore, an extra step could be included, involving the addition of carbonate ions to promote $CaCO_3$ formation instead of C–(A)–S–H. A schematic diagram of the proposed treatment is shown in Figure 3-12.

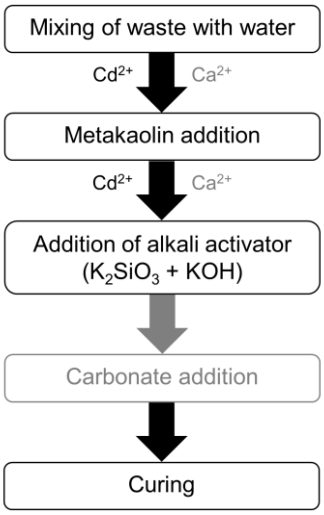

Figure 3-12. Schematic diagram of the proposed treatment for cadmium-containing waste

3.4 Conclusion

This study has investigated the effects of initial heavy metal speciation and concentration on its final speciation form in a geopolymer. The initial speciation (i.e., salt or ion) leads to different immobilization forms and/or geopolymer characteristics. The species can be controlled by mixing procedures. Introducing Cd and Hg to the geopolymer system in a salt form produces metal hydroxide and oxide, respectively. Cadmium hydroxide is unstable at low pH, whereas HgO is hydrolyzed at any pH. Dissolving the heavy metal salts in water makes the resultant geopolymers more homogeneous. This procedure, applied to heavy metal concentrations of 0.02–1.00 wt.%, yielded the same Cd species and geopolymer characteristics, highlighting its applicability to processing and managing waste of various concentrations. Differently, high mercury concentrations form HgO. This formation results in high Hg leaching, while very low mercury concentrations can be better immobilized. Different leaching behaviors, depending on the stabilized form of cadmium, demonstrate the importance of choosing

the appropriate mixing procedure to process contaminated waste and for its long-term stability.

3.5 References

[1] U.S. Environmental Protection Agency, "WATER-RELATED ENVIRONMENTAL FATE OF 129 PRIORITY POLLUTANTS Volume I: Introduction and Technical Background, Metals and Inorganics, Pesticides and PCBs," Washington, D.C., 1979.

[2] U.S. Environmental Protection Agency, "Mercury Study Report to Congress Volume V: Health Effects of Mercury and Mercury Compounds," Dec. 1997.

[3] G. C. Kisku, S. Yadav, R. K. Sharma, and M. P. S. Negi, "Potential environmental pollution hazards by coal based power plant at Jhansi (UP) India," *Environ Earth Sci*, vol. 67, no. 7, pp. 2109–2120, Dec. 2012, doi: 10.1007/s12665-012-1651-x.

[4] W. Zucha, G. Weibel, M. Wolffers, and U. Eggenberger, "Inventory of MSWI fly ash in Switzerland: Heavy metal recovery potential and their properties for acid leaching," *Processes*, vol. 8, no. 12, pp. 1–13, Dec. 2020, doi: 10.3390/pr8121668.

[5] G. K. Kinuthia, V. Ngure, D. Beti, R. Lugalia, A. Wangila, and L. Kamau, "Levels of heavy metals in wastewater and soil samples from open drainage channels in Nairobi, Kenya: community health implication," *Sci Rep*, vol. 10, no. 8434, pp. 1–13, Dec. 2020, doi: 10.1038/s41598-020-65359-5.

[6] X. Zhao, J. Yang, N. Ning, and Z. Yang, "Chemical stabilization of heavy metals in municipal solid waste incineration fly ash: a review," *Environmental Science and Pollution Research*, vol. 29, no. 27, pp. 40384–40402, Jun. 2022, doi: 10.1007/s11356-022-19649-2.

[7] W. Chen, Y. Wang, Y. Sun, G. Fang, and Y. Li, "Release of soluble ions and heavy metal during fly ash washing by deionized water and sodium carbonate solution," *Chemosphere*, vol. 307, pp. 1–8, Nov. 2022, doi: 10.1016/j.chemosphere.2022.135860.

[8] A. V. Dahlan, H. Kitamura, H. Sakanakura, T. Shimaoka, T. Yamamoto, and F. Takahashi, "Possible metal speciation in the fly ash produced from a fluidized bed incinerator of municipal solid waste," in *The 31st Annual Conference of JSMCWM*, online, Sep. 2020, pp. 505–506.

[9] Y. Liang *et al.*, "Kinetics of Cd(II) adsorption and desorption on ferrihydrite: experiments and modeling," *Environ Sci Process Impacts*, vol. 20, no. 6, pp. 934–942, Jun. 2018, doi: 10.1039/c8em00068a.

[10] J. L. Provis and S. A. Bernal, "Geopolymers and related alkali-activated materials," *Annu Rev Mater Res*, vol. 44, pp. 299–327, 2014, doi: 10.1146/annurev-matsci-070813-113515.

[11] X. Niu, Y. Elakneswaran, C. R. Islam, J. L. Provis, and T. Sato, “Adsorption behaviour of simulant radionuclide cations and anions in metakaolin-based geopolymer,” *J Hazard Mater*, vol. 429, pp. 1–11, May 2022, doi: 10.1016/j.jhazmat.2022.128373.

[12] N. Soonthornwiphat *et al.*, “Encapsulation of Sr-loaded titanate spent adsorbents in potassium aluminosilicate geopolymer,” *J Nucl Sci Technol*, vol. 57, no. 10, pp. 1181–1188, Oct. 2020, doi: 10.1080/00223131.2020.1775717.

[13] R. I. Chaerun *et al.*, “Retention mechanism of cesium in chabazite embedded into metakaolin-based alkali activated materials,” *J Hazard Mater*, vol. 440, pp. 1–10, Oct. 2022, doi: 10.1016/j.jhazmat.2022.129732.

[14] P. Rożek, M. Król, and W. Mozgawa, “Geopolymer-zeolite composites: A review,” *J Clean Prod*, vol. 230, pp. 557–579, Sep. 2019, doi: 10.1016/j.jclepro.2019.05.152.

[15] J. G. S. Van Jaarsveld, J. S. J. Van Deventer, and A. Schwartzman, “THE POTENTIAL USE OF GEOPOLYMERIC MATERIALS TO IMMOBILISE TOXIC METALS: PART II. MATERIAL AND LEACHING CHARACTERISTICS,” *Miner Eng*, vol. 12, no. I, pp. 75–91, 1999.

[16] T. da S. Rocha, D. P. Dias, F. C. C. França, R. R. de S. Guerra, and L. R. da C. de O. Marques, “Metakaolin-based geopolymer mortars with different alkaline activators (Na+ and K+),” *Constr Build Mater*, vol. 178, pp. 453–461, Jul. 2018, doi: 10.1016/j.conbuildmat.2018.05.172.

[17] Z. Ji and Y. Pei, “Immobilization efficiency and mechanism of metal cations (Cd2+, Pb2+ and Zn2+) and anions (AsO43- and Cr2O72-) in wastes-based geopolymer,” *J Hazard Mater*, vol. 384, pp. 1–11, Feb. 2020, doi: 10.1016/j.jhazmat.2019.121290.

[18] B. I. El-Eswed, “Chemical evaluation of immobilization of wastes containing Pb, Cd, Cu and Zn in alkali-activated materials: A critical review,” *J Environ Chem Eng*, vol. 8, no. 5, pp. 1–9, Oct. 2020, doi: 10.1016/j.jece.2020.104194.

[19] E. Gomaa, S. Sargon, C. Kashosi, A. Gheni, and M. A. ElGawady, “Mechanical Properties of High Early Strength Class C Fly Ash-Based Alkali Activated Concrete,” *Transp Res Rec*, vol. 2674, no. 5, pp. 430–443, May 2020, doi: 10.1177/0361198120915892.

[20] S. Donatello, A. Fernández-Jiménez, and A. Palomo, “An assessment of Mercury immobilisation in alkali activated fly ash (AAFA) cements,” *J Hazard Mater*, vol. 213–214, pp. 207–215, Apr. 2012, doi: 10.1016/j.jhazmat.2012.01.081.

[21] J. Zhang, J. L. Provis, D. Feng, and J. S. J. van Deventer, “Geopolymers for immobilization of Cr6+, Cd2+, and Pb2+,” *J Hazard Mater*, vol. 157, no. 2–3, pp. 587–598, Sep. 2008, doi: 10.1016/j.jhazmat.2008.01.053.

[22] B. I. El-Eswed, R. I. Yousef, M. Alshaaer, I. Hamadneh, S. I. Al-Gharabli, and F. Khalili, “Stabilization/solidification of heavy metals in kaolin/zeolite based geopolymers,” *Int J Miner Process*, vol. 137, pp. 34–42, Apr. 2015, doi: 10.1016/j.minpro.2015.03.002.

[23] G. Qian, D. D. Sun, and J. H. Tay, “Immobilization of mercury and zinc in an alkali-activated slag matrix,” *J Hazard Mater*, vol. 101, no. 1, pp. 65–77, Jul. 2003, doi: 10.1016/S0304-3894(03)00143-2.

[24] Z. Ji and Y. Pei, “Geopolymers produced from drinking water treatment residue and bottom ash for the immobilization of heavy metals,” *Chemosphere*, vol. 225, pp. 579–587, Jun. 2019, doi: 10.1016/j.chemosphere.2019.03.056.

[25] N. Mladenović *et al.*, “The Applications of New Inorganic Polymer for Adsorption Cadmium from Waste Water,” *J Inorg Organomet Polym Mater*, vol. 30, no. 2, pp. 554–563, Feb. 2020, doi: 10.1007/s10904-019-01215-y.

[26] M. Ivanović *et al.*, “The Influence Of Thermodynamic Parameters On Alkaline Activators Of Geopolymers And The Structure Of Geopolymers,” *Macedonian Journal of Chemistry and Chemical Engineering*, vol. 40, no. 1, pp. 99–109, 2021, doi: 10.20450/MJCCE.2021.2127.

[27] L. Zhang, F. Zhang, M. Liu, and X. Hu, “Novel sustainable geopolymer based syntactic foams: An eco-friendly alternative to polymer based syntactic foams,” *Chemical Engineering Journal*, vol. 313, pp. 74–82, 2017, doi: 10.1016/j.cej.2016.12.046.

[28] L. Vidal *et al.*, “Determination of the polymerization degree of various alkaline solutions: Raman investigation,” *J Solgel Sci Technol*, vol. 83, no. 1, pp. 1–11, Jul. 2017, doi: 10.1007/s10971-017-4394-z.

[29] A. Depla *et al.*, “UV-Raman and 29Si NMR spectroscopy investigation of the nature of silicate oligomers formed by acid catalyzed hydrolysis and polycondensation of tetramethylorthosilicate,” *Journal of Physical Chemistry C*, vol. 115, no. 22, pp. 11077–11088, Jun. 2011, doi: 10.1021/jp200568j.

[30] H. D. Lutz, H. Mdller, and M. Schmidt, “Lattice vibration spectra. Part LXXXII. Brucite-type hydroxides M(OH)2 (M = Ca, Mn, Co, Fe, Cd)-IR and Raman spectra, neutron diffraction of Fe(OH)2*,” *J Mol Struct*, vol. 328, pp. 121–132, 1994.

[31] R. P. J. Cooney and J. R. Hall, “VIBRATIONAL SPECTRA OF MERCURY(l) AND MERCURY(II) ACETATE COMPOUNDS,” *J. inorg. nucl. Chem.*, vol. 34, pp. 1519–1527, 1972.

[32] F. K. Cartledge *et al.*, “Immobilization Mechanisms in Solidification/Stabilization of Cd and Pb Salts Using Portland Cement Fixing Agents,” *Environ. Sci. Technol.* , vol. 24, no. 6, pp. 867–873, 1990.

[33] J. Liu, D. Wu, X. Tan, P. Yu, and L. Xu, “Review of the Interactions between Conventional Cementitious Materials and Heavy Metal Ions in Stabilization/Solidification Processing,” *Materials*, vol. 16, no. 9, pp. 1–23, May 2023, doi: 10.3390/ma16093444.

CHAPTER 4. DIFFERENCE OF IMMOBILIZATION CHARACTERISTICS BETWEEN HEAVY METALS IN K-GEOPOLYMER

4.1 Introduction

Heavy metals contamination has become a concern all over the world. These metals are highly toxic and become priority pollutants to be regulated [1]. Anthropogenic activities have increased the possibility of heavy metal contamination in the environment [2]. Activities like mining, coal power plants, various industries, and municipal waste incineration produce waste containing heavy metals [3]. Several heavy metals commonly found in those wastes are Cd, Hg, Zn, and Pb [4], [5], [6], [7]. These metals can exist as desorbed ions in sludge as well as soluble chloride or sulfate salts in fly ash [8], [9]. These forms are more prone to leaching. Therefore, dumping sludge and fly ash in landfills without prior treatment can increase the opportunity for secondary waste contamination [10]. The waste treatment becomes essential because heavy metals can cause adverse health effects [11], [12]. Cadmium causes bone disease and prostate cancer and damages the lungs. Exposure to mercury causes birth defects and permanent damage to the brain and nervous system. Lead can inhibit renal dysfunction and brain damage, while zinc causes nausea, abdominal pain, and anemia [13].

Solidification/stabilization is an appropriate treatment for preventing secondary waste contamination. This treatment includes the addition of a binder to the solid wastes. Geopolymer is one kind of binder deemed suitable for stabilizing heavy metals [14], [15]. This material is acid and thermal-resistant, has low permeability, and produces low CO_2 emission compared to the manufacture of Portland cement [16], [17]. Geopolymer is an alkali-activated material consisting of silica and alumina tetrahedra joined alternately by sharing oxygen atoms creating a three-dimensional framework [18]. Its main structure is N-A-S-H or K-A-S-H, depending on the alkali activator [19]. Geopolymer has a very similar structure to zeolite but lacks crystallinity [20]. However, Na-geopolymer is reported to be able to transform into zeolite at low temperatures [21]. This raises a concern about the use of Na-geopolymer for heavy metal immobilization, since the metal may leach out to the environment during Na-geopolymer transformation into a more ordered and compact structure. Compared to Na-geopolymer, K-geopolymer remains amorphous, suggesting its prospect for long-term immobilization for heavy metals [22]. However, K-geopolymer is less studied.

A study on the immobilization of Cd and Hg in K-geopolymer has been conducted. The previous chapter proposed an appropriate procedure for mixing geopolymer components with heavy metal contaminants. Providing the metals as ions by mixing the contaminant with water before the geopolymerization process results in very low Cd leaching and relatively homogeneous geopolymer [23]. Confirmation is needed to prove the replicability of this procedure for other heavy metals. The previous study also shows a distinct behavior of Cd and Hg in K-geopolymer although they belong to the same group in the periodic table, meaning that they have similar electron configurations. The study needs to be extended by evaluating Zn, which is also a member of group 12. Another metal located in the same row of Hg, such as Pb, also needs to be examined to understand these distinct behaviors.

Previous studies have proposed the immobilization mechanisms for Zn, Cd, Hg, and Pb in Na-geopolymer [15], [24], [25], [26], [27], [28], [29]. However, the studies concluded different kinds of mechanisms even within a particular metal. Previous studies on the immobilization of heavy metals in Na-geopolymer is presented in Table 4-1. The different mechanisms may be due to the variation of aluminosilicate precursors, metal concentrations, and mixing procedures providing the initial heavy metal species either as salt or ion. The previous chapter shows that incorporating cadmium ions at different concentrations results in the same immobilization and geopolymer characteristics. The use of metakaolin as an aluminosilicate precursor also leads to the formation of pure K-geopolymer, making it easier to study.

Table 4-1. Previous studies on the immobilization of heavy metals in Na-geopolymer

Researcher	Metal	Precursor	Metal Concentration (wt.%)	Mechanisms
Ji and Pei [24]	Zn	Bottom ash + drinking water treatment residue	2 and 4	Covalent bonding
Wan, *et al*. [25]	Zn	Mine tailing + metakaolin	0.14 and 0.81	Physical encapsulation of nonreactive ZnO
Zhang *et al*. [26]	Zn	Al_2O_3 + SiO_2	5 and 10	Ion exchange
Ji and Pei [24]	Cd	Bottom ash + drinking water treatment residue	1, 2, and 4	Covalent bonding
Qian *et al.* [27]	Hg	Blast furnace slag	0.5 and 2	Hg-silicate precipitate; C-S-H lattice incorporation; Physical encapsulation of HgO
Donatello *et al.* [28]	Hg	Fly ash	0.5 and 5	HgS; HgO/Hg-silicate; Hg absorbed onto N-A-S-H
Ji and Pei [24]	Pb	Bottom ash + drinking water treatment residue	1, 2, and 4	$PbSiO_3$ precipitate
Nikolić [29]	Pb	Fly ash	10 and 30	Pb_5SiO_7 precipitate; Pb-silicate hydroxide
Zhang *et al*. [15]	Pb	Fly ash + sand	0.5	Pb_3SiO_5 precipitate
Zhang *et al*. [26]	Pb	Al_2O_3 + SiO_2	5 and 10	Ion exchange; covalent bonding

By applying a mixing procedure proposed in the previous chapter, the avoidance of metal hydroxide/oxide formation and the instigation of better immobilization mechanisms are expected. Clarification on the immobilization mechanisms of Zn, Cd, Hg, and Pb is required to predict their long-term stability in K-geopolymer. The differences and/or similarities in heavy metals immobilization mechanisms in K-geopolymer also need to be explained to draw a general conclusion and predict the behavior of other metals.

4.2 Materials and Methods

4.2.1 Materials

Metakaolin from Sobueclay Co., Ltd. (Nagoya, Japan) with a chemical composition shown in Table 4-1 acted as an aluminosilicate precursor for manufacturing geopolymer. Alkali activator consisted of a potassium silicate solution (Fujifilm Wako Pure Chemical Corporation, Japan), with 21.90 wt.% of K_2O and 29.00 wt.% of SiO_2, and potassium hydroxide (Kanto Chemical Co., Inc., Japan), with 86.0 wt.% purity. The molar ratio of SiO_2:K_2O within the alkali activator was kept at 1:1. Their ratio with ultrapure water was also kept at 1:13 to keep its optimum workability [30]. Several salts were used as artificial contaminants, namely cadmium chloride 2.5-hydrate with 98 wt.% purity (Kanto Chemical Co., Inc., Japan), mercury (II) chloride with 99.5 wt.% purity (Fujifilm Wako Pure Chemical Corporation, Japan), lead nitrate of 99.999 wt.% purity (Sigma-Aldrich, Japan), and zinc chloride of 98 wt.% purity (Fujifilm Wako Pure Chemical Corporation, Japan).

Table 4-1. Chemical composition of Sobueclay metakaolin

Component	Percentage (wt.%)
SiO_2	51.25
Al_2O_3	45.82
TiO_2	1.19
Fe_2O_3	0.58
Na_2O	0.06
K_2O	0.15
CaO	0.23
MgO	0.02
P_2O_5	0.13

4.2.2 Methods

4.2.2.1 Sample Preparation

A geopolymer control (GP-control) was prepared by mixing metakaolin with an alkali activator and water. The amount of alkali activator was adjusted to make a ratio of Al_2O_3 in metakaolin-to-K_2O in alkali activator equals 1. The mixture was hand-mixed for 15 min, cast into PVC molds of 1.3 cm diameter × 1.5 cm height, and covered with parafilm on both sides. Meanwhile, zinc geopolymer (Zn-GP), cadmium geopolymer (Cd-GP), mercury geopolymer (Hg-GP), and lead geopolymer (Pb-GP) were prepared by

first dissolving the metal salts into ultrapure water. The solution was poured onto metakaolin and then mixed with the alkali activator. The amount of heavy metals was adjusted to make a concentration of 1 wt.%. After 15 min of mixing, the mixture was poured into PVC molds. All geopolymers were cured at 40°C for 24 h and at 25°C for another 24 h.

4.2.2.2 Leaching Test

A leaching test was conducted based on the ANSI/ANS-16.1-2003 standard. Each geopolymer sample was submerged in 88 mL of deionized water and moved into a new batch of deionized water after 30 s, 2 h, 7 h, and 1, 2, 3, 4, 5, 19, 47, and 90 d. The leaching was carried out at a constant temperature of 25°C.

4.2.2.3 Liquid Sample Analysis

The concentration of Zn, Cd, Hg, and Pb in leachates was analyzed using an iCAP RQplus inductively coupled plasma mass spectrometry (ICP-MS; Thermo Scientific, USA). Calibration standards in the range of 0.01–10 ppb were made with the custom assurance standard XSTC-331 (SPEX CertiPrep; Seishin Trading Company, Japan) and a mercury standard solution (Hg 1000; Fujifilm Wako Pure Chemical Corporation, Japan) Yttrium, indium and bismuth were used as internal standards.

4.2.2.4 Solid Sample Analysis

All geopolymer samples were analyzed by X-ray diffraction (RINT2100; Rigaku; Japan) to determine their crystallography. The CuKα radiation source was operated at 30 kV and 20 mA. The scanning was conducted at 0.02°/s for a 2θ of 10°–70°. An XploRA PLUS Raman microscope (Horiba, Japan) was also used to examine the samples. The spectra were collected using a 532 nm excitation wavelength with a 50× objective lens, 100 μm entrance slit, and 1800 groove/mm grating. The chemical state of the surface composition was determined with a JPS-9200 X-ray photoelectron spectrometer (XPS; JEOL, Japan). Powdered samples were attached to carbon tape and subjected to MgKα radiation at 12 kV and 25 mA. The analyses were carried out over a 3 mm measurement area with a pass energy of 10 eV, 0.1 eV energy step, and dwell time of 0.1 s. The binding energy was calibrated based on the carbon 1s peak at 284.8 eV. Lastly, geopolymer morphology, crystallography, and chemical composition were investigated at the nano-scale level by a JEM-2010 transmission electron microscope (TEM; JEOL, Japan) at an accelerating voltage of 200 kV.

4.3 Results and Discussion

4.3.1 Overall Results

Leaching test results in Figure 4-1 show that, except for mercury, other metals are well-immobilized within geopolymer. More than 99.8% of Zn, Cd, and Pb can be retained in the geopolymer. The leaching behavior also tends to be constant after several days, indicating stability in the long run. Differently, mercury is hardly retained in K-geopolymer. Only less than 30% of Hg remains in the geopolymer after 90 days of leaching. This metal has an increasing leaching behavior, suggesting more mercury may be leached out after 90 days.

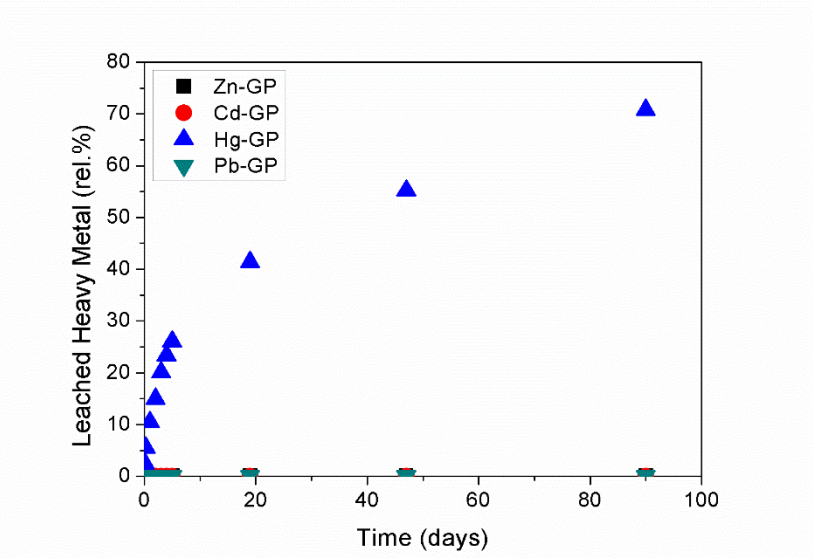

Figure 4-1. Cumulative amount of leaching relative to the initial amount of heavy metal

The X-ray diffraction pattern of mercury geopolymer in Figure 4-2 shows the presence of peaks at 30.1°, 31.5°, 37.3°, 50.3°, and 62.0° belonging to HgO. Being the dominant species, HgO is accountable for the high mercury leaching rate. The results indicate that the HgO species is unstable in a geopolymer environment and has high solubility. Meanwhile, a crystalline phase is not formed for other heavy metal samples. The only peaks that emerged are at 28.36°, 40.56°, and 66.4° from the zinc geopolymer sample due to the formation of KCl. This crystal formation is enabled by the contribution of K^+ from the alkali activator and Cl^- from the chloride salt. Eventually, the main immobilization mechanisms for Zn, Cd, and Pb are not by the precipitate formation. A closer examination of each sample is needed to determine the possible immobilization mechanisms.

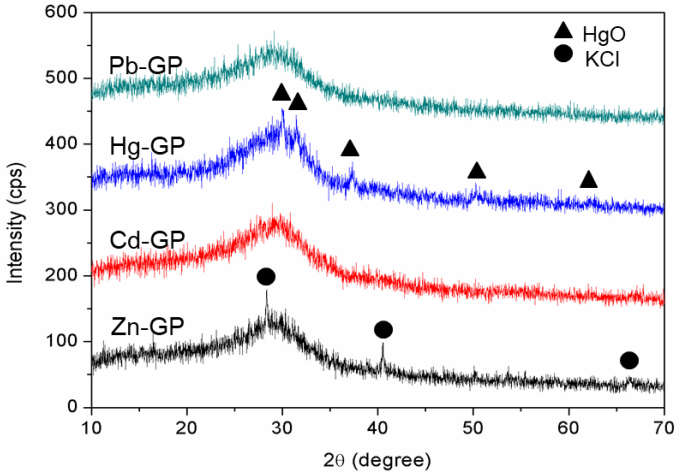

Figure 4-2. X-ray diffraction pattern of various heavy metal-geopolymer

4.3.2 Zinc Geopolymer

A nano-scale observation was conducted for heavy metal samples to assess the effect of metal incorporation on the morphology and crystallography of geopolymer. Figures 4-3a and b show the morphology of geopolymer control and selected area electron diffraction (SAED) pattern that translates to the amorphous structure of geopolymer. The diffuse and thick rings in the SAED pattern indicate that the amorphous sample randomly scatters electrons. Figure 4-3c shows the energy dispersive spectroscopy (EDS) results, giving information on geopolymer composition mainly of O, Si, Al, and K. The effect of Zn incorporation can be determined by comparing the results of zinc geopolymer with geopolymer control. Zinc geopolymer successfully incorporated Zn as indicated by the appearance of a Zn peak in the EDS result (Figure 4-3f). The incorporation does not change the amorphousness of geopolymer as shown by a halo around the bright central spot in the SAED pattern (Figure 4-3d and e). After 90 days of leaching, Zn is still well-incorporated in K-geopolymer as seen in Figure 4-3i, and keeps the amorphousness of geopolymer, as indicated in Figure 4-3g and h.

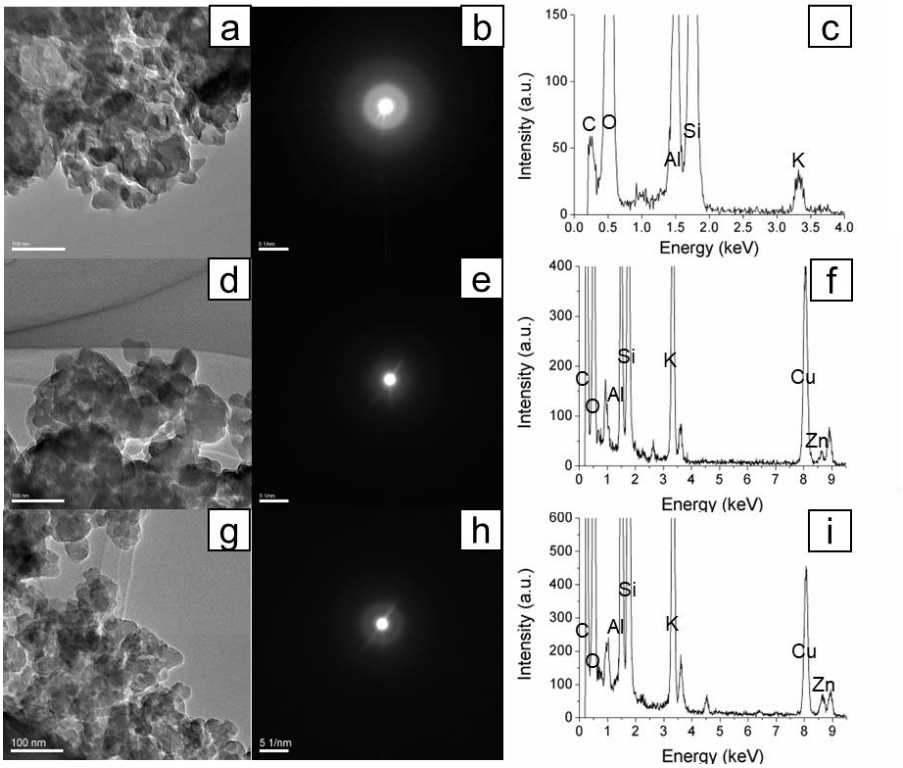

Figure 4-3. a) Morphology, b) SAED pattern, and c) EDS result of geopolymer control, d) Morphology, e) SAED pattern, and f) EDS result of zinc geopolymer, g) Morphology, h) SAED pattern, and i) EDS result of zinc geopolymer after leaching for 90 days

The state and location at which Zn is incorporated in the K-geopolymer are revealed by XPS results in Figure 4-4. Zinc is found to be present in K-geopolymer in its divalent state, indicated by $Zn2p_{3/2}$ binding energy of 1021 eV [31]. The presence of Zn shifts the binding energies of Al2p, Si2p, and O1s to a higher level. The binding energies of Al2p, Si2p, and O1s in the geopolymer control are 74.5, 102.6, and 531.3 eV,

respectively. These binding energies shift to 75.2, 103.1, and 531.6 eV with the presence of Zn^{2+}. The results indicate that Zn^{2+} bonds with silicate and aluminate much strongly than K^{+}. Zinc attracts electrons from Al, Si, and O and reduces the electron cloud density around them. This phenomenon leads to a decrease in the shielding effect and an increase in the binding energies [32].

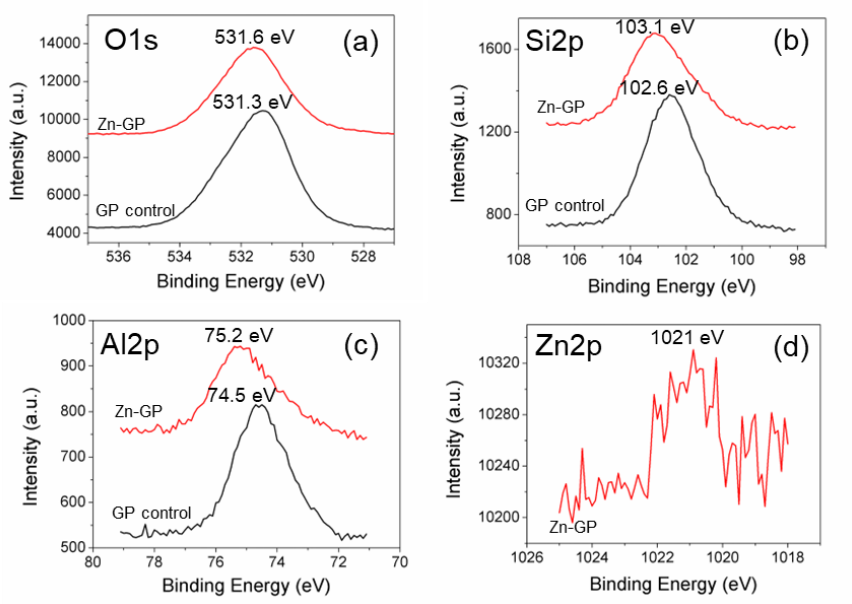

Figure 4-4. XPS spectra of (a) O1s, (b) Si2p, (c) Al2p, and (d) Zn2p from the geopolymer control and zinc geopolymer

4.3.3 Cadmium Geopolymer

Cadmium geopolymer has similar results to zinc. The TEM results are shown in Figure 4-5. Cadmium addition does not change K-geopolymer morphology (Figure 4-5a and d). The EDS result (Figure 4-5c) shows that Cd is present alongside other main constituents of geopolymer, namely O, Al, Si, and K. The low intensity of the Cd peak compared to other elements is in line with its low concentration and shows that Cd is surrounded by a K-geopolymer framework. The presence of Cd still allows a random electron scattering by geopolymer, resulting in diffused rings in the SAED pattern, highlighting its amorphousness. After 90 days of the leaching experiment, Cd is still held by K-geopolymer in the same manner, as suggested by the SAED pattern and EDS result (Figure 4-5e and f).

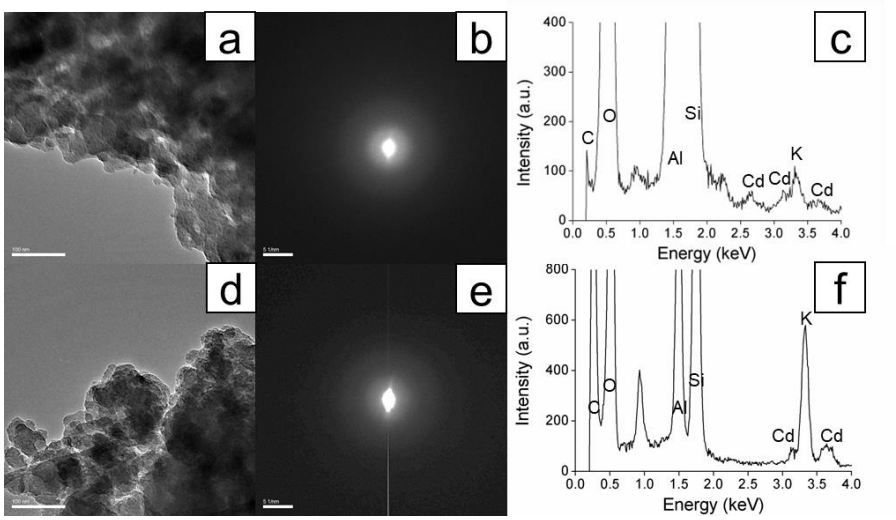

Figure 4-5. a) Morphology, b) SAED pattern, and c) EDS result of cadmium geopolymer, d) Morphology, e) SAED pattern, and f) EDS result of cadmium geopolymer after leaching for 90 days

The comparison of XPS spectra between cadmium geopolymer and geopolymer control is shown in Figure 4-6. The binding energy of $Cd3d_{5/2}$ and $Cd3d_{3/2}$ at 405.4 and 412.2 eV correspond to its divalent state in geopolymer [31]. The binding energy of Al2p, Si2p, and O1s shift with the presence of this cation. Those binding energies move from 74.5, 102.6, and 531.3 eV to a higher energy level of 74.7, 102.8, and 531.5, respectively. These results account for the bonding between Cd^{2+} with aluminate and silicate. The results indicate that the immobilization mechanisms of Cd in K-geopolymer are the same as Zn.

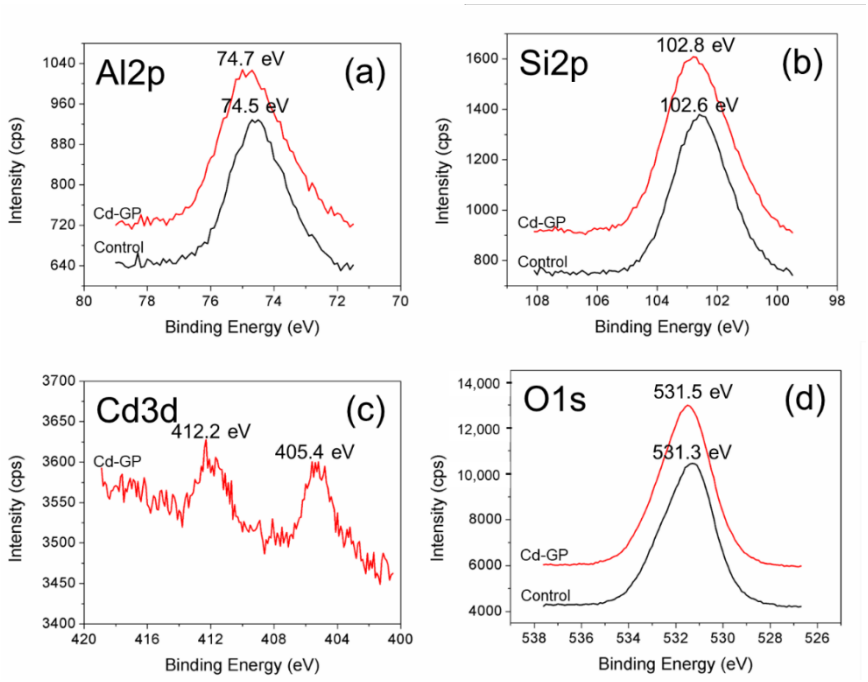

Figure 4-6. XPS spectra of (a) Al2p, (b) Si2p, (c) Cd3d, and (d) O1s from the geopolymer control and cadmium geopolymer

4.3.4 Lead Geopolymer

A nano-scale observation on lead geopolymer shows two different tendencies of Pb interaction within K-geopolymer. The observation results are provided in Figure 4-7. Two kinds of morphologies are discovered, one phase is similar to geopolymer control (Figure 4-7a and g), while another phase has a darker and more arranged structure (Figure 4-7d and j). The intensity of Pb is also different in those two phases. Less Pb is found in the amorphous phase (Figure 4-7b and c), while more Pb can be found in a more arranged and comparatively more crystalline structure (Figure 4-7e and f). After 90 days of leaching, the amorphous phase still maintains the Pb content as indicated by Figure 4-7h and i. Meanwhile, crystallinity increases in a phase with higher Pb content, as seen in Figure 4-7k and i. Two bright spots surrounding the central spot are present in the electron diffraction of this crystalline phase. Both crystals have a d-spacing of 2.9 A, which most likely belongs to $PbSiO_3$. It shows the tendency of Pb to bond with silicate and form a stable crystal.

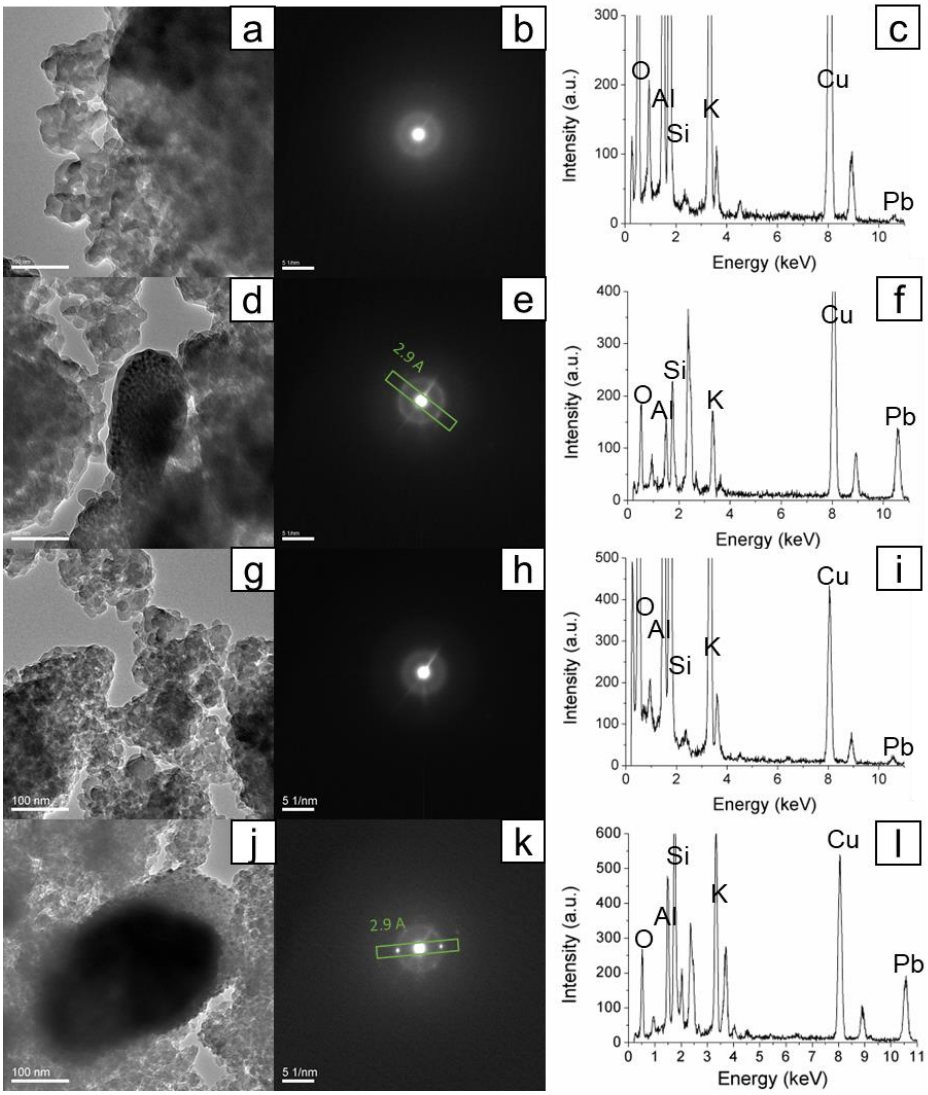

Figure 4-7. a) Morphology, b) SAED pattern, and c) EDS result of lead geopolymer, d) Morphology, e) SAED pattern, and f) EDS result of crystalline lead geopolymer, g) Morphology, h) SAED pattern, and i) EDS result of lead geopolymer after leaching for 90 days, j) Morphology, k) SAED pattern, and l) EDS result of crystalline lead geopolymer after leaching for 90 days

Figure 4-8 shows the Raman spectra of lead geopolymer. Lead is detected with $Pb4f_{7/2}$ and $Pb4f_{5/2}$ binding energy of 139 and 143.9 eV. This character is owned by the divalent state of Pb [31]. The presence of this cation also changes the binding energy of other geopolymer constituents, which are O, Si, and Al. Geopolymer initially has O1s, Si2p, and Al2p binding energy of 531.3, 102.6, and 74.5 eV, respectively. Lead incorporation affects the electron clouds and leads to a change of O1s, Si2p, and Al2p binding energy to 531.6, 102.8, and 74.7 eV. These results imply the strong bonding between Pb and aluminate and silicate.

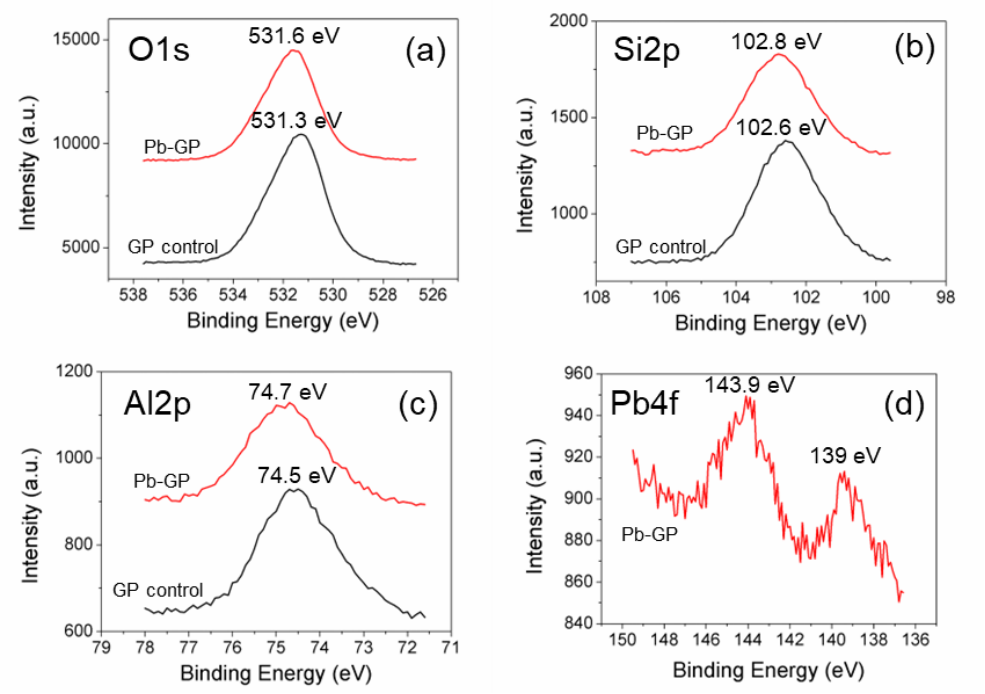

Figure 4-8. XPS spectra of (a) O1s, (b) Si2p, (c) Al2p, and (d) Pb4f from the geopolymer control and lead geopolymer

4.3.5 Factors Affecting Heavy Metals Immobilization

Immobilization of Zn, Cd, Hg, and Pb in K-geopolymer have similarities as well as differences. A closer analysis implies that Zn, Cd, and Pb are dominantly retained by bonding with aluminate and silicate while keeping the amorphous phase of K-geopolymer. Among those, a slight difference is observed in Pb which has more preference for forming a crystal with silicate. Another difference is between those three metals with Hg, in which Hg prefers to form HgO in the geopolymer system. These immobilization mechanisms are affected by three factors.

4.3.5.1 Ionic Potential

The ionic potential is the ability of an ion to attract or repulse electrons. Ionic potential (φ) can be calculated by dividing the ionic charge (Z*) by its ionic radius (r) [33].

$$\varphi = \frac{Z^*}{r} \tag{4-1}$$

For cations, greater ionic potential corresponds to their higher ability to attract electrons. For anions, smaller ionic potential means that they can reject more electrons. Ionic potential depends on the coordination number of elements since different coordination number has a slightly different ionic radius [34]. Every element can have various coordination numbers, but some are more common than others. The common coordination numbers for K are 10 and 12-coordination [35]. Zinc and cadmium have

coordination numbers of 4 and 6-coordination [36], [37], [38], [39], [40]. Coordination numbers for Hg are mostly 2 and 4-coordination, while for Pb are 4, 6, and 8-coordination [41], [42], [43]. The ionic potential of metals in various coordination numbers is provided in Figure 4-9.

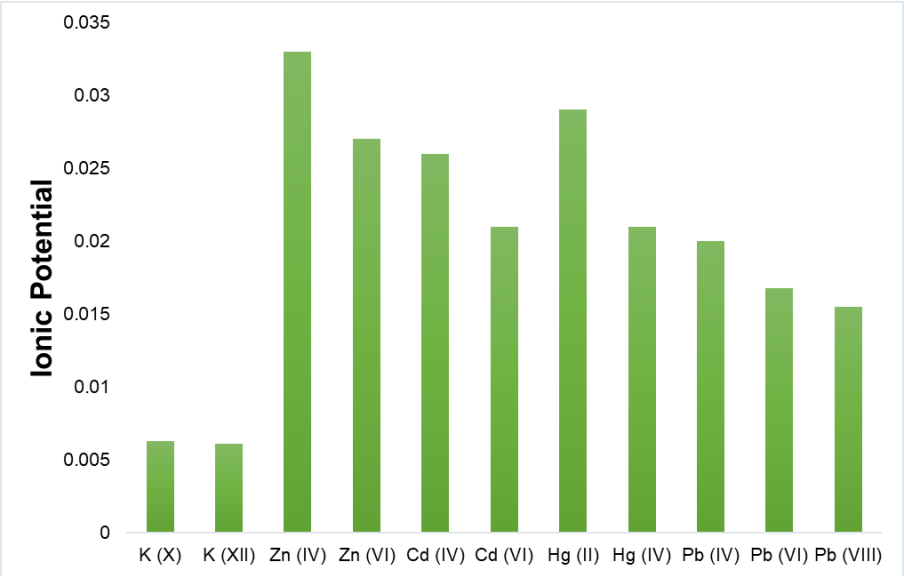

Figure 4-9. Ionic potential of several metals

The ionic potential for all heavy metals is much higher compared to K^+. Heavy metals can outperform K^+ in attracting electrons. Eventually, all heavy metals can replace K^+ in balancing the negatively charged alumina tetrahedra and bond more strongly. The strong bonding is also affected by the second factor. An illustration of this bonding is provided in Figure 4-10.

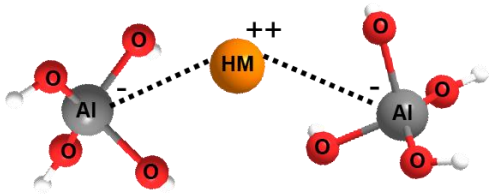

Figure 4-10. Bonding between heavy metal and alumina tetrahedra promoted by high ionic potential

4.3.5.2 Electronegativity

Electronegativity signifies the ability of an atom in a compound to attract shared-pair electrons toward itself [44]. Electronegativity determines the type of bonding between one atom and another. Atoms with similar electronegativity will have a stronger covalent bonding, while atoms with different electronegativity have ionic binding. The electronegativity of some atoms in K-geopolymer is shown in Figure 4-11.

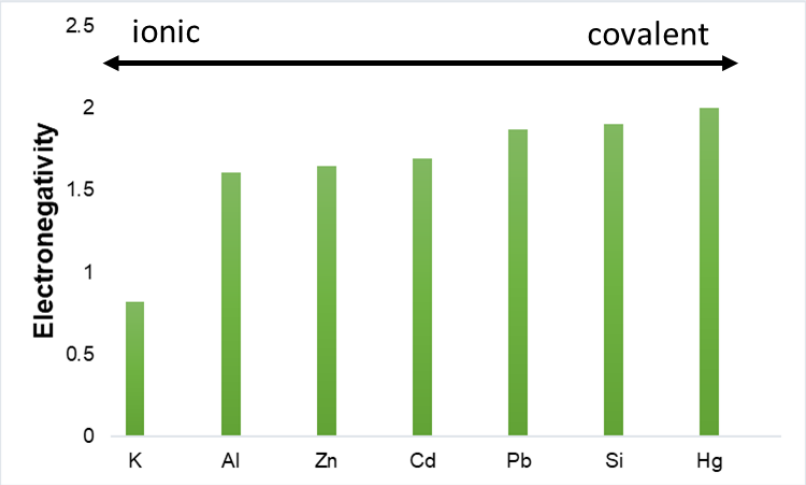

Figure 4-11. Electronegativity of several atoms [45]

Heavy metals have a relatively high electronegativity in the sequence of Zn < Cd < Pb < Hg [45]. The high electronegativity allows all heavy metals to form a bond by attracting electrons from silica and alumina tetrahedra. As a result, heavy metals will have a strong covalent bonding with silicate and aluminate. An illustration of this bonding is shown in Figure 4-12. While the electronegativity of Zn and Cd is similar to Al, the electronegativity of Pb and Hg is more identical to Si. Lead preference for silicate may be explained by this electronegativity similarity, which leads to a stronger covalent bonding.

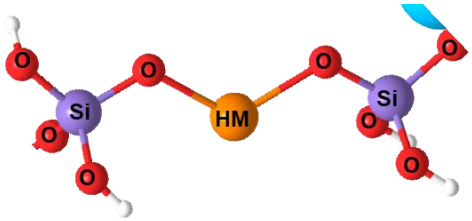

Figure 4-12. Bonding between heavy metal and silicate promoted by high electronegativity

4.3.5.3 Electron Configuration and Relativistic Effect

According to Einstein's relativistic theory, the mass (m) of a moving electron in an atom increases with respect to its rest mass (m_0) with the increase of its velocity (v).

$$m = \frac{m_0}{\sqrt{1-\frac{v^2}{c^2}}} = \gamma\, m_0 \qquad (4\text{-}2)$$

taking c = velocity of light and γ = relativistic factor

The velocity of the electron in 1s shell has a linear correlation with its atomic number (Z).

$$v = \frac{Z}{137} c \quad (4\text{-}3)$$

Electron velocity decreases with the value of n. Thus, the relativistic effect is more apparent in the smaller value of n and heavier elements. This effect causes an orbital contraction in the order of s > p > d > f, as stated in the following equation.

$$r_{rel} = \frac{r}{\gamma} \quad (4\text{-}4)$$

taking r_{rel} = relativistic radius and r = nonrelativistic radius

Consequently, there is a contraction of the s and p orbital, called the direct relativistic effect [46]. The contracted s and p orbital effectively shield the d and f orbital, making them experience less nucleus attraction and undergo expansion, also called indirect relativistic effect.

The relativistic parameters for Zn, Cd, Hg, and Pb are calculated and provided in Table 4-2. From the calculation, the effect of relativity is negligible for Zn and Cd due to their small atomic number. On the contrary, this effect cannot be ruled out for Hg and Pb as it accounts for 23% and 25% of orbital contraction. This marks the difference between Hg and the other elements of group 12 (Zn and Cd). Given the electron configuration of Hg^{2+} = [Xe] $4f^{14}$ $5d^{10}$, the relativistic effect will cause a contraction of the 6s orbital and expansion of the 5d orbital, decreasing the energy difference between those orbitals. The small difference allows a hybridization scheme that leads to the preference for linear coordination. Since the geopolymerization process involves a high concentration of OH^-, Hg^{2+} prefers to bond with the hydroxide to form linearly coordinated HgO. However, this linear coordination is not preferable for Pb^{2+} with an electron configuration of [Xe] $4f^{14}$ $5d^{10}$ $6s^2$. The valence orbital of 6s tends to form conventional orbital hybridization with 6p orbital. This leads to the Pb tendency for four coordination or more. Nonetheless, Pb acts similarly to Zn and Cd and preferably bonds with silica and alumina tetrahedra in K-geopolymer.

Table 4-2. Relativistic parameters of heavy metals

Heavy Metal	Z	v	m	Relativistic contraction orbital
Zn	30	0.22 c	1.02 m_0	2%
Cd	48	0.35 c	1.07 m_0	7%
Hg	80	0.58 c	1.23 m_0	23%
Pb	82	0.60 c	1.25 m_0	25%

4.4 Conclusion

Zinc, cadmium, and lead are well-immobilized within K-geopolymer. Incorporating these metals into geopolymer changes the binding energy of the main constituents but keeps its amorphousness. Zinc, cadmium, and lead are immobilized through covalent bonding with silicate and aluminate. The high ionic potential and electronegativity make these bonds possible and are stronger than those of K^+. Since Pb has an electronegativity that is more similar to Si, Pb tends to bond with silicate to form

a stable crystal. Due to its high ionic potential and electronegativity, Hg can be immobilized similarly to other metals. However, Hg in high concentration prefers bonding with oxygen and forms linear coordination in the geopolymer system. This preference is affected by the electron configuration and relativistic effects. Consequently, Hg is easily leached out from the geopolymer due to the high solubility of HgO. This suggests the need for an additive to transform Hg into a much more stable form.

4.5 References

[1] U.S. Environmental Protection Agency, "WATER-RELATED ENVIRONMENTAL FATE OF 129 PRIORITY POLLUTANTS Volume I: Introduction and Technical Background, Metals and Inorganics, Pesticides and PCBs," Washington, D.C., 1979.

[2] J. P. Vareda, A. J. M. Valente, and L. Durães, "Assessment of heavy metal pollution from anthropogenic activities and remediation strategies: A review," *J Environ Manage*, vol. 246, pp. 101–118, Sep. 2019, doi: 10.1016/j.jenvman.2019.05.126.

[3] J. Mishra, R. Saini, and D. Singh, "Review paper on removal of heavy metal ions from industrial waste water effluent," in *IOP Conference Series: Materials Science and Engineering*, IOP Publishing, Jul. 2021, pp. 1–21. doi: 10.1088/1757-899x/1168/1/012027.

[4] G. C. Kisku, S. Yadav, R. K. Sharma, and M. P. S. Negi, "Potential environmental pollution hazards by coal based power plant at Jhansi (UP) India," *Environ Earth Sci*, vol. 67, no. 7, pp. 2109–2120, Dec. 2012, doi: 10.1007/s12665-012-1651-x.

[5] W. Zucha, G. Weibel, M. Wolffers, and U. Eggenberger, "Inventory of MSWI fly ash in Switzerland: Heavy metal recovery potential and their properties for acid leaching," *Processes*, vol. 8, no. 12, pp. 1–13, Dec. 2020, doi: 10.3390/pr8121668.

[6] D. Xiao, H. Li, Y. Wang, G. Wen, and C. Wang, "Distribution Characteristics of Typical Heavy Metals in Sludge from Wastewater Plants in Jiangsu Province (China) and Their Potential Risks," *Water (Switzerland)*, vol. 15, no. 2, pp. 1–13, Jan. 2023, doi: 10.3390/w15020313.

[7] A. Ito, T. Umita, J. Aizawa M, T. Takachi, and K. Morinaga, "REMOVAL OF HEAVY METALS FROM ANAEROBICALLY DIGESTED SEWAGE SLUDGE BY A NEW CHEMICAL METHOD USING FERRIC SULFATE," *Wat. Res.* , vol. 34, no. 3, pp. 751–758, 2000, [Online]. Available: www.elsevier.com/locate/watres

[8] W. Chen, Y. Wang, Y. Sun, G. Fang, and Y. Li, "Release of soluble ions and heavy metal during fly ash washing by deionized water and sodium carbonate solution," *Chemosphere*, vol. 307, pp. 1–8, Nov. 2022, doi: 10.1016/j.chemosphere.2022.135860.

[9] A. V. Dahlan, H. Kitamura, H. Sakanakura, T. Shimaoka, T. Yamamoto, and F. Takahashi, “Possible metal speciation in the fly ash produced from a fluidized bed incinerator of municipal solid waste,” in *The 31st Annual Conference of JSMCWM*, online, Sep. 2020, pp. 505–506.

[10] V. Nevondo, T. Malehase, A. P. Daso, and O. J. Okonkwo, “Leachate seepage from landfill: A source of groundwater mercury contamination in South Africa,” *Water SA*, vol. 45, no. 2, pp. 225–231, Apr. 2019, doi: 10.4314/wsa.v45i2.09.

[11] M. Mahurpawar, “Effects of heavy metals on human health,” *Social Issues and Environmental Problems*, pp. 1–7, 2015.

[12] P. B. Tchounwou, C. G. Yedjou, A. K. Patlolla, and D. J. Sutton, “Heavy metal toxicity and the environment,” *EXS*, vol. 101, pp. 133–164, 2012, doi: 10.1007/978-3-7643-8340-4_6.

[13] L. M. Plum, L. Rink, and H. Hajo, “The essential toxin: Impact of zinc on human health,” *Int J Environ Res Public Health*, vol. 7, no. 4, pp. 1342–1365, 2010, doi: 10.3390/ijerph7041342.

[14] Z. Ji and Y. Pei, “Immobilization efficiency and mechanism of metal cations (Cd2+, Pb2+ and Zn2+) and anions (AsO43- and Cr2O72-) in wastes-based geopolymer,” *J Hazard Mater*, vol. 384, pp. 1–11, Feb. 2020, doi: 10.1016/j.jhazmat.2019.121290.

[15] J. Zhang, J. L. Provis, D. Feng, and J. S. J. van Deventer, “Geopolymers for immobilization of Cr6+, Cd2+, and Pb2+,” *J Hazard Mater*, vol. 157, no. 2–3, pp. 587–598, Sep. 2008, doi: 10.1016/j.jhazmat.2008.01.053.

[16] M. Nodehi and V. M. Taghvaee, “Alkali-Activated Materials and Geopolymer: a Review of Common Precursors and Activators Addressing Circular Economy,” *Circular Economy and Sustainability*, vol. 2, no. 1, pp. 165–196, Mar. 2022, doi: 10.1007/s43615-021-00029-w.

[17] J. Davidovits, “Geopolymer cement to minimize carbon-dioxde greenhouse-warming,” *Ceramic Transactions*, vol. 37, no. 1, pp. 165–182, 1993, [Online]. Available: https://www.researchgate.net/publication/284682578

[18] J. Davidovits, “Geopolymers: Ceramic-like inorganic polymers,” *Journal of Ceramic Science and Technology*, vol. 8, no. 3, pp. 335–350, 2017, doi: 10.4416/JCST2017-00038.

[19] J. Davidovits, “PROPERTIES OF GEOPOLYMER CEMENTS,” in *Alkaline Cements and Concretes*, 1994, pp. 131–149. [Online]. Available: www.geopolymer.org

[20] J. G. S. Van Jaarsveld, J. S. J. Van Deventer, and L. Lorenzeni, “THE POTENTIAL USE OF GEOPOLYMERIC MATERIALS TO IMMOBILISE TOXIC METALS:

PART I. THEORY AND APPLICATIONS," *Miner Eng*, vol. 10, no. 7, pp. 659–669, 1997.

[21] P. De Silva and K. Sagoe-Crenstil, "Medium-term phase stability of Na2O-Al2O3-SiO2-H2O geopolymer systems," *Cem Concr Res*, vol. 38, no. 6, pp. 870–876, Jun. 2008, doi: 10.1016/j.cemconres.2007.10.003.

[22] B. Liu *et al.*, "Insights into the microstructure of hydrothermal synthesized nanoscale k2o-al2o3-sio2-h2o particles," *Nanomaterials*, vol. 10, no. 1, pp. 1–18, Jan. 2020, doi: 10.3390/nano10010063.

[23] P. Prihutami, R. I. Chaerun, Y. Ohya, T. Otake, R. Kikuchi, and T. Sato, "Immobilization Forms of Cadmium and Mercury in a Potassium-Activated Metakaolin-Based Geopolymer," *Minerals*, vol. 14, no. 3, pp. 1–15, Mar. 2024, doi: 10.3390/min14030311.

[24] Z. Ji and Y. Pei, "Geopolymers produced from drinking water treatment residue and bottom ash for the immobilization of heavy metals," *Chemosphere*, vol. 225, pp. 579–587, Jun. 2019, doi: 10.1016/j.chemosphere.2019.03.056.

[25] Q. Wan, F. Rao, S. Song, and Y. Zhang, "Immobilization forms of ZnO in the solidification/stabilization (S/S) of a zinc mine tailing through geopolymerization," *Journal of Materials Research and Technology*, vol. 8, no. 6, pp. 5728–5735, Nov. 2019, doi: 10.1016/j.jmrt.2019.09.040.

[26] Q. Zhang *et al.*, "Lead zinc slag-based geopolymer: Demonstration of heavy metal solidification mechanism from the new perspectives of electronegativity and ion potential," *Environmental Pollution*, vol. 293, pp. 1–10, Jan. 2022, doi: 10.1016/j.envpol.2021.118509.

[27] G. Qian, D. D. Sun, and J. H. Tay, "Immobilization of mercury and zinc in an alkali-activated slag matrix," *J Hazard Mater*, vol. 101, no. 1, pp. 65–77, Jul. 2003, doi: 10.1016/S0304-3894(03)00143-2.

[28] S. Donatello, A. Fernández-Jiménez, and A. Palomo, "An assessment of Mercury immobilisation in alkali activated fly ash (AAFA) cements," *J Hazard Mater*, vol. 213–214, pp. 207–215, Apr. 2012, doi: 10.1016/j.jhazmat.2012.01.081.

[29] V. Nikolić, "Structural changes of fly ash-based geopolymers induced by a large amount of lead," *Global Sustainability Challenges* , 2023, [Online]. Available: https://gsc.unionnikolatesla.edu.rs/index.php/gsc/index

[30] X. Niu, Y. Elakneswaran, C. R. Islam, J. L. Provis, and T. Sato, "Adsorption behaviour of simulant radionuclide cations and anions in metakaolin-based geopolymer," *J Hazard Mater*, vol. 429, pp. 1–11, May 2022, doi: 10.1016/j.jhazmat.2022.128373.

[31] J. F. Moulder, W. F. Stickle, P. E. Sobol, and K. D. Bomben, *Handbook of X-ray Photoelectron Spectroscopy*. Eden Prairie: Perkin-Elmer Corporation, 1992.

[32] X. Wei *et al.*, “Structural Evolution of Geopolymers Incorporated with Heavy Metals: Solidification Mechanism of Pb2+ and Cd2+,” *Journal of Physical Chemistry C*, vol. 127, no. 39, pp. 19563–19573, Oct. 2023, doi: 10.1021/acs.jpcc.3c03924.

[33] W. Hai-Jun and W. Hai-Ju, “Ion Potential Principle Summary,” *London Journal of Research in Science: Natural and Formal*, vol. 19, no. 2, pp. 33–44, 2019.

[34] R. D. Shannon, “Revised Effective Ionic Radii and Systematic Studies of Interatomie Distances in Halides and Chaleogenides,” *Acta Cryst*, vol. 32, pp. 751–767, 1976.

[35] V. P. Solov, M. S. Stuklova, E. V Koltunova, and N. N. Kochanova, “Coordination Numbers of Central Atoms in Coordination Compounds,” *Russian Journal of Coordination Chemistry*, vol. 29, no. 9, pp. 711–720, 2003.

[36] S. Sen, M. Kumar Saha, P. Kundu, S. Mitra, C. Kruger, and J. Bruckmann, “Synthesis and structure of a heptacoordinated cadmium(II) complex,” *Inorganica Chim Acta*, vol. 288, pp. 118–121, 1999.

[37] M. Remelli, V. M. Nurchi, J. I. Lachowicz, S. Medici, M. A. Zoroddu, and M. Peana, “Competition between Cd(II) and other divalent transition metal ions during complex formation with amino acids, peptides, and chelating agents,” *Coord Chem Rev*, vol. 327–328, pp. 55–69, Nov. 2016, doi: 10.1016/j.ccr.2016.07.004.

[38] M. Borsari, “Cadmium: Coordination Chemistry,” in *Encyclopedia of Inorganic and Bioinorganic Chemistry*, Wiley, 2014, pp. 1–16. doi: 10.1002/9781119951438.eibc2261.

[39] J. Burgess and R. H. Prince, “Zinc: Inorganic & Coordination Chemistry,” in *Encyclopedia of Inorganic Chemistry*, Wiley, 2006, pp. 1–26. doi: 10.1002/0470862106.ia260.

[40] N. J. Ataie *et al.*, “Zinc coordination geometry and ligand binding affinity: The structural and kinetic analysis of the second-shell serine 228 residue and the methionine 180 residue of the aminopeptidase from Vibrio proteolyticus,” *Biochemistry*, vol. 47, no. 29, pp. 7673–7683, Jul. 2008, doi: 10.1021/bi702188e.

[41] D. C. Bebout, “Mercury: Inorganic & Coordination Chemistry,” in *Encyclopedia of Inorganic and Bioinorganic Chemistry*, Wiley, 2006, pp. 1–15. doi: 10.1002/9781119951438.eibc0124.

[42] A. Morsali and M. Y. Masoomi, “Structures and properties of mercury(II) coordination polymers,” *Coord Chem Rev*, vol. 253, no. 13–14, pp. 1882–1905, Jul. 2009, doi: 10.1016/j.ccr.2009.02.018.

[43] M. S. Bharara and D. A. Atwood, “Lead: Inorganic Chemistry,” in *Encyclopedia of Inorganic and Bioinorganic Chemistry*, Wiley, 2006, pp. 1–14. doi: 10.1002/9781119951438.eibc0111.

[44] A. L. Allred and E. G. Rochow, “A scale of electronegativity based on electrostatic force,” *J. Inorg. Nucl. Chem*, vol. 5, no. 1, pp. 264–268, 1958.

[45] M. Laing, “The electronegativity of a metal and its E°: should they correlate?,” *S Afr J Sci*, vol. 98, p. 580, 2002.

[46] A. Das, U. Das, and A. K. Das, “Relativistic effects on the chemical bonding properties of the heavier elements and their compounds,” *Coord Chem Rev*, vol. 479, pp. 1–24, Mar. 2023, doi: 10.1016/j.ccr.2022.215000.

CHAPTER 5. IMMOBILIZATION OF MERCURY IN K-GEOPOLYMER USING HYDROSULFIDE

5.1 Introduction

Various human activities have increased the risk of heavy metals contamination [1]. Activities such as mining, coal power plants, municipal waste incineration, and several industries produce wastes containing heavy metals. These metals are contained in fly ash and wastewater which is further treated into sludge [2], [3], [4]. Either fly ash or sludge is usually disposed of by dumping in landfills. However, this kind of disposal is susceptible to leaching [5], [6]. Rainwater and soil moisture can desorb or dissolve soluble metals from the waste and cause secondary waste contamination. The contamination can be prevented by applying a solidification/stabilization technique for treating fly ash and sludge before final disposal.

Geopolymer has emerged as a potential binder for the solidification/stabilization of waste containing heavy metals [7]. It is an alkali-activated material consisting of three-dimensional alumina and silica tetrahedra joined alternately by sharing oxygen atoms [8]. The main structure of geopolymer is either N-A-S-H or K-A-S-H, depending on the alkali activator [9]. This material is acid-resistant and emits lower CO_2 than the conventional binder, which is Portland cement [10], [11]. Geopolymer also has another superior ability in immobilizing radioactive like cesium [12]. This characteristic becomes important due to the various combinations of waste. Some waste can contain both heavy metals and radioactive, for example, fly ash produced from the Fukushima Daiichi Nuclear Power Plant accident [13]. K-geopolymer is more prospective for long-term immobilization due to the ability to maintain its amorphousness [14].

The previous chapter has conducted studies on the immobilization of several heavy metals in K-geopolymer. Among them, mercury exhibits a distinct behavior and cannot be well-immobilized at high concentrations [15]. Mercury strongly prefers linear coordination with oxygen in the geopolymer system, forming HgO [16]. This species is highly soluble, marking the difficulty in stabilizing the metal [17]. However, mercury is highly toxic. This metal has strong chemical and biological activity. It is present in the environment as inorganic and organic mercury compounds. Organic mercury, especially methylmercury, is generally more toxic [18]. This species is easily absorbed by aquatic life and bioaccumulated, causing ecological damage. Mercury ingests into humans through food chains and brings about adverse health effects [19]. This metal causes nausea, lung damage, birth defects, and permanent damage to the brain and nervous system [20]. In addition, inorganic mercury is primarily contained in fly ash and can transform into organic mercury through dissolution into freshwater and seawater [21]. Therefore, preventing the leaching of inorganic mercury from contaminated waste is crucial.

Mercury needs to be transformed into its most stable form to ensure long-term safety disposal. One of the most stable mercury forms is mercury sulfide with solubility in water of 2×10^{-24} g/L at 25ºC [22]. Several studies have reported the excellence of HgS formation for stabilizing mercury from waste [23], [24]. Sulfide and hydrosulfide are common reactants for this precipitation [25], [26]. The reaction paths at neutral to alkaline conditions are presented below [26].

$$Hg(OH)_2 + H_2S \rightleftharpoons HgS + 2H_2O \quad (5\text{-}1)$$

$$Hg(OH)_2 + HS^- \rightleftharpoons HgS + H_2O + OH^- \quad (5\text{-}2)$$

During the reaction with hydrosulfide, mercury initially forms an unstable chain (-S-Hg-S-Hg-S-) that rapidly transforms to four-coordinate HgS with short ordering and eventually yields crystal [27].

In this study, hydrosulfide is used to stabilize mercury in K-geopolymer. Hydrosulfide is expected to help stabilize high mercury concentrations and prevent the formation of highly soluble HgO, according to the stability diagram of Hg in H_2O system in the presence of HS^- shown in Figure 5-1. Stabilization mechanisms are evaluated by employing different methods. The molar ratio of Hg:S, a primary stabilization variable, is also examined. Finally, this study aims to provide the most appropriate procedure to immobilize mercury in K-geopolymer.

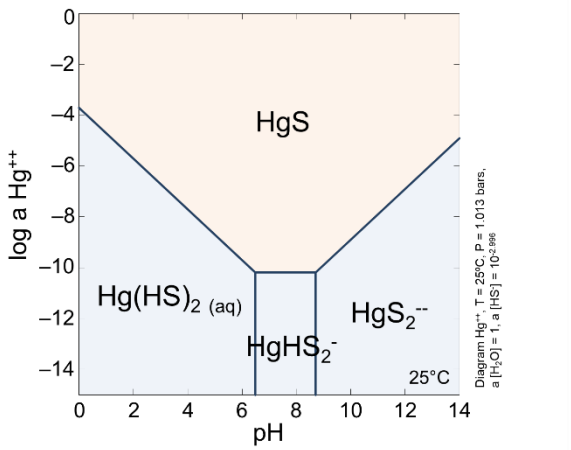

Figure 5-1. Solubility diagrams of mercury in the presence of hydrosulfide calculated with the Visual MINTEQ database

5.2 Materials and Methods

5.2.1 Materials

Metakaolin from Sobueclay Co., Ltd. (Japan) with a composition listed in Table 5-1 was used as an aluminosilicate precursor. Potassium silicate solution (21.90 wt.% of K_2O and 29.00 wt.% of SiO_2) was obtained from Fujifilm Wako Pure Chemical Corporation, while potassium hydroxide (86.0 wt.% purity) was bought from Kanto Chemical Co., Inc., Japan. Potassium silicate and potassium hydroxide were used as an alkali activator and were mixed, later with ultrapure water, with a molar ratio of SiO_2:K_2O:H_2O equals 1:1:13 [28]. Mercury(II) chloride (99.5 wt.% purity) was acquired from Fujifilm Wako Pure Chemical Corporation, Japan, and was used as an artificial contaminant. Potassium hydrosulfide solution (19.7 wt.% of KHS) was obtained from Kanto Chemical Co., Inc., Japan, and used as an additive.

Table 5-1. Chemical composition of the Sobueclay metakaolin

Component	Percentage (wt.%)
SiO_2	51.25
Al_2O_3	45.82
TiO_2	1.19
Fe_2O_3	0.58
Na_2O	0.06
K_2O	0.15
CaO	0.23
MgO	0.02
P_2O_5	0.13

5.2.2 Methods

5.2.2.1 Sample Preparation

Mercury geopolymers were made by two methods, namely the Simultaneous and Encapsulation method.

i. Simultaneous: Mercury(II) chloride was first dissolved in ultrapure water. The dissolved mercury was then mixed with metakaolin, an alkali activator, and potassium hydrosulfide solution. The mixture was hand-mixed for 15 minutes before molding.
ii. Encapsulation: Mercury(II) chloride was first dissolved in ultrapure water. The solution was then mixed with potassium hydrosulfide solution for 15 min. After that, metakaolin and alkali activator were added and mixed for another 15 min.

The above procedure was followed by molding the geopolymer gel in PVC molds (1.3 cm diameter × 1.5 cm height) and curing at 40°C for 24 h and another 24 h at 25°C. The experiments were carried out at a mercury concentration of 1 wt.%. The amount of the alkali activator used was adjusted to the Al_2O_3 content in the metakaolin to obtain an Al_2O_3:K_2O molar ratio of 1. The amount of potassium hydrosulfide used was also adjusted to obtain a Hg:S ratio of 1:1. Other samples were also made with the Simultaneous method by changing the Hg:S ratio to 1:2.

5.2.2.2 Leaching Test

A leaching test was performed by modifying the ANSI/ANS-16.1-2003 standard. Mercury geopolymers were submerged in 88 mL of deionized water and then moved into a new batch of deionized water after 30 s, 2 h, 7 h, and 1, 2, 3, 4, 5, 19, 47, and 90 d. During the leaching experiment, the temperature was kept constant at 25°C.

5.2.2.3 Liquid Sample Analysis

Mercury concentrations in the leachates were analyzed using an iCAP RQplus inductively coupled plasma mass spectrometry (ICP-MS; Thermo Scientific, USA). A mercury standard solution (Hg 1000; Fujifilm Wako Pure Chemical Corporation, Japan) was used to make a calibration standard with concentrations of 0.01–10 ppb. During the measurement, bismuth was used as the internal standard.

5.2.2.4 Solid Sample Analysis

The crystallography of mercury geopolymers was analyzed by X-ray diffraction (RINT2100; Rigaku; Japan). The CuKα radiation source used was 30 kV and 20 mA. The scanning was conducted from 2θ of 10° to 70° with 0.02°/s. Covalent bonding in the samples was examined with an XploRA PLUS Raman microscope (Horiba, Japan). Raman spectra were collected using a 532 nm excitation wavelength with a 50× objective lens, 100 µm entrance slit, and 1800 groove/mm grating. A JEM-2010 transmission electron microscope (TEM; JEOL, Japan) at an accelerating voltage of 200 kV was used to investigate nano-scale sample morphology, crystallography, and chemical composition.

5.3 Results and Discussion

5.3.1 Effect of Incorporation Method

Leaching test results for mercury geopolymer made with the addition of hydrosulfide are shown in Figure 5-2. The results show that hydrosulfide successfully decreases mercury leaching from K-geopolymer. Mercury is well-immobilized with less than 0.005% leaching for the sample made with the Simultaneous method and around 0.16% leaching for the Encapsulation method. Despite the low rate, both methods show different leaching behavior. Mercury leaching tends to be constant after several days for the Simultaneous method. Meanwhile, an increasing leaching pattern is obtained from the Encapsulation method.

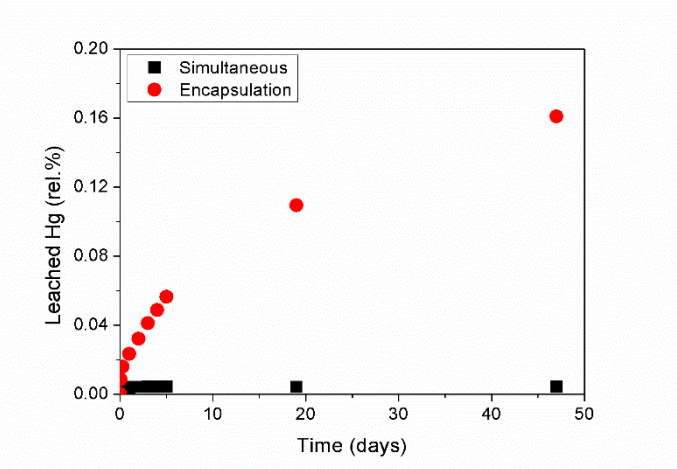

Figure 5-2. Cumulative amount of leaching relative to the initial amount of mercury made with different methods

X-ray diffraction patterns of mercury geopolymer added with hydrosulfide made via the Simultaneous and Encapsulation method are provided in Figure 5-3. A broad hump centered at ~28° is observed. This indicates the formation of amorphous silica which is a characteristic of geopolymer [29]. Several sharp peaks appear at 2θ of 26.38°, 30.68°, 43.72°, 51.74° and 54.22° in Simultaneous sample. Similar peaks at 26.46°, 30.62°, 43.78°, 51.82°, and 54.22° are also found in the geopolymer sample made via the Encapsulation method. Those peaks belong to metacinnabar. Metacinnabar is a cubic

polymorph of HgS consisting of four-coordinated Hg. This crystal is formed instead of the other polymorph because it is kinetically preferable [25]. During the geopolymerization reaction, Hg reacts with hydrosulfide to produce HgS (metacinnabar). The results show that in either method, the main immobilization mechanism for Hg in K-geopolymer with hydrosulfide addition is through the formation of a stable HgS precipitate.

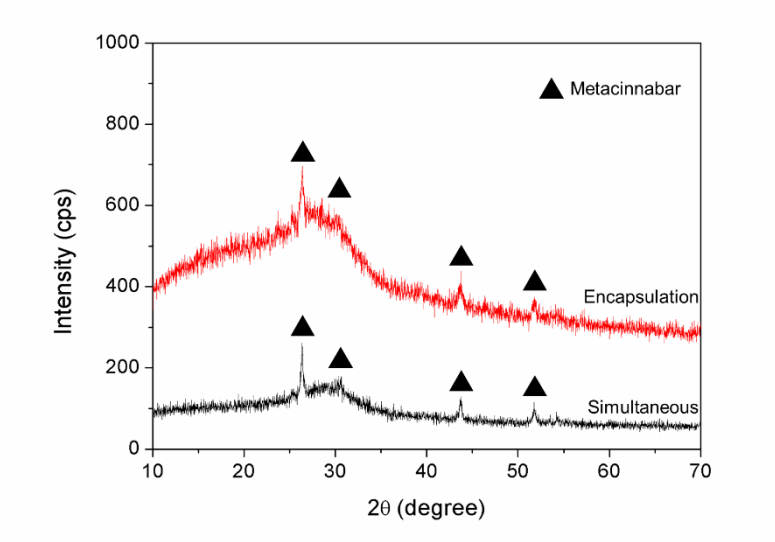

Figure 5-3. X-ray diffraction pattern of mercury geopolymer made by different incorporation methods

Figure 5-4 shows a nano-scale analysis of mercury precipitate in K-geopolymer. The morphology (Figure 5-4a) shows two separate phases. One phase consists of a more random structure and has a lighter color. This phase belongs to the geopolymer framework. The other phase is darker and more structured. Selected area electron diffraction (SAED) analysis on this phase results in regular spots, indicating a single crystal (Figure 5-4b). The main constituents of this crystal are Hg and S as suggested by the energy dispersive X-ray spectroscopy (EDS) result in Figure 5-4c. The SAED pattern reveals the d-spacing of the crystal to be 3.4, 1.689, and 1.13 A, belonging to metacinnabar. This crystal does not seem to chemically interact with geopolymer as they are seen to form two segregated phases. Therefore, geopolymer mostly acts as a binder that physically encapsulates metacinnabar. Besides the physical encapsulation of mercury precipitate, the distinction in the leaching behavior of Simultaneous and Encapsulation samples suggests other mechanisms may take a role in immobilizing Hg.

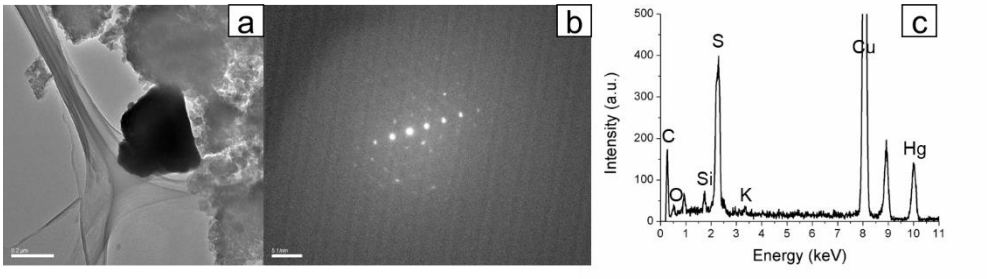

Figure 5-4. a) Morphology, b) SAED pattern, and c) EDS result of mercury precipitate in K-geopolymer

Nano-scale analysis on the Simultaneous sample shows another type of immobilization mechanism. Figure 5-5a shows the morphology of mercury geopolymer consisting of an amorphous phase. The crystalline form is absent as indicated by the selected area diffraction pattern in Figure 5-5b which is composed of a halo surrounding the central bright spot. However, the EDS result (Figure 5-5c) shows the existence of Hg alongside the constituents of the geopolymer framework. It indicates that mercury can be immobilized within K-geopolymer in a form other than HgS precipitate. The Simultaneous method allows Hg to form bonds with the geopolymer framework.

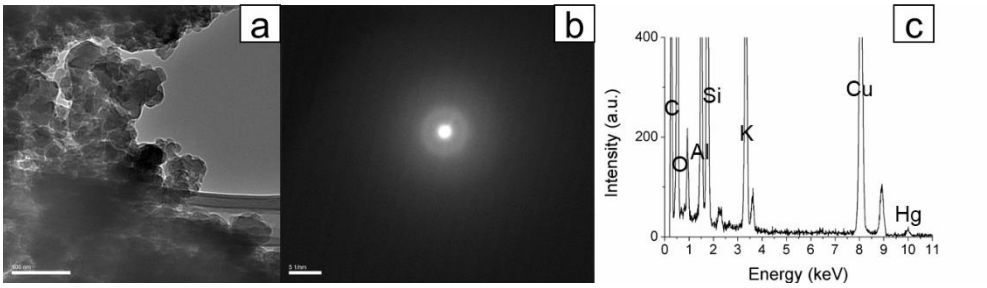

Figure 5-5. a) Morphology, b) SAED pattern, and c) EDS result of mercury geopolymer made via Simultaneous method

In the Encapsulation method, Hg was first reacted with hydrosulfide and later introduced to an aluminosilicate precursor and alkali activator. This method forms HgS in the initial stage and encapsulates the crystal within the geopolymer in the next stage. The increasing leaching pattern may be due to the formation of other soluble Hg forms, such as mercury polysulfide. A late introduction to the geopolymer system makes this method rely solely on precipitate formation and its encapsulation. Differently, the Simultaneous method allows the formation of HgS to happen simultaneously with the geopolymerization process. It leads to the possibility of Hg reacting with different reactants other than hydrosulfide. The formation of soluble species can be suppressed as Hg forms bonds with silica and alumina tetrahedra instead. Consequently, Hg is immobilized better and has a constant leaching behavior. An illustration of these immobilization mechanisms is provided in Figure 5-6.

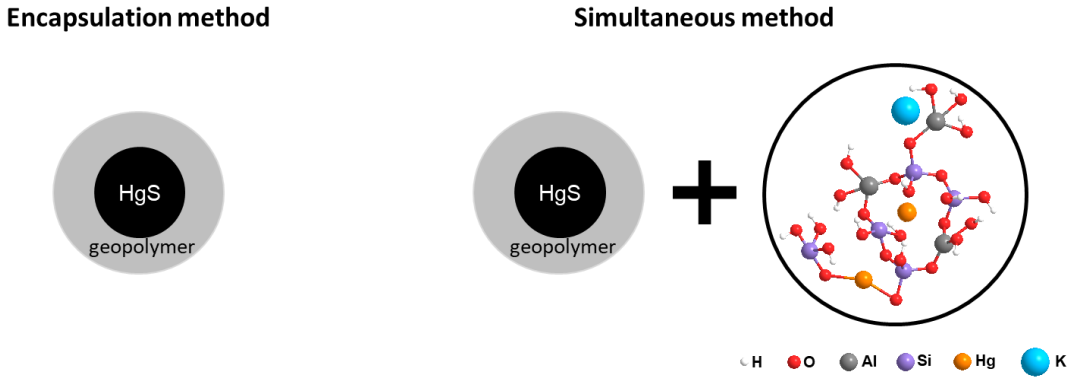

Figure 5-6. Immobilization mechanisms of Hg in K-geopolymer made via Encapsulation and Simultaneous method

5.3.2 Effect of Hg:S Ratio

Leaching test results for mercury geopolymer made with different Hg:S ratio is provided in Figure 5-7. The figure shows that mercury leaching is low regardless of the hydrosulfide concentration. Increasing the hydrosulfide concentration does not have a significant effect on mercury immobilization. Instead, the leaching rate for Hg:S ratio of 1:2 is similar to 1:1 in terms of the leached amount of Hg and leaching behavior. The Hg:S ratio of 1:2 also gives a relatively constant leaching pattern.

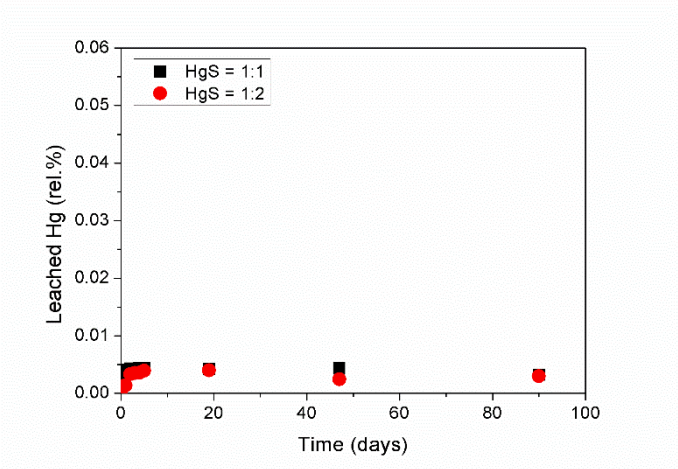

Figure 5-7. Cumulative amount of leaching relative to the initial amount of mercury made with different Hg:S ratio

A diffraction pattern of mercury geopolymer made with a Hg:S ratio of 1:2 is shown in Figure 5-8. This pattern consists of a broad hump centered at ~28°. The hump belongs to amorphous silica, which is a characteristic of geopolymer. In addition, peaks at 2θ of 26.56°, 30.86°, 43.92°, and 51.94° belonging to metacinnabar are also found. This result suggests that the same mercury speciation is formed even with a higher hydrosulfide concentration.

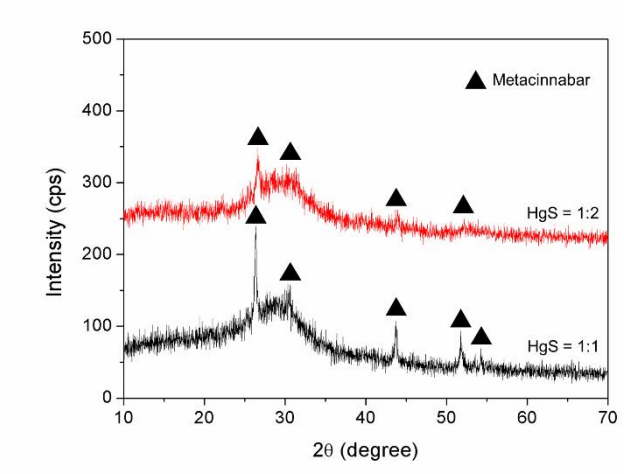

Figure 5-8. X-ray diffraction patterns of mercury geopolymer made with different Hg:S ratio

A slight difference with the use of various Hg:S ratios is observed from the Raman spectra shown in Figure 5-9. All samples exhibit the same peaks at 396, 502, 570, and 637 cm^{-1}, which correspond to the Si-O-Al bending mode, Si-O-Si stretching vibration from long and short chains, and T-O symmetric stretching mode [30], [31], [32], [33]. At higher wavelengths, peaks are found at 851 and 1056, correlating to the Si-O symmetric stretching [32]. All peaks indicate typical bonds owned by K-geopolymer. A new peak emerges at 970 cm^{-1} for both samples made with Hg:S ratio of 1:1 and 1:2. In addition, a different peak is present at 457 cm^{-1} for a Hg:S ratio of 1:2. These peaks belong to symmetric stretching of S-O [34]. The intensity of these peaks is proportional to the hydrosulfide concentration. These peaks represent unreacted hydrosulfide. After 90 days of leaching, a decrease in both peaks' intensity is observed. K-geopolymer poorly holds the negatively charged compound and enables its release. Therefore, the use of a Hg:S ratio of 1:2 is inefficient due to more unreacted sulfide.

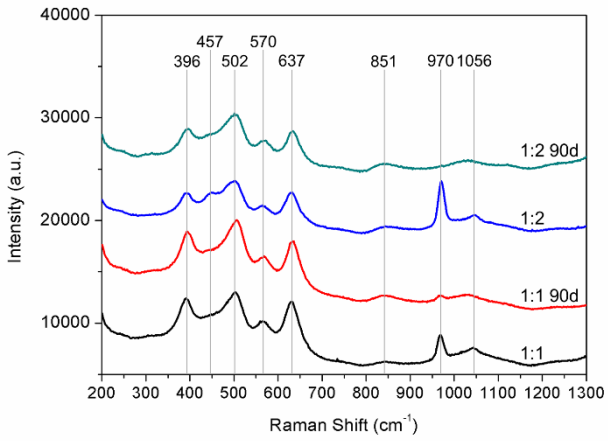

Figure 5-9. Raman spectra of mercury geopolymer made with different Hg:S ratios before and after 90 days of leaching

5.4 Conclusion

High mercury concentration can be well immobilized within K-geopolymer with hydrosulfide addition. The reaction between Hg and hydrosulfide produces metacinnabar (HgS) which is physically encapsulated by K-geopolymer and results in low mercury leaching. The methodology in which mercury is incorporated affects the leaching behavior. Simultaneous mixing of dissolved mercury with aluminosilicate precursor, KHS, and K-activator provides the stabilization of mercury not only through precipitate formation but also through bonding to silica and alumina tetrahedra, resulting in more stable forms and constant leaching pattern. Meanwhile, different uses of the Hg:S ratio do not induce distinct leaching behavior. Metacinnabar is the main stabilization product even when hydrosulfide concentration is increased. However, high hydrosulfide concentration has an excess that does not take part in the immobilization process and is easily leached out from the geopolymer. Simultaneous mixing of dissolved mercury with geopolymer components and KHS with a ratio of 1:1 is recommended for immobilizing high mercury concentrations in K-geopolymer.

5.5 References

[1] J. P. Vareda, A. J. M. Valente, and L. Durães, "Assessment of heavy metal pollution from anthropogenic activities and remediation strategies: A review," *J Environ Manage*, vol. 246, pp. 101–118, Sep. 2019, doi: 10.1016/j.jenvman.2019.05.126.

[2] N. A. A. Qasem, R. H. Mohammed, and D. U. Lawal, "Removal of heavy metal ions from wastewater: a comprehensive and critical review," *NPJ Clean Water*, vol. 4, no. 1, pp. 1–36, Dec. 2021, doi: 10.1038/s41545-021-00127-0.

[3] V. K. Sangal, S. Rajoria, and M. Vashishtha, "Heavy Metal Ions in Wastewater: A Review on Detection and Toxicity," *Chem Eng Process Tech*, vol. 8, no. 3, pp. 1082–1087, 2023.

[4] A. Altlkulaç *et al.*, "Assessment of the Enrichment of Heavy Metals in Coal and Its Combustion Residues," *ACS Omega*, vol. 7, no. 24, pp. 21239–21245, Jun. 2022, doi: 10.1021/acsomega.2c02308.

[5] A. Iravanian and S. O. Ravari, "Types of Contamination in Landfills and Effects on the Environment: A Review Study," in *IOP Conference Series: Earth and Environmental Science*, IOP Publishing Ltd, Dec. 2020, pp. 1–8. doi: 10.1088/1755-1315/614/1/012083.

[6] V. Nevondo, T. Malehase, A. P. Daso, and O. J. Okonkwo, "Leachate seepage from landfill: A source of groundwater mercury contamination in South Africa," *Water SA*, vol. 45, no. 2, pp. 225–231, Apr. 2019, doi: 10.4314/wsa.v45i2.09.

[7] T. H. Vu and N. Gowripalan, “Mechanisms of heavy metal immobilisation using geopolymerisation techniques – A review,” *Journal of Advanced Concrete Technology*, vol. 16, no. 3, pp. 124–135, 2018, doi: 10.3151/jact.16.124.

[8] J. Davidovits, “PROPERTIES OF GEOPOLYMER CEMENTS,” in *Alkaline Cements and Concretes*, 1994, pp. 131–149. [Online]. Available: www.geopolymer.org

[9] J. Davidovits, “Geopolymers: Ceramic-like inorganic polymers,” *Journal of Ceramic Science and Technology*, vol. 8, no. 3, pp. 335–350, 2017, doi: 10.4416/JCST2017-00038.

[10] M. Nodehi and V. M. Taghvaee, “Alkali-Activated Materials and Geopolymer: a Review of Common Precursors and Activators Addressing Circular Economy,” *Circular Economy and Sustainability*, vol. 2, no. 1, pp. 165–196, Mar. 2022, doi: 10.1007/s43615-021-00029-w.

[11] J. Davidovits, “Geopolymer cement to minimize carbon-dioxde greenhouse-warming,” *Ceramic Transactions*, vol. 37, no. 1, pp. 165–182, 1993, [Online]. Available: https://www.researchgate.net/publication/284682578

[12] R. I. Chaerun *et al.*, “Retention mechanism of cesium in chabazite embedded into metakaolin-based alkali activated materials,” *J Hazard Mater*, vol. 440, pp. 1–10, Oct. 2022, doi: 10.1016/j.jhazmat.2022.129732.

[13] Y. Koike, K. Fujii, R. Saito, N. Ogawa, and A. Ohbuchi, “Chemical State Analysis of Heavy Metals and Radioactive Cesium in Municipal Solid Waste Incineration Fly Ash Contaminated with Radioactive Cesium Released by the FDNPP Accident,” *Analytical Sciences*, vol. 37, no. 11, pp. 1565–1570, 2021, doi: 10.2116/analsci.21P022.

[14] B. Liu *et al.*, “Insights into the microstructure of hydrothermal synthesized nanoscale k2o-al2o3-sio2-h2o particles,” *Nanomaterials*, vol. 10, no. 1, pp. 1–18, Jan. 2020, doi: 10.3390/nano10010063.

[15] P. Prihutami, R. I. Chaerun, Y. Ohya, T. Otake, R. Kikuchi, and T. Sato, “Immobilization Forms of Cadmium and Mercury in a Potassium-Activated Metakaolin-Based Geopolymer,” *Minerals*, vol. 14, no. 3, pp. 1–15, Mar. 2024, doi: 10.3390/min14030311.

[16] A. Das, U. Das, R. Das, and A. K. Das, “Relativistic effects on the chemistry of heavier elements: Why not given proper importance in chemistry education at the undergraduate and postgraduate level?,” *Chemistry Teacher International*, vol. 5, no. 4, pp. 365–378, Dec. 2023, doi: 10.1515/cti-2023-0043.

[17] A. Hocsman, S. Di Nezio, L. Charlet, and M. Avena, “On the mechanisms of dissolution of montroydite [HgO(s)]: Dependence of the dissolution rate on pH,

temperature, and stirring rate," *J Colloid Interface Sci*, vol. 297, no. 2, pp. 696–704, May 2006, doi: 10.1016/j.jcis.2005.11.020.

[18] Y. S. Hong, Y. M. Kim, and K. E. Lee, "Methylmercury exposure and health effects," *Journal of Preventive Medicine and Public Health*, vol. 45, no. 6, pp. 353–363, Nov. 2012, doi: 10.3961/jpmph.2012.45.6.353.

[19] A. Renzoni, F. Zino, and E. Franchi, "Mercury Levels along the Food Chain and Risk for Exposed Populations 1," *ENVIRONMENTAL RESEARCH, SECTION A* , vol. 77, pp. 68–72, 1998.

[20] U.S. Environmental Protection Agency, "Mercury Study Report to Congress Volume V: Health Effects of Mercury and Mercury Compounds," Dec. 1997.

[21] Q. Chen *et al.*, "Increasing mercury risk of fly ash generated from coal-fired power plants in China," *J Hazard Mater*, vol. 429, pp. 1–8, May 2022, doi: 10.1016/j.jhazmat.2022.128296.

[22] D. O'Connor *et al.*, "Mercury speciation, transformation, and transportation in soils, atmospheric flux, and implications for risk management: A critical review," *Environ Int*, vol. 126, pp. 747–761, May 2019, doi: 10.1016/j.envint.2019.03.019.

[23] D. D. Sun, L. Zhang, and D. Lai, "Stabilization of mercury using waste ladle furnace slag," *J Air Waste Manage Assoc*, vol. 63, no. 12, pp. 1469–1478, 2013, doi: 10.1080/10962247.2013.796899.

[24] H. Piao and P. L. Bishop, "Stabilization of mercury-containing wastes using sulfide," *Environmental Pollution*, vol. 139, no. 3, pp. 498–506, Feb. 2006, doi: 10.1016/j.envpol.2005.06.005.

[25] A. R. Lennie, J. M. Charnock, and R. A. D. Pattrick, "Structure of mercury(II)-sulfur complexes by EXAFS spectroscopic measurements," *Chem Geol*, vol. 199, no. 3–4, pp. 199–207, Sep. 2003, doi: 10.1016/S0009-2541(03)00118-9.

[26] L.-Y. Chai, Q.-W. Wang, Y.-Y. Wang, Q.-Z. Li, Z.-H. Yang, and Y.-D. Shu, "Thermodynamic study on reaction path of Hg(II) with S(II) in solution," *J. Cent. South Univ. Technol*, vol. 17, pp. 289–294, 2010, doi: 10.1007/s11771−010−0044−0.

[27] M. Enescu, K. L. Nagy, and A. Manceau, "Nucleation of mercury sulfide by dealkylation," *Sci Rep*, vol. 6, pp. 1–6, Dec. 2016, doi: 10.1038/srep39359.

[28] X. Niu, Y. Elakneswaran, C. R. Islam, J. L. Provis, and T. Sato, "Adsorption behaviour of simulant radionuclide cations and anions in metakaolin-based geopolymer," *J Hazard Mater*, vol. 429, pp. 1–11, May 2022, doi: 10.1016/j.jhazmat.2022.128373.

[29] N. Mladenović *et al.*, “The Applications of New Inorganic Polymer for Adsorption Cadmium from Waste Water,” *J Inorg Organomet Polym Mater*, vol. 30, no. 2, pp. 554–563, Feb. 2020, doi: 10.1007/s10904-019-01215-y.

[30] M. Ivanović *et al.*, “The Influence Of Thermodynamic Parameters On Alkaline Activators Of Geopolymers And The Structure Of Geopolymers,” *Macedonian Journal of Chemistry and Chemical Engineering*, vol. 40, no. 1, pp. 99–109, 2021, doi: 10.20450/MJCCE.2021.2127.

[31] L. Zhang, F. Zhang, M. Liu, and X. Hu, “Novel sustainable geopolymer based syntactic foams: An eco-friendly alternative to polymer based syntactic foams,” *Chemical Engineering Journal*, vol. 313, pp. 74–82, 2017, doi: 10.1016/j.cej.2016.12.046.

[32] L. Vidal *et al.*, “Determination of the polymerization degree of various alkaline solutions: Raman investigation,” *J Solgel Sci Technol*, vol. 83, no. 1, pp. 1–11, Jul. 2017, doi: 10.1007/s10971-017-4394-z.

[33] A. Depla *et al.*, “UV-Raman and 29Si NMR spectroscopy investigation of the nature of silicate oligomers formed by acid catalyzed hydrolysis and polycondensation of tetramethylorthosilicate,” *Journal of Physical Chemistry C*, vol. 115, no. 22, pp. 11077–11088, Jun. 2011, doi: 10.1021/jp200568j.

[34] K. Ben Mabrouk, T. Kauffmann, H. Aroui, and F. Raman, “Raman study of cation effect on sulfate vibration modes in solid state and in aqueous solutions,” *Journal of Raman Spectroscopy*, vol. 44, no. 11, pp. 1603–1608, 2013, doi: 10.1002/jrs.4374ï.

CHAPTER 6. EFFECT OF HYDROSULFIDE ADDITION ON ZINC, CADMIUM, AND LEAD IN K-GEOPOLYMER

6.1 Introduction

Heavy metals are considerably toxic contaminants [1]. Several of these metals are mercury, cadmium, zinc, and lead. Exposure to heavy metals causes adverse clinical effects such as nausea, abdominal pain, renal dysfunction, lung damage, birth defects, bone disease, and permanent damage to the brain and nervous system [2], [3], [4], [5]. The risk of contamination has increased with anthropological activities, including mining, coal power plants, waste incineration, and various industries [6]. Those activities produce wastes such as fly ash and sludge from wastewater treatment containing heavy metals [7], [8], [9]. One of the disposal methods for those wastes is dumping in landfills. However, rainwater and soil moisture can leach out the heavy metals, causing secondary environmental contamination [10].

Solidification/stabilization of waste containing heavy metals becomes necessary to prevent contamination. The treatment can be done by using a binder. The conventional binder is Portland cement [11], [12]. This material is well-established but emits enormous CO_2 in its production [13]. This disadvantage, as well as its vulnerability to acid attack and inability to immobilize radioactive, has encouraged the development of another binder called geopolymer [14], [15]. Geopolymer is acid and thermal-resistant, it emits low CO_2 and can retain radioactive which sometimes exists with heavy metals [15], [16], [17]. This material consists of silica and alumina tetrahedra joined alternately forming a three-dimensional framework [18]. Four coordination of alumina induces a negative charge that is balanced by cations like Na^+ or K^+. Therefore, the main structure of geopolymer is either N-A-S-H or K-A-S-H [19]. K-geopolymer is a prospective binder for long-term waste stability due to its better flowability and ability to remain amorphous than the counterpart Na-geopolymer [20], [21], [22].

Previous chapters have reported the ability of K-geopolymer to immobilize heavy metals. Some metals, like Zn, Cd, and Pb, are stabilized directly in the geopolymer framework through electrostatic attraction and covalent bonds. However, mercury, especially at high concentrations, prefers the formation of highly soluble HgO [23], [24], [25]. An additive is required to increase mercury stabilization. Hydrosulfide is the additive that is proven to help stabilize mercury in K-geopolymer. It decreases mercury leaching from 70.81% to less than 0.005%. Hydrosulfide avoids HgO formation by instead forming metacinnabar (HgS) with mercury [26]. This crystal is then physically encapsulated within K-geopolymer. Since mercury exists in solid wastes along with other metals, studying the effect of hydrosulfide addition on other heavy metals in K-geopolymer is necessary. In this research, zinc, cadmium, and lead are subjected to the study due to their common existence in solid wastes aside from mercury [27], [28], [29].

6.2 Materials and Methods

6.2.1 Materials

Metakaolin (Sobueclay Co., Ltd., Japan) was used as the aluminosilicate precursor to make geopolymer. The metakaolin mainly consists of SiO_2 and Al_2O_3, with low CaO

content (Table 6-1). Potassium silicate solution (Fujifilm Wako Pure Chemical Corporation, Japan) and potassium hydroxide (Kanto Chemical Co., Inc., Japan) were employed as an alkali activator. Potassium silicate solution has K_2O and SiO_2 contents of 21.90 and 29.00 wt.%, respectively. Potassium hydroxide has 86.0 wt.% purity. Heavy metal salts were used to make artificial contaminants. Zinc chloride (99.5 wt.% purity) and cadmium chloride 2.5-hydrate (98 wt.% purity) were obtained from Fujifilm Wako Pure Chemical Corporation, Japan. Meanwhile, lead nitrate of 99.999 wt.% purity was bought from Sigma-Aldrich, Japan. Potassium hydrosulfide solution (19.7 wt.% of KHS) was obtained from Kanto Chemical Co., Inc., Japan, and used as an additive.

Table 6-1. Chemical composition of the Sobueclay metakaolin

Component	Percentage (wt.%)
SiO_2	51.25
Al_2O_3	45.82
TiO_2	1.19
Fe_2O_3	0.58
Na_2O	0.06
K_2O	0.15
CaO	0.23
MgO	0.02
P_2O_5	0.13

6.2.2 Methods

6.2.2.1 Sample Preparation

Zinc geopolymer (Zn-GP), cadmium geopolymer (Cd-GP), and lead geopolymer (Pb-GP) were made by first dissolving heavy metal salt in ultrapure water. The dissolved metal was then mixed with potassium hydrosulfide solution for 15 min. The ratio of heavy metal-to-hydrosulfide was kept at 1:1. After that, the mixture was added with metakaolin and alkali activator and mixed for another 15 min. The molar ratio of SiO_2:K_2O:H_2O in the alkali activator was kept constant at 1:1:13 to ensure the highest workability of the geopolymer [11]. The amount of the alkali activator used was then adjusted to the Al_2O_3 content in the metakaolin to obtain an Al_2O_3:K_2O molar ratio of 1. At the end of the mixing process, the mixture was poured into PVC molds (1.3 cm diameter × 1.5 cm height) and cured at 40°C for 24 h and for another 24 h at 25°C.

6.2.2.2 Leaching Test

ANSI/ANS-16.1-2003 standard was employed for the leaching test. Heavy metal geopolymers were submerged in 88 mL of deionized water and then moved into a new batch of deionized water after 30 s, 2 h, 7 h, and 1, 2, 3, 4, 5, 19 d, 47 d, and 90 d. The temperature was kept constant at 25°C during leaching.

6.2.2.3 Liquid Sample Analysis

Heavy metal concentrations in the leachates were analyzed using an iCAP RQplus inductively coupled plasma mass spectrometry (ICP-MS; Thermo Scientific, USA). A calibration standard of Zn, Cd, and Pb from 0.01 to 10 ppb was made with the custom

assurance standard XSTC-331 (SPEX CertiPrep; Seishin Trading Company, Japan). Yttrium and indium were introduced during measurement as internal standards.

6.2.2.4 Solid Sample Analysis

The crystallography of heavy metal geopolymers was analyzed by X-ray diffraction (RINT2100; Rigaku; Japan). The CuKα radiation source used was 30 kV and 20 mA. The scanning was conducted from 2θ of 10° to 70° with 0.02°/s. A JEM-2010 transmission electron microscope (TEM; JEOL, Japan) at an accelerating voltage of 200 kV was used to investigate nano-scale sample morphology, crystallography, and chemical composition.

6.3 Results and Discussion

Leaching test results for zinc, cadmium, and mercury geopolymer added with hydrosulfide are provided in Figure 6-1. All samples result in a high heavy metal immobilization efficiency with less than 0.12 wt.% leaching. All heavy metals have the same leaching pattern, in which constant leaching is achieved after several days. These results indicate that hydrosulfide addition has a positive effect on immobilizing Zn, Cd, and Pb.

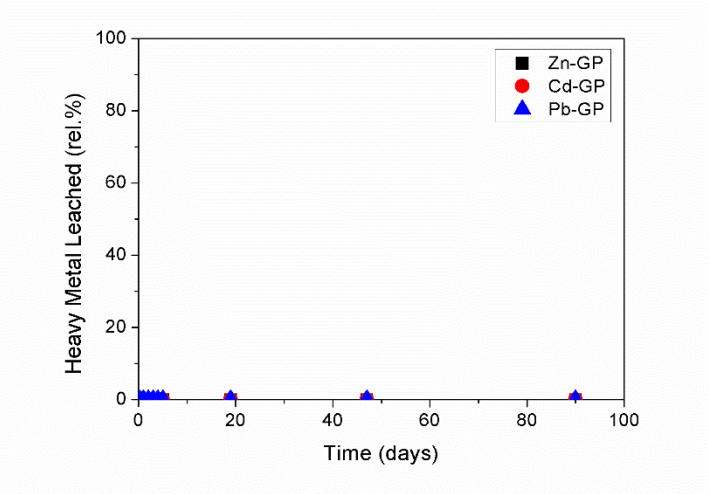

Figure 6-1. Cumulative amount of leaching relative to the initial amount of heavy metal

Heavy metal geopolymers were made by first reacting the metals with hydrosulfide. Products of this reaction are expected to be sulfide precipitates as predicted by solubility diagrams presented in Figure 6-2. The mixtures were then introduced into the geopolymerization process by adding an aluminosilicate precursor and alkali activator. By this method, sulfide precipitates are to be encapsulated by geopolymer to make a stable solid. According to the previous chapter, the encapsulation of sulfide precipitate results in comparatively more leaching, making it the determinant immobilization mechanism. The encapsulation method can provide a better condition to observe hydrosulfide interaction with heavy metals and K-geopolymer.

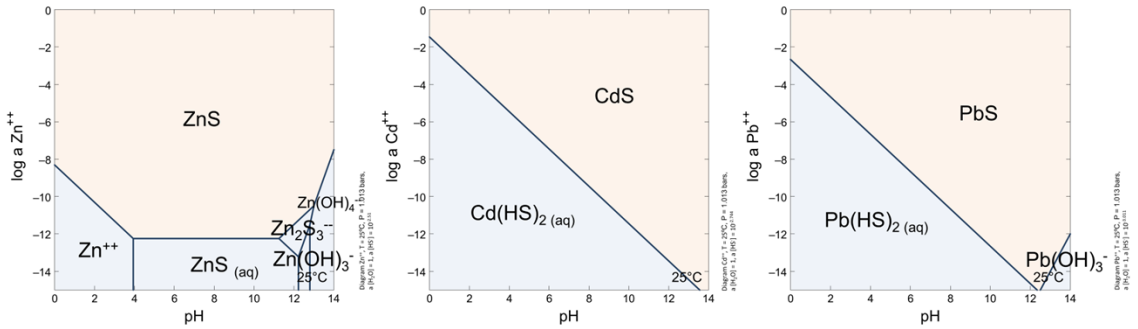

Figure 6-2. Solubility diagrams of zinc, cadmium, and lead in the presence of hydrosulfide calculated with the Visual MINTEQ database

The precipitation product for each metal is investigated through an X-ray diffraction analysis. The results are shown in Figure 6-3. All samples exhibit a broad hump centered around 28° which indicates amorphous silica and confirms the formation of geopolymer [30]. In addition, cadmium geopolymer possesses peaks at 25.28°, 26.72°, 28.4°, 44.08°, 48.3°, and 52.44° which belong to CdS. Peaks at 26.02°, 30.16°, 43.02°, and 51.1° corresponding to PbS are found in lead geopolymer. The diffraction patterns indicate that Cd and Pb interact with hydrosulfide, forming sulfide precipitates. However, a different result is observed for zinc geopolymer. Zinc speciation is not observed in the X-ray diffraction pattern.

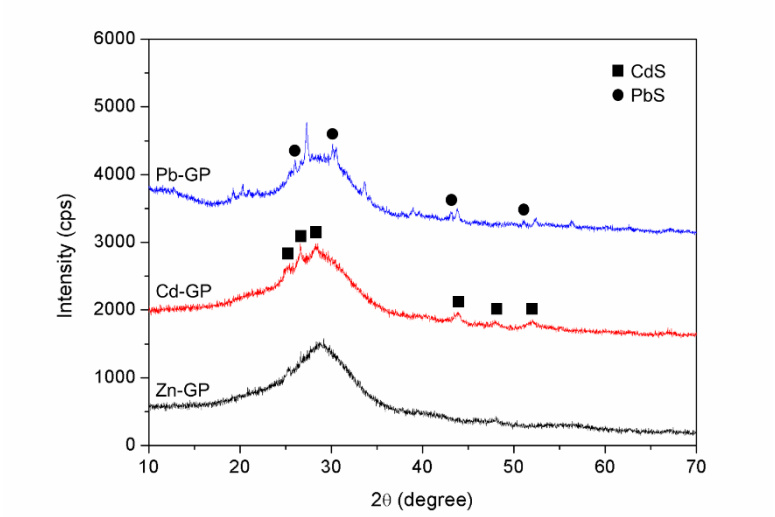

Figure 6-3. X-ray diffraction patterns of heavy metal geopolymers with hydrosulfide addition

Nano-scale analysis was conducted for all geopolymer samples to find out the precipitate interaction with geopolymer. Figure 6-4 shows the TEM analysis results for lead geopolymer made with hydrosulfide addition. The geopolymer matrix and precipitate are seen in Figure 6-4a to have a separate phase. A selected area electron diffraction of the precipitate results in two bright spots surrounding the central spot. The d-spacing is calculated from the distance between those spots with the central one and is

found to be 2.96 A. This d-spacing is the characteristic of PbS. The EDS result in Figure 6-4c also agrees with this result as the main constituents for this phase are mostly Pb and S. Lead sulfide is formed with hydrosulfide addition and is physically encapsulated within K-geopolymer.

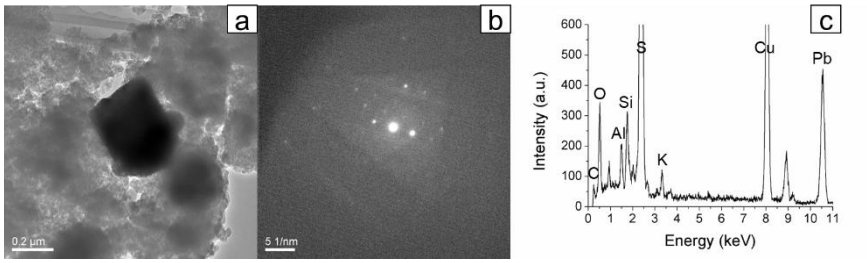

Figure 6-4. a) Morphology, b) SAED pattern, and c) EDS result of lead geopolymer with hydrosulfide addition

A similar result is also observed for cadmium geopolymer made with hydrosulfide addition. Figure 6-5a shows the morphology of cadmium geopolymer morphology which is also separated between the geopolymer phase and precipitate phase. The SAED pattern for the precipitate phase is shown in Figure 6-5b. The central spot is surrounded by bright spots that translate to a d-spacing of 3.58 A. This d-spacing belongs to CdS. This result is also supported by the EDS result (Figure 6-5c) as Cd is in high intensity along with S. After the formation of CdS, the geopolymer surrounds the precipitate and physically encapsulates it.

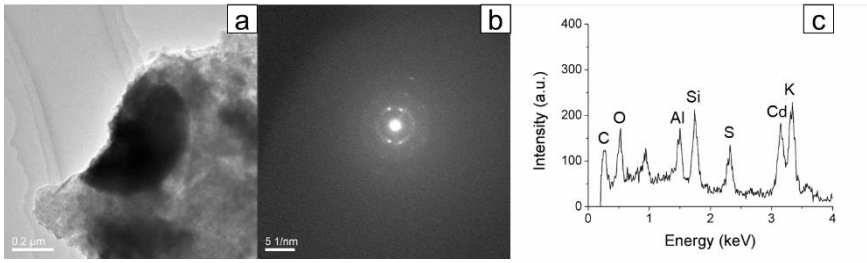

Figure 6-5. a) Morphology, b) SAED pattern, and c) EDS result of cadmium geopolymer with hydrosulfide addition

Although not apparent from the XRD analysis, the precipitate of zinc is observed from the TEM analysis. Figure 6-6a shows the crystal morphology of zinc precipitate and Figure 6-6b shows its SAED pattern. The regular spots in the SAED pattern translate to a single crystal structure. Calculation upon the pattern results in the d-spacing of 3.12 A and 1.57 A which are the characteristics of ZnS. These results indicate that hydrosulfide addition produces a sulfide precipitate that helps immobilize zinc in K-geopolymer.

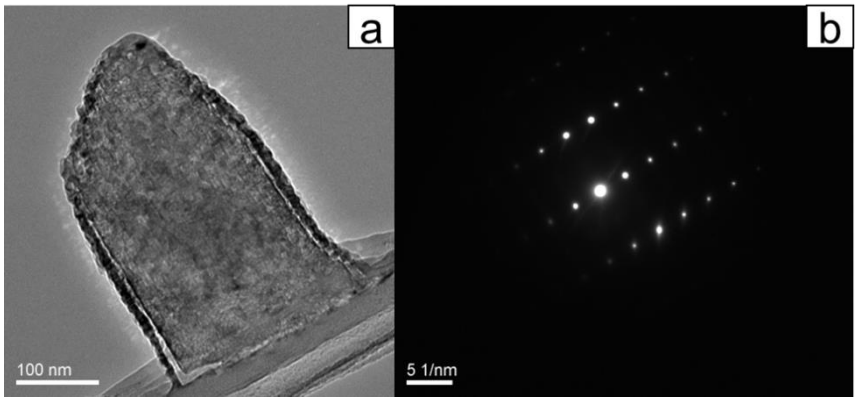

Figure 6-6. a) Morphology and b) SAED pattern of crystal structure in zinc geopolymer with hydrosulfide addition

Besides precipitate, the addition of hydrosulfide does not inhibit the direct interaction between heavy metal and geopolymer framework. Figure 6-7 shows the other type of Zn immobilization in K-geopolymer. The morphology of geopolymer is amorphous as seen in Figure 6-7a. The SAED pattern in Figure 6-7b also shows a halo surrounding the central spot which supports the amorphous phase. However, the EDS result in Figure 6-7c shows that besides the main constituents of geopolymer, which are Si, Al, K, and O, Zn is also observed. Besides hydrosulfide, the heavy metal reacts with the other reactants of geopolymer constituents and is immobilized by bonding within the K-geopolymer framework.

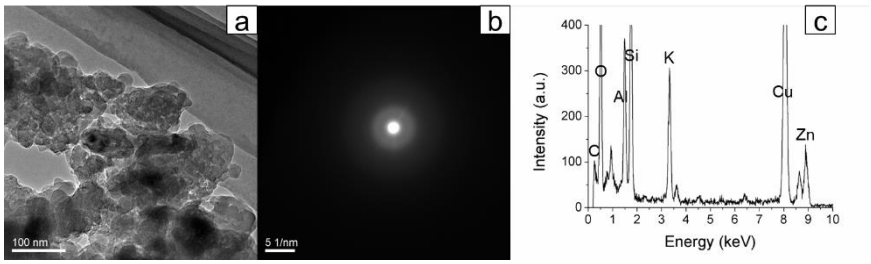

Figure 6-7. a) Morphology, b) SAED pattern, and c) EDS of amorphous structure in zinc geopolymer with hydrosulfide addition

6.4 Conclusion

Zinc, cadmium, and lead are well-immobilized in K-geopolymer with the addition of hydrosulfide. The leaching rate of those metals is low and constant after several days. This hydrosulfide interacts with heavy metals to produce stable sulfide precipitates. K-geopolymer is proven to be able to encapsulate the precipitates and form stable solids. In addition, K-geopolymer can still form stable bonds with unreacted metal cations. Hydrosulfide addition, therefore, has positive effects on heavy metals immobilization in K-geopolymer through the formation of stable precipitates and by not restraining the reaction between heavy metal and geopolymer framework.

6.5 References

[1] M. Bibi, Samiullah, F. Behlil, S. Afzal, and Sahifa, "Essential and non-essential heavy metals sources and impacts on human health and plants," *Pure and Applied Biology*, vol. 12, no. 2, pp. 835–847, Jun. 2023, doi: 10.19045/bspab.2023.120083.

[2] M. Mahurpawar, "Effects of heavy metals on human health," *Social Issues and Environmental Problems*, pp. 1–7, 2015.

[3] P. B. Tchounwou, C. G. Yedjou, A. K. Patlolla, and D. J. Sutton, "Heavy metal toxicity and the environment," *EXS*, vol. 101, pp. 133–164, 2012, doi: 10.1007/978-3-7643-8340-4_6.

[4] L. M. Plum, L. Rink, and H. Hajo, "The essential toxin: Impact of zinc on human health," *Int J Environ Res Public Health*, vol. 7, no. 4, pp. 1342–1365, 2010, doi: 10.3390/ijerph7041342.

[5] U.S. Environmental Protection Agency, "Mercury Study Report to Congress Volume V: Health Effects of Mercury and Mercury Compounds," Dec. 1997.

[6] J. P. Vareda, A. J. M. Valente, and L. Durães, "Assessment of heavy metal pollution from anthropogenic activities and remediation strategies: A review," *J Environ Manage*, vol. 246, pp. 101–118, Sep. 2019, doi: 10.1016/j.jenvman.2019.05.126.

[7] N. A. A. Qasem, R. H. Mohammed, and D. U. Lawal, "Removal of heavy metal ions from wastewater: a comprehensive and critical review," *NPJ Clean Water*, vol. 4, no. 1, pp. 1–36, Dec. 2021, doi: 10.1038/s41545-021-00127-0.

[8] V. K. Sangal, S. Rajoria, and M. Vashishtha, "Heavy Metal Ions in Wastewater: A Review on Detection and Toxicity," *Chem Eng Process Tech*, vol. 8, no. 3, pp. 1082–1087, 2023.

[9] A. Altlkulaç *et al.*, "Assessment of the Enrichment of Heavy Metals in Coal and Its Combustion Residues," *ACS Omega*, vol. 7, no. 24, pp. 21239–21245, Jun. 2022, doi: 10.1021/acsomega.2c02308.

[10] A. Iravanian and S. O. Ravari, "Types of Contamination in Landfills and Effects on the Environment: A Review Study," in *IOP Conference Series: Earth and Environmental Science*, IOP Publishing Ltd, Dec. 2020, pp. 1–8. doi: 10.1088/1755-1315/614/1/012083.

[11] Y. J. Du and N. J. Jiang, "Stabilization/solidification of contaminated soils: A case study," in *Low Carbon Stabilization and Solidification of Hazardous Wastes*, Elsevier, 2021, pp. 75–92. doi: 10.1016/B978-0-12-824004-5.00007-4.

[12] U.S. Environmental Protection Agency, "Treatment Technologies For Mercury in Soil, Waste, and Water," 2007.

[13] Z. He, X. Zhu, J. Wang, M. Mu, and Y. Wang, “Comparison of CO2 emissions from OPC and recycled cement production,” *Constr Build Mater*, vol. 211, pp. 965–973, Jun. 2019, doi: 10.1016/j.conbuildmat.2019.03.289.

[14] S. Goyal, M. Kumar, D. S. Sidhu, and B. Bhattacharjee, “Resistance of Mineral Admixture Concrete to Acid Attack,” *Journal of Advanced Concrete Technology*, vol. 7, no. 2, pp. 273–283, 2009.

[15] R. I. Chaerun *et al.*, “Retention mechanism of cesium in chabazite embedded into metakaolin-based alkali activated materials,” *J Hazard Mater*, vol. 440, pp. 1–10, Oct. 2022, doi: 10.1016/j.jhazmat.2022.129732.

[16] M. Nodehi and V. M. Taghvaee, “Alkali-Activated Materials and Geopolymer: a Review of Common Precursors and Activators Addressing Circular Economy,” *Circular Economy and Sustainability*, vol. 2, no. 1, pp. 165–196, Mar. 2022, doi: 10.1007/s43615-021-00029-w.

[17] J. Davidovits, “Geopolymer cement to minimize carbon-dioxde greenhouse-warming,” *Ceramic Transactions*, vol. 37, no. 1, pp. 165–182, 1993, [Online]. Available: https://www.researchgate.net/publication/284682578

[18] J. Davidovits, “Geopolymers: Ceramic-like inorganic polymers,” *Journal of Ceramic Science and Technology*, vol. 8, no. 3, pp. 335–350, 2017, doi: 10.4416/JCST2017-00038.

[19] J. Davidovits, “PROPERTIES OF GEOPOLYMER CEMENTS,” in *Alkaline Cements and Concretes*, 1994, pp. 131–149. [Online]. Available: www.geopolymer.org

[20] A. C. Constâncio Trindade, I. Curosu, M. Liebscher, V. Mechtcherine, and F. de Andrade Silva, “On the mechanical performance of K- and Na-based strain-hardening geopolymer composites (SHGC) reinforced with PVA fibers,” *Constr Build Mater*, vol. 248, pp. 1–16, Jul. 2020, doi: 10.1016/j.conbuildmat.2020.118558.

[21] M. Uehara, “New Concrete with Low Environmental Load Using the Geopolymer Method,” *QR of RTRI*, vol. 51, no. 1, pp. 1–7, 2010.

[22] B. Liu *et al.*, “Insights into the microstructure of hydrothermal synthesized nanoscale k2o-al2o3-sio2-h2o particles,” *Nanomaterials*, vol. 10, no. 1, pp. 1–18, Jan. 2020, doi: 10.3390/nano10010063.

[23] A. Das, U. Das, R. Das, and A. K. Das, “Relativistic effects on the chemistry of heavier elements: Why not given proper importance in chemistry education at the undergraduate and postgraduate level?,” *Chemistry Teacher International*, vol. 5, no. 4, pp. 365–378, Dec. 2023, doi: 10.1515/cti-2023-0043.

[24] A. Hocsman, S. Di Nezio, L. Charlet, and M. Avena, “On the mechanisms of dissolution of montroydite [HgO(s)]: Dependence of the dissolution rate on pH,

temperature, and stirring rate," *J Colloid Interface Sci*, vol. 297, no. 2, pp. 696–704, May 2006, doi: 10.1016/j.jcis.2005.11.020.

[25] D. O'Connor *et al.*, "Mercury speciation, transformation, and transportation in soils, atmospheric flux, and implications for risk management: A critical review," *Environ Int*, vol. 126, pp. 747–761, May 2019, doi: 10.1016/j.envint.2019.03.019.

[26] A. R. Lennie, J. M. Charnock, and R. A. D. Pattrick, "Structure of mercury(II)-sulfur complexes by EXAFS spectroscopic measurements," *Chem Geol*, vol. 199, no. 3–4, pp. 199–207, Sep. 2003, doi: 10.1016/S0009-2541(03)00118-9.

[27] D. Xiao, H. Li, Y. Wang, G. Wen, and C. Wang, "Distribution Characteristics of Typical Heavy Metals in Sludge from Wastewater Plants in Jiangsu Province (China) and Their Potential Risks," *Water (Switzerland)*, vol. 15, no. 2, pp. 1–13, Jan. 2023, doi: 10.3390/w15020313.

[28] G. C. Kisku, S. Yadav, R. K. Sharma, and M. P. S. Negi, "Potential environmental pollution hazards by coal based power plant at Jhansi (UP) India," *Environ Earth Sci*, vol. 67, no. 7, pp. 2109–2120, Dec. 2012, doi: 10.1007/s12665-012-1651-x.

[29] W. Zucha, G. Weibel, M. Wolffers, and U. Eggenberger, "Inventory of MSWI fly ash in Switzerland: Heavy metal recovery potential and their properties for acid leaching," *Processes*, vol. 8, no. 12, pp. 1–13, Dec. 2020, doi: 10.3390/pr8121668.

[30] N. Mladenović *et al.*, "The Applications of New Inorganic Polymer for Adsorption Cadmium from Waste Water," *J Inorg Organomet Polym Mater*, vol. 30, no. 2, pp. 554–563, Feb. 2020, doi: 10.1007/s10904-019-01215-y.

[31] M. Ivanović *et al.*, "The Influence Of Thermodynamic Parameters On Alkaline Activators Of Geopolymers And The Structure Of Geopolymers," *Macedonian Journal of Chemistry and Chemical Engineering*, vol. 40, no. 1, pp. 99–109, 2021, doi: 10.20450/MJCCE.2021.2127.

[32] L. Zhang, F. Zhang, M. Liu, and X. Hu, "Novel sustainable geopolymer based syntactic foams: An eco-friendly alternative to polymer based syntactic foams," *Chemical Engineering Journal*, vol. 313, pp. 74–82, 2017, doi: 10.1016/j.cej.2016.12.046.

[33] L. Vidal *et al.*, "Determination of the polymerization degree of various alkaline solutions: Raman investigation," *J Solgel Sci Technol*, vol. 83, no. 1, pp. 1–11, Jul. 2017, doi: 10.1007/s10971-017-4394-z.

[34] A. Depla *et al.*, "UV-Raman and 29Si NMR spectroscopy investigation of the nature of silicate oligomers formed by acid catalyzed hydrolysis and polycondensation of tetramethylorthosilicate," *Journal of Physical Chemistry C*, vol. 115, no. 22, pp. 11077–11088, Jun. 2011, doi: 10.1021/jp200568j.

[35] K. Ben Mabrouk, T. Kauffmann, H. Aroui, and F. Raman, "Raman study of cation effect on sulfate vibration modes in solid state and in aqueous solutions," *Journal*

of Raman Spectroscopy, vol. 44, no. 11, pp. 1603–1608, 2013, doi: 10.1002/jrs.4374ï.

[36] L. P. Wang *et al.*, “Selective Precipitation of Copper and Zinc over Iron from Acid Mine Drainage by Neutralization and Sulfidization for Recovery,” *J. Soc. Mater. Eng. Resour*, vol. 20, no. 2, pp. 136–140, 2014.

CHAPTER 7. GENERAL CONCLUSION AND FUTURE WORKS

7.1 General Conclusion

This study depicts the importance of understanding the initial and final heavy metal species for its stabilization within K-geopolymer. Cadmium and mercury can be introduced into the geopolymer system in two forms and produce distinct results. Introducing Cd and Hg in salt forms produces $Cd(OH)_2$ and HgO of high solubility, especially at low pH conditions. These precipitates reside at the bottom, resulting in nonhomogeneous geopolymers. Meanwhile, introducing Cd and Hg in their ion forms produces more homogeneous geopolymers. Cadmium does not form $Cd(OH)_2$, resulting in better immobilization. Initial heavy metal species, whether salt or ion, clearly affect their final species and immobilization efficiency. This study points out the importance of choosing the most appropriate mixing procedure as it can determine the heavy metal form during geopolymerization, in which providing heavy metal in dissolved ions is more beneficial. This procedure can be well-executed by a K-activator due to its higher flowability compared to the Na counterpart. This study also highlights the effect of heavy metals concentration on their immobilization within K-geopolymer. High concentrations of Hg are more difficult to retain than low-concentration ones due to the formation of highly soluble HgO. Meanwhile, Cd is well-immobilized at any concentration, indicating the ability of K-geopolymer to stabilize the metal of various concentrations.

This study also clarifies the immobilization mechanisms of some heavy metals in K-geopolymer and the factors affecting them. Zinc, cadmium, and lead are revealed to be immobilized through bonding with alumina tetrahedra. The bonding is made feasible by the higher ionic potential of Zn^{2+}, Cd^{2+}, and Pb^{2+} compared to K^+. Bonding through an oxygen atom from aluminate and silicate is also plausible because Zn, Cd, and Pb have high electronegativity similar to Al and Si. High ionic potential and electronegativity also explain the bonding of Hg within the geopolymer framework at low concentrations. However, at high concentrations, Hg prefers linear coordination with oxygen affected by relativistic effects and its electron configuration.

Since Hg leads to the formation of highly soluble HgO at high concentrations, considering a more stable heavy metal species is important to immobilize the metal within K-geopolymer. Mercury stabilization is helped by hydrosulfide addition to form HgS. However, this study shows that relying solely on HgS formation is not as effective as letting the formation of bonds between Hg and geopolymer framework alongside HgS formation. The latter mechanisms can be achieved by simultaneous mixing of contaminant, aluminosilicate precursor, hydrosulfide, and alkali activator. The study also found that hydrosulfide does not change the main structure of K-geopolymer. Excess hydrosulfide easily leaches out after contact with water.

Hydrosulfide addition can also form low-solubility Zn, Cd, and Pb precipitates. These precipitates are well encapsulated in K-geopolymer, suggested by their low leaching. Besides, similar to the mercury case, hydrosulfide does not hinder the immobilization mechanisms of heavy metals through bonds with the geopolymer framework. The results depict that K-geopolymer can manage wastes containing various

combinations of heavy metals, including high concentrations of Hg, by using hydrosulfide as an additive.

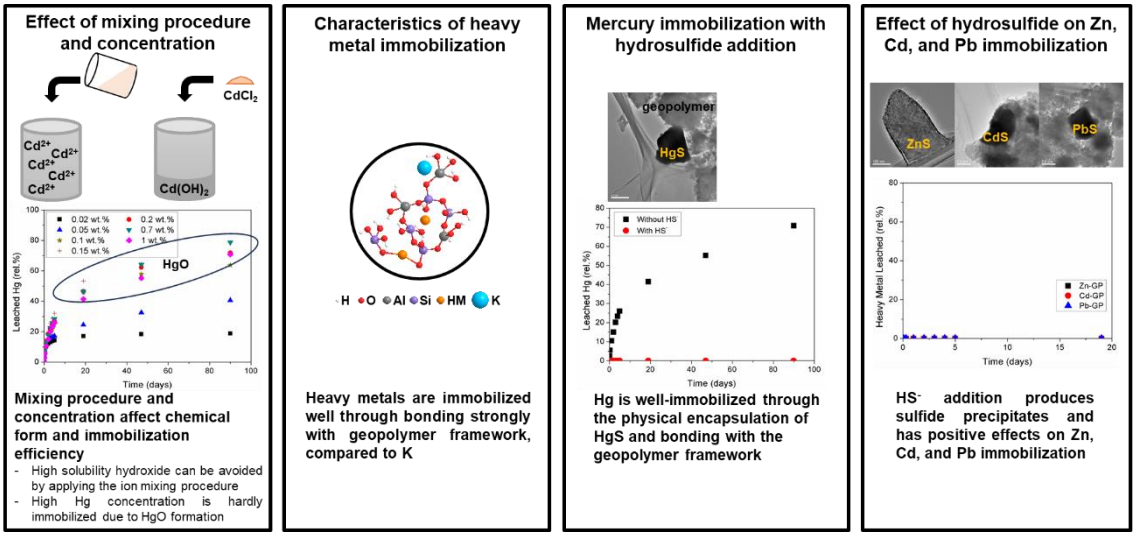

Figure 7-1. Novel findings regarding immobilization of heavy metals in K-geopolymer

Knowing the immobilization mechanisms of Zn, Cd, Hg, and Pb and the factors affecting them, the immobilization mechanisms of other metals can be predicted. The prediction is limited to divalent heavy metals, following the previously investigated ones. Immobilization mechanisms are predicted for Mn, Co, Ni, and Cu. Those metals have low atomic numbers, thus the relativistic effect can be neglected. Unlike Hg, Mn, Co, Ni, and Cu will not strongly prefer linear coordination with oxygen.

The ionic potential of Mn, Co, Ni, Cu, and several other heavy metals in 6-coordination are shown in Figure 7-2. All of the predicted heavy metals have ionic potential higher than K^+. The higher ionic potentials allow the heavy metals to replace K^+ and bond with alumina tetrahedra. The bonding is stronger than the K^+ and alumina tetrahedra bond. Aside from K^+, Figure 7-2 also shows the ionic potential of Ca^{2+} and Na^+. Those three are common ions in groundwater that may come in contact with geopolymer. However, all those ions have ionic potential much lower than heavy metals, meaning neither K^+, Ca^{2+}, nor Na^+ can replace heavy metals after they bond with alumina tetrahedra. This ensures the stability of heavy metals in K-geopolymer for the long term.

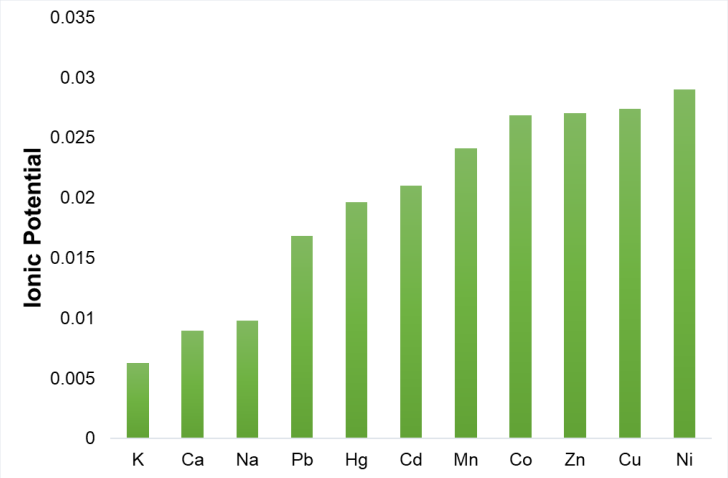

Figure 7-2. Ionic potential of previously investigated and predicted metals

Figure 7-3 presents the electronegativity value of the predicted and previously investigated metals. Manganese, cobalt, nickel, and copper have high electronegativity values identical to Al and Si. This similarity allows covalent bonding between heavy metals and aluminate and silicate. Among others, Mn has an electronegativity value similar to Zn and Cd. Therefore, Mn most likely bonds to alumina and silica tetrahedra, like Zn and Cd. Meanwhile, the electronegativity values of Co, Cu, and Ni are more similar to Pb. These three metals are most likely to behave similarly to Pb, which will have strong bonds with silicate.

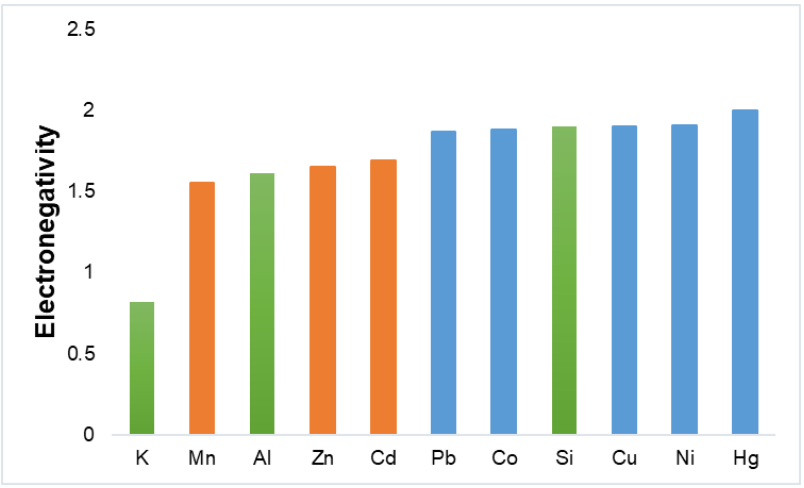

Figure 7-3. Electronegativity value of previously investigated and predicted metals

Heavy metal speciation plays a pivotal role in its immobilization within K-geopolymer. Heavy metal hydroxide and oxide are mostly only stable at high pH conditions. This species is disadvantageous for final waste disposal since the waste may interact with groundwater, decreasing surrounding pH, and result in heavy metal leaching. Providing heavy metals in their ion form during geopolymerization can avoid the formation of metal hydroxide and allow metal immobilization through covalent bonding within the geopolymer framework. This bonding is stable at decreasing pH. When highly

soluble metal oxide formation cannot be avoided, an additive is needed to transform the metal into a much more stable form. Heavy metal sulfide is a more stable form as predicted by thermodynamics calculation. However, in the long run, interaction with oxygen may transform it into sulfate form and change its stability. When a slow heavy metal release occurs due to this phenomenon, the use of K-geopolymer as the binder is very beneficial. The released metal can bond with the geopolymer matrix, preventing its release into the environment. Besides the strong interaction between geopolymer framework and heavy metals, geopolymer resistance to oxidation and acidic attack made this mechanism possible.

Considering all the novel findings in this study, K-geopolymer has the potential to treat a wide variety of solid wastes containing heavy metals. This variety includes various combinations of heavy metals and various concentrations. In processing real waste, heavy metal concentration is an important parameter that determines the formation of a highly soluble precipitate. In principle, hydroxides and mercury oxide formation need to be avoided and heavy metals bonding with geopolymer framework should be promoted. This can be done by applying an appropriate mixing procedure and adding an additive as can be seen from Figure 7-4.

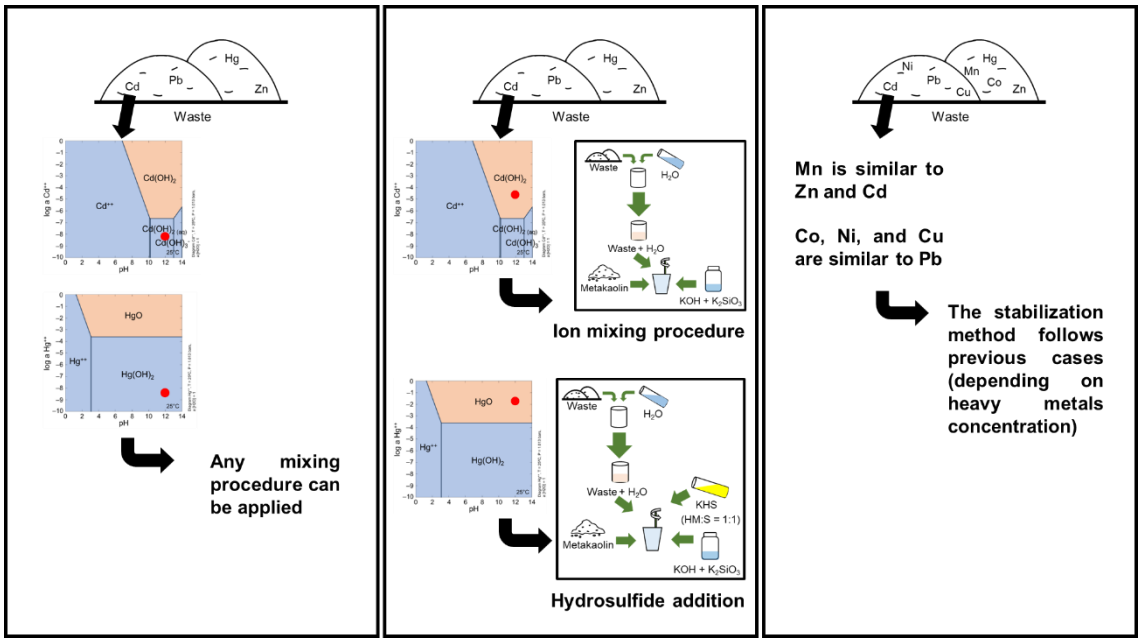

Figure 7-4. Implication for real waste solidification/stabilization

The method selection for real waste solidification/stabilization using K-geopolymer is provided in Figure 7-5. Before treating, determining the major content of the waste is a crucial step. This step can tell an additional matrix that will be formed within the waste. Iron sludge, for example, has high ferrihydrite content which is stable at high pH. Therefore, this matrix will not interfere with geopolymer formation and heavy metals' stabilization within its framework. Heavy metal content then determines the method for iron sludge solidification/stabilization. In the case of Fukushima and ordinary fly ash, a C-S-H or C-A-S-H matrix may be produced depending on Ca content. The

formation of this matrix should be avoided as it cannot retain Cs in Fukushima fly ash. Differently, C-S-H or C-A-S-H can retain divalent heavy metals. However, the metals are mostly immobilized as hydroxides or other mechanisms with low stability. Therefore, K_2CO_3 should be added to form $CaCO_3$ instead of C-S-H or C-A-S-H.

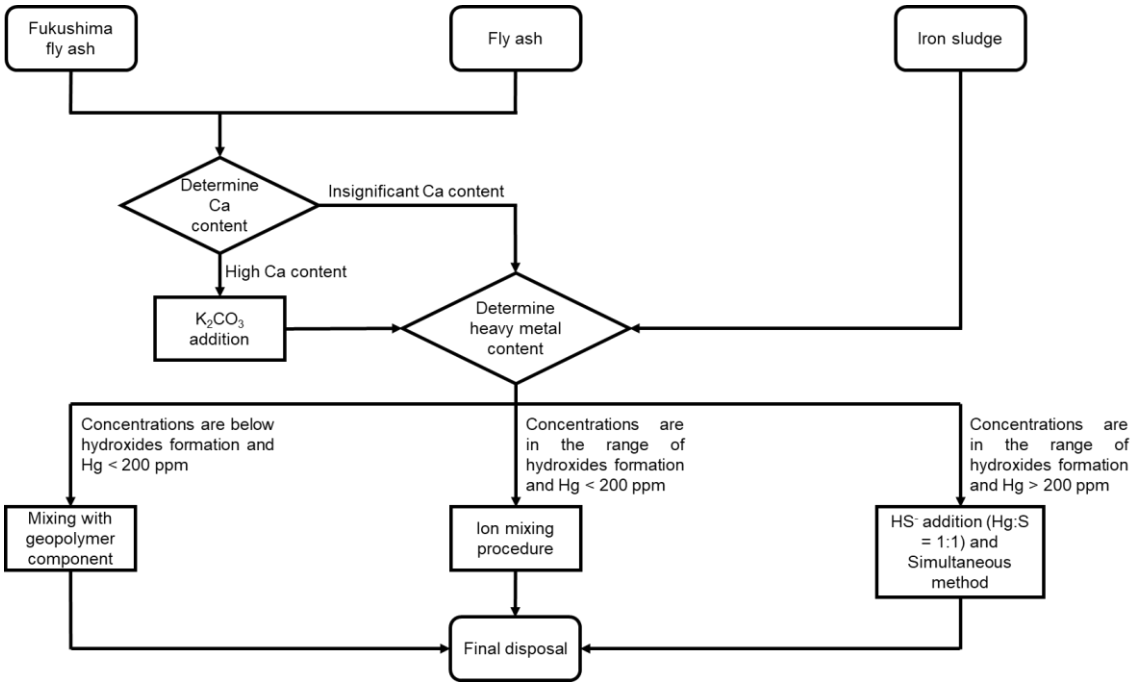

Figure 7-5. Method selection for waste solidification/stabilization using K-geopolymer

7.2 Suggestions for Future Works

7.2.1 Broadening the understanding of heavy metals immobilization for other valence cations and oxyanions

This study has investigated the immobilization mechanisms of Zn, Cd, Hg, and Pb as well as extended the postulated mechanisms for other similar metals, namely divalent metal cations with high ionic potential and electronegativity. However, real wastes can contain heavy metals other than divalent cations. Several metals exist as 1-valence cations like Hg(I), 3-valence cations such as As(III) and Cr(III), 4-valence cations like Mn(IV), 5-valence cations such as As(V) and 6-valence cations like Cr(VI). Heavy metals can also present as oxyanions, for example, AsO_4^{3-} and $Cr_2O_7^{2-}$. Therefore, conducting research that focuses on the immobilization mechanisms of other valence cations and oxyanions is important. Investigation into other valence cations is needed to confirm whether they follow the same theoretical approach in this study. Meanwhile, a study on oxyanions immobilization can focus on the most appropriate additive to well-immobilize them in K-geopolymer. The additive effect on K-geopolymer as well as other heavy metals is also crucial to study for the practicality and long-term immobilization. A comprehensive study on various heavy metal species will open the door for the utilization of K-geopolymer to treat a wider variety of waste.

7.2.2 Understanding the effect of calcium concentration on heavy metal immobilization

This study aims to offer an alternative binder to treat solid wastes containing heavy metals. However, the composition of solid wastes is very varied. They can contain not only various heavy metals, but also various concentrations of SiO_2, Al_2O_3, and even CaO. Calcium content becomes important in determining the formation of C-(A)-S-H. Future works can focus on the effect of calcium concentration on C-(A)-S-H formation and its effect on heavy metal immobilization mechanisms. Considering C-(A)-S-H limitation in immobilizing some contaminants, its formation during alkali activation needs to be avoided. The study should aim to find the concentration limit at which K_2CO_3 addition is required to eliminate C-(A)-S-H formation. Finally, a standardized procedure is expected to act as a blueprint for making stable waste for final disposal.

Expanding the scope of the K-geopolymer study to immobilize heavy metals is essential for deeply understanding their interaction with geopolymer and assessing the feasibility of K-geopolymer in treating solid wastes. The research will be important for the development of safer waste disposal.